Michael J. R. Fasham (Ed.)

Ocean Biogeochemistry

The Role of the Ocean Carbon Cycle in Global Change

Chapter 3

Continental Margin Exchanges

Chen-Tung Arthur Chen · Kon-Kee Liu · Robie Macdonald

Springer, 2003

Chapter 3

Continental Margin Exchanges

Chen-Tung Arthur Chen · Kon-Kee Liu · Robie Macdonald

3.1 Introduction

Biogeochemical processes principally occur in the upper 200 metres of the sea and are often associated with continental margins. Although the continental margins, with waters shallower than 200 m, occupy a mere 7% of the ocean surface and even less than 0.5% of the ocean volume, they still play a major role in oceanic biogeochemical cycling. Significantly higher rates of organic productivity occur, in fact, in the coastal oceans than in the open oceans because of rapid turnover and the higher supply of nutrients from upwelling and riverine inputs. Also, 8 to 30 times more organic carbon and 4 to 15 times more calcium carbonate per unit area accumulate in the coastal oceans than in the open oceans. Similarly, gas exchange fluxes of carbon and nitrogen are considerably higher in coastal waters than in the open oceans per unit area. As a result, it has been reported that around 14% of total global ocean production, along with 80–90% of new production and as much as up to 50% of denitrification takes place in the coastal oceans. The burial sites of 80% of the organic carbon derived from both oceanic processes and terrestrial sources, in excess of 50% of present day global carbonate deposition, are also located in the coastal oceans. The unburied portion of organic carbon may be respired on the shelf, thus forming a potential natural source of atmospheric carbon dioxide. However, how much is actually respired is unknown since much of this carbon is highly inert and only mixes conservatively with seawater (Smith and Mackenzie 1987; Mantoura et al. 1991; Wollast 1998).

Humans strongly interfere with the global biogeochemical cycle of carbon, nitrogen and phosphorus and this has led to substantially increased loadings of chemicals from their activities on land and in the atmosphere. The horizontal fluxes of these elements to the coastal oceans via rivers, groundwaters and the atmosphere have a strong impact on biogeochemical dynamics, cycling, and the metabolism of coastal waters. Potential feedback may result from the anthropogenic eutrophication of continental shelf areas due to increases in nutrient availability, which may then lead to a reduction of oxygen concentration in subsurface waters as a result of increased microbial respiration. In this way, denitrification and methanogenesis are promoted, resulting in the release of N_2, N_2O and CH_4. Eutrophication accelerates the cycle of organic synthesis and regeneration of nutrients other than silicate; however, calcareous shells and skeletons are preserved. On the other hand, the damming of major rivers may reduce freshwater output and the buoyancy effect on the shelves, which in turn reduces upwelling and nutrient input. Subsequently, productivity and eutrophication are diminished. These processes, however, cannot yet be accurately quantified (Walsh et al. 1985; Christensen 1994; Galloway et al. 1995; Kempe 1995).

The flux of carbon from the terrestrial biosphere to the oceans takes place via river transport. The global river discharge of carbon in both organic and inorganic form may approximate 1–1.4 Gt C yr^{-1} (Schlesinger and Melack 1981; Degens et al. 1991; Meybeck 1993). A substantial fraction of this transport (up to 0.8 Gt C yr^{-1}), however, reflects the natural geochemical cycling of carbon and does not in any way affect the global budget of anthropogenic CO_2 perturbation. Furthermore, to a large extent anthropogenically-induced river carbon fluxes are indicative of increased soil erosion rather than a removal of excess atmospheric CO_2. The above mentioned discharges of organic matter and nutrients from coastal communities do not have a significant impact on the open world oceans but can have important effects on the coastal oceans (Chen and Tsunogai 1998). Smith and Hollibaugh (1993) suggested that the observed invasion of fluxes of anthropogenic CO_2 in coastal oceans should be increased by 0.08 Gt C yr^{-1} to accurately represent the perturbed carbon fluxes because, under natural conditions, they are net sources of CO_2.

The discharge of excess nutrients by rivers may have significantly stimulated carbon fixation (up to 0.5–1 Gt C yr^{-1}). Bolin (1977) and Walsh et al. (1981) claimed that the acceleration in the amount of organic carbon storage in the coastal sediments can partially be attributed to the increased primary productivity due to large increases in anthropogenic nitrate inputs from rivers. They proposed that this process could account for the "missing billion metric tons of carbon" in global CO_2 budgets. Their hypotheses cannot be confirmed be-

cause the productivity increase over the continental marginal seas is still small when compared with total primary productivity. The excess organic carbon production due to nutrient input is estimated at only 3% of gross primary productivity. Furthermore, much of the unused shelf primary productivity is not available for export or deposition but is remineralized on the shelf instead (Berner 1992; Kempe and Pegler 1991; Biscaye et al. 1994). The results of the one Shelf Edge Exchange Processes Study (SEEP; Rowe et al. 1996) indeed raised the question: "Do continental shelves export organic matter?" Perhaps, in response, Bauer and Druffel (1998) suggested that dissolved organic carbon and particulate organic carbon inputs from ocean margins to the open ocean interior may be more than one order of magnitude greater than inputs of recently produced organic matter derived from the open surface ocean.

At present, it is not clear how much of this excess organic carbon is simply reoxidized and how much is permanently sequestered by export to the deep oceans or in sediments on the shelves and shallow seas. Because of the limited surface area, a burial rate significantly exceeding 0.5 Gt C yr^{-1} is not very likely, as this would require that all coastal seas be on average more than 50 μatm undersaturated in pCO_2 annually, in order to supply carbon from the atmosphere. Even though such undersaturations have been documented, as in the North Sea and the East China Sea (ECS) for example, (Kempe and Pegler 1991; Chen and Wang 1999), it is not certain to what extent these measurements are representative of all coastal oceans. For instance, Holligan and Reiners (1992) estimated a net flux of approximately 0.4 Gt C yr^{-1} to the atmosphere from the coastal oceans because of supersaturation. Ver et al. (1999) also gave a sea-to-air flux of 0.1 Gt C yr^{-1} as of 2000.

To sum up, based on the above considerations, the role of the coastal oceans has not been thoroughly, let alone accurately, assessed. In order to determine the contribution of continental margins and seas to CO_2 sequestration and the horizontal flux of carbon, nitrogen and phosphorus across the ocean-continental margin boundary, the JGOFS/LOICZ Continental Margins Task Team (CMTT) was established (Chen et al. 1994). The specific objectives are to:

i identify relevant and appropriate data sets from continental margin studies and investigate their applicability to IGBP projects;
ii develop a conceptual framework so as to integrate continental margin carbon, nitrogen and phosphorus fluxes and to assess the influence of anthropogenic factors on the fluxes;
iii quantify, as best possible, the vertical and horizontal carbon, nitrogen and phosphorus fluxes in different types of continental margins, such as: (*a*) eastern boundary currents, (*b*) western boundary currents, (*c*) marginal seas, (*d*) polar margins, and (*e*) tropical coasts;
iv establish an overall synthesis and assessment of carbon, nitrogen and phosphorus fluxes on and across continental margins to feed into the IGBP program; and
v determine major gaps and uncertainties in the current understanding of continental margin carbon, nitrogen and phosphorus fluxes and recommend a priority of needs for further observational and modeling endeavors.

Selected national and international projects are identified in Fig. 3.1. General descriptions of the continental margins and marginal seas are given in Appendix 3.1.

The first CMTT effort to study cross-shelf exchanges and regionalization was aimed at differentiating between systems where budgets for C, N, P and water already exist, or at least are close to completion. It should be noted that some of these systems fall at least partially outside the definition of 'continental margins'. The CMTT recognized that the goal of obtaining a budget for each and every system in the world is unrealistic. To compensate for this, however, key shelf characteristics have been identified and the systems have been categorized into two broad groups, namely the recycling and export systems based on specific defining characteristics (Table 3.1). It has also been recognized that in a number of regions there is fairly distinct continuum between the two extremes. For example, some important systems (notably the North Sea and the ECS) may function like recycling systems towards their landward side and like export systems towards their seaward side.

Water exchange time is perhaps the single defining difference between 'recycling' and 'export' systems with respect to CNP budgets. The recycling system is frequently influenced and often dominated by rivers, whereas the export system is frequently governed by the oceans. JGOFS (1997) has considered some of the features that control exchange time, and these include:

- shelf width, depth and shelf-edge depth: where a narrow width and deep shelf break suggest short exchange time;
- long-shore relative to cross-shelf scales: when long-shore transport is larger than the cross-shelf transport, the retention of material on the shelf is favored;
- river input: large rivers discharge beyond the shelf-break, while small rivers discharge onto the shelf, affecting fresh-water buoyancy control. If the river flow is larger than 10% of the shelf volume, the buoyancy effect is significant;
- winds and orientation to the coast: this induces entrainment, circulation, upwelling or downwelling cycles;
- insolation and heat balance: this affects stratification, making the system one- or two-layered; and
- retention time: whether it is less than or greater than one month seems to be significant in the balance between 'recycling' or 'export' system processes.

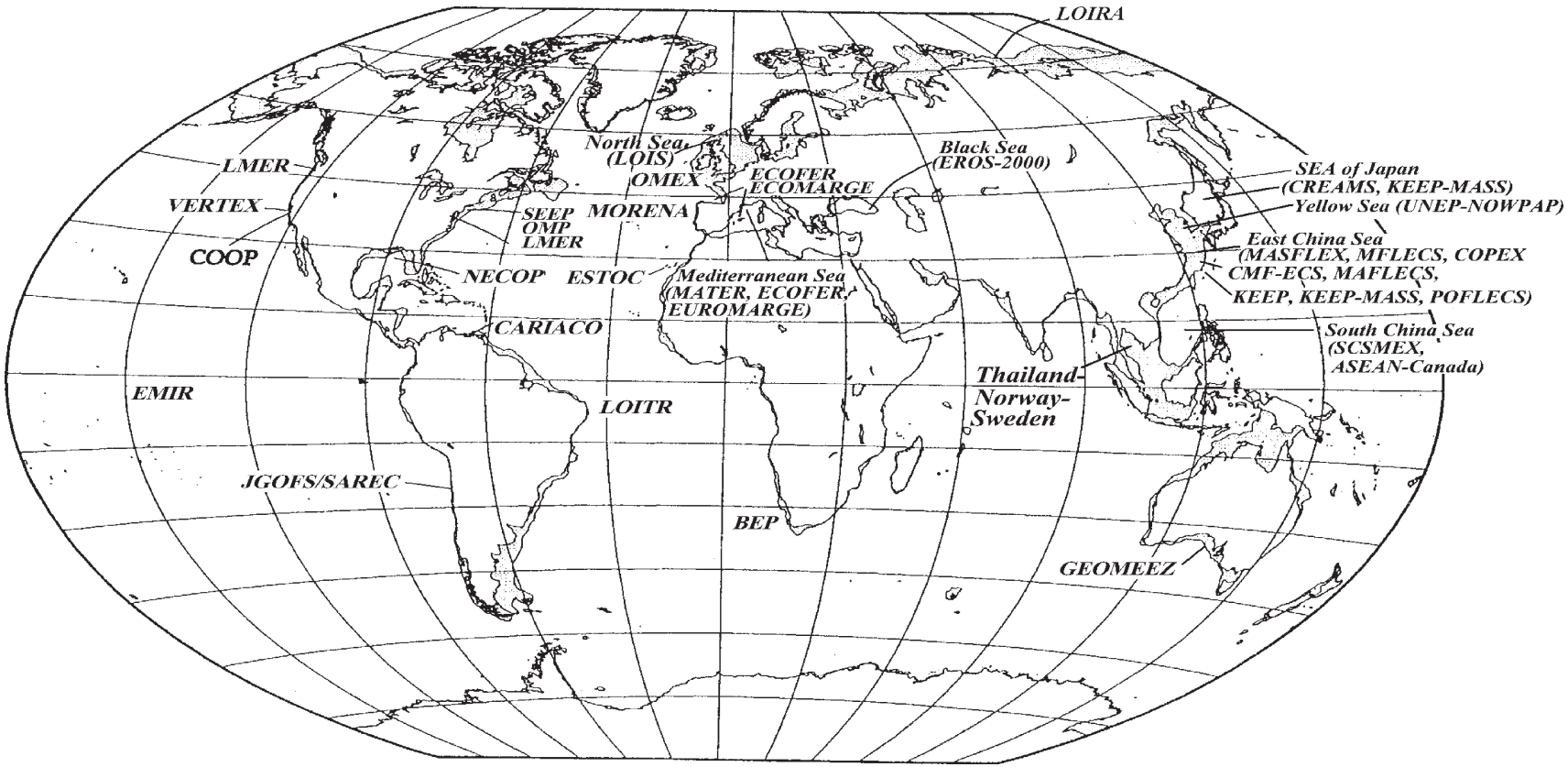

Fig. 3.1. Map of continental margins. Stippled areas represent the continental shelves with depths less than 200 m. Selected programs for continental margin studies, both completed and ongoing, are shown. The acronyms are as follows: *BEP* (Benguela Ecology Programme); *CARIACO* (Carbon Retention In a Colored Ocean); *CMF-ECS* (Continental Margin Flux-East China Sea); *COPEX* (The Coastal Ocean Processes Experiment of the East China Sea); *COOP* (Coastal Ocean Processes); *CREAMS* (The Circulation Research Experiment in Asian Marginal Sea); *ECOFER* (Ecosysteme du canyon du cap Ferret program); *ECOMARGE* (Ecosystems de Marge); *EMIR* (Exportation de Carbon sur une Marge Insulaire Recifale); *EROS-2000* (European River-Ocean System); *ESTOC* (European Station for Time-Series on the Ocean, Canary Islands); *GEOMEEZ* (Marine Geolological and Oceanographic computer model for Management of Australia's EEZ); *JGOFS/SAREC* (Eastern Boundary Current Programme); *KEEP* (Kuroshio Edge Exchange Processes); *KEEP-MASS* (Kuroshio Edge Exchange Processes-Marginal Seas Studies); *LMER* (Land Margin Ecosystem Research); *LOIRA* (Land/Ocean Interactions in the Russian Arctic); *LOISE* (Land Ocean Interaction Study); *LOITRO* (Land-Ocean Interaction in Tropical Regions); *MAFLECS* (Marginal Flux in the East China Sea); *MASFLEX* (The Marginal Sea Flux Experiment); *MATER* (Mass Transfer and Ecosystem Response); *MFLECS* (The Margin Flux in the East China Sea Program); *MORENA* (Multidisciplinary Oceanographic Research in the Eastern Boundary of the North Atlantic); *NECOP* (Nutrient Enhanced Coastal Ocean Productivity); *OMEX* (The Ocean Margin Exchange); *OMP* (US Ocean Margins Programme); *POFLECS* (The Key Processes of Ocean Fluxes in the East China Sea); *SEEP* (Shelf Edge Exchange Processes); *UNEP-NOWPAP* (The United Nations Environment Program – Northern Western Pacific Area Protection); *VERTEX* (Vertical Transport and Exchange)

Table 3.1
Comparisons between systems dominated by recycling systems and systems dominated by material export (modified from JGOFS 1997)

River dominated, recycling systems	Ocean dominated, export systems
Biologically mediated; Tidal, geostrophic circulation; Benthic bioturbation	Physically forced; Ekman shelf-edge baroclinic upwelling; Boundary currents; Can be forced by high river input – especially rivers with shelf-edge deltas
Broad shelves (>50 km)	Narrow shelves (<50 km)
Forcing, responses on seasonal time scales	Forcing, responses episodic
Long water exchange time (≫1 month)	Short water exchange time (≪1 month)
May have $(p - r) = +$ (autotrophic) or – (heterotrophic), but generally near 1.0	If upwelling dominated or dominated by rivers with high inorganic nutrients, $(p - r) > 0$ (autotrophic); if dominated by sediment-laden rivers, $(p - r) < 0$ (heterotrophic)
Examples	Examples
East China Sea, North Sea, Baltic, Sea of Japan, Sea of Okhotsk, South China Sea, NW Atlantic, Great Barrier Reef, Barents Sea	Western Boundary Currents of the Americas and Africa, and Amazon, Mackenzie, and Mississippi Rivers

3.2 Recycling Systems

Recycling systems are those with wide shelves and a relatively long residence time. Those with large freshwater input have a strong buoyancy effect which, in combination with wind stress and tidal mixing, results in strong upwelling and vertical mixing. Because of the external input of nutrients, the shelves tend to be autotrophic, i.e., biological production exceeds respiration. Small rivers, however, trap sediments mainly in bays and estuaries where turbidity hinders primary production. In such a case, the respiration of organic matter associated with these sediments tends to push the systems towards heterotrophy; in other words, the respiration of organic matter exceeds production.

The East China Sea (ECS), the Atlantic Bight and the North Sea are the most studied recycling margins in the world. Although still far from being able to construct a fully balanced carbon model for these regions, many important fluxes are known. For instance, it was found that the organic carbon in the North Sea turns over every 1.3 days on average, which is very quick indeed. As a result, only less than 1% of the net primary production reaches the bottom (Kempe 1995). It is particularly important to learn that the North Sea is, on average, a net sink for atmospheric CO_2. At some places, the pCO_2 drops below 100 ppmv due to the intensive spring phytoplankton bloom along the Danish-German-Dutch coast. The ECS is also undersaturated with respect to CO_2 in all seasons.

Since the ECS has the most detailed budgets available, it is discussed in greater detail. The Gulf of Bohai and the Yellow and East China Seas have a total area of 1.15×10^6 km^2, about 0.9×10^6 km^2 of which is the continental shelf, one of the largest in the world. Compared with other oceans, it is also one of the most productive areas. Two of the largest rivers in the world, the Yangtze River (Changjiang) and the Yellow River (Huanghe), empty onto the shelf with large, ever increasing nutrient and carbon input.

The Kuroshio flows northeastwardly along the eastern margin of the continental shelf. Subsurface waters, even the Kuroshio Intermediate Water, contribute up to 30% of the onshore water transport due to the upwelling and cross-shelf mixing (Chen et al. 1995b; Chen 1996). A similar situation is found in the South Atlantic Bight where the Antarctic Intermediate Water contributes 20–25% of the water on the shelf (Kashgarian and Tanaka 1991). Though the major currents are parallel to the isobath, the surface water on the shelf has a net transport offshore because of net precipitation and the fresh water discharge from rivers, while subsurface Kuroshio waters have net onshore transport. Added to this is an input through the Taiwan Strait.

The water and salt balances for the shelf at a steady state have been used to calculate the fluxes of water. It is also possible to use a simple box model for nutrient budgets and to calculate the offshore transport of organic matter in the suspended sediments from the ECS shelf. It is clear from looking at the P fluxes in Fig. 3.2 that the rivers only play a very minor role in that they contribute a mere 7% of the total input. The major contributors of phosphorus in the inorganic form are the subsurface Kuroshio waters. Most of the incoming inorganic P is converted to the organic form which is either deposited on the shelf or transported offshore as particulate. It is to be noted even in the presence of any man-made eutrophication or increased biomass production due to the increased anthropogenic input of phosphorus, the increase is probably very small. On the other hand, enhanced or damped upwelling due to changes in climatic forcing would bring about a large change in the biological pump. There is evidence to show that aeolian

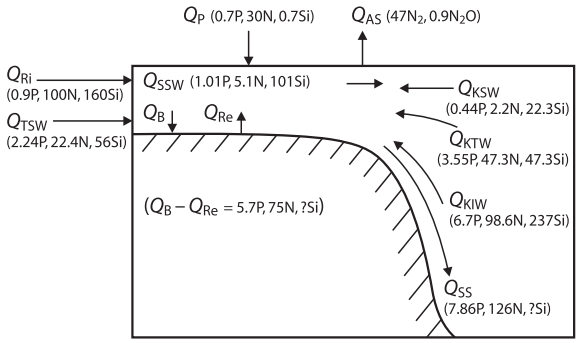

Fig. 3.2. Schematic diagram for the annual nutrient budgets (numbers in 10^9 mol yr^{-1}) in the East China Sea where *Q* is the flux, subscripts *Ri*, *P*, *TSW*, *KSW*, *KTW*, *KIW* and *SSW* denote river input, precipitation, Taiwan Strait Water, Kuroshio Surface Water, Kuroshio Tropical Water, Kuroshio Intermediate Water and shelf surface water, respectively; *P* denotes phosphorus, *N* denotes nitrogen, *Si* denotes silicate, *Re* denotes the release from sediments, *AS* denotes the air-sea exchange, *B* denotes the nutrients buried, and *SS* denotes suspended sediments transported offshore

fluxes may have increased during the past few hundred years (Chen et al. 2001a). Anthropogenic iron input or enhanced aeolion input of loess, being rich in iron and phosphorus, may increase primary productivity in the high nutrient-low chlorophyll regions or in waters where molecular-nitrogen-fixing, blue-green algae (*cyanobacteria*) bloom. The nitrogen-fixing *Trichodesmium* is abundant in the ECS (Chen et al. 1996b), and nitrogen fixation may account for 20% of the new N input in this upwelling zone (Liu et al. 1996).

The nitrogen budget (Fig. 3.2) is more complicated since denitrification converts nitrate to NH_3, N_2O and N_2 with the latter two degassing at the air-sea interface. On the other hand, nitrogen fixation by plankton utilizes N_2. The input from rivers is still smaller than that from the incoming water masses, but the difference is not as sharp as for phosphorus. Not much nitrogen leaves the ECS with the outflowing seawater. Instead, the largest sinks are the net burial on the shelf, the offshore transport in the form of sediments and that in the form of degassing as N_2. The box model gives the offshore N transport as 0.38 ±0.19 mmol N $m^{-2}\,d^{-1}$, and the net denitrification rate as equivalent to 0.103 ±0.050 mol N $m^{-2}\,yr^{-1}$. Seitzinger and Giblin (1996) gave an average denitrification rate of 0.252 mol N $m^{-2}\,yr^{-1}$ for continental shelf sediments in the North Atlantic.

After the completion of the SEEP project, the question as to the sources of N for the shelf to be able to support the measured primary production was considered unresolved. Biscaye et al. (1994) found it difficult to explain the flux of nitrate onto the shelf without imposing an export of flux of water. The above calculations, made by the present authors, however, indicate that the upwelling of nutrient-rich subsurface water would balance the export of nutrient-depleted surface waters and sediments.

It is important to keep in mind that for the ECS, the riverine N/P ratio is 111, a value much higher than the Redfield N/P ratio of 16 for phytoplankton. This makes P more limiting than N in terms of net organic production in the estuaries because the maximum amount of new organic matter that could be produced with land-derived inorganic nutrients is determined by the major nutrients which run out first. The total seawater flux of N and P to the ECS, however, has a ratio of 21 which is much closer to the Redfield ratio. As a result, the phosphorus shortage in the ECS, as a whole, is not as dramatic owing to the large influx from the subsurface Kuroshio waters. Changes in the nutrient structure of small riverine inputs are also not expected to affect the stoichiometric nutrient balance of the phytoplankton ecosystem in the ECS. The Si budget is also given in Fig. 3.2. The riverine input is still smaller than the oceanic input, but the budget is not balanced because it has yet to be determined how to estimate the Q_B, Q_{Re} and Q_{ss} values for Si.

The upwelled Kuroshio Intermediate Water (KIW) actually originates in the South China Sea (SCS) and is high in nutrients, which it contributes more generously to the shelf than do the much smaller riverine fluxes. Furthermore, the PO_4 flux from the Changjiang River can only be identified in the estuary. The NO_3 flux extends farther but can still only be identified in the Yangtze River Plume. This suggests that productivity in much of the ECS is mainly influenced by the upwelled subsurface Kuroshio waters. Any potential change in the upwelling rate would, therefore, have a much larger effect than would a change in the nutrient input from the rivers (Chen and Wang 1999). For instance, cutting back the Yangtze River outflow by 10% would reduce the cross-shelf water exchange by roughly 9%. The nutrient supply would then be reduced by that much as well. This means that new production, primary production and the fish catch in the ECS would be proportionately reduced as well. On the other hand, the passage of typhoons, which enhances vertical mixing, freshwater inflow and the resuspension of bottom sediments are three factors causing the shelf ecosystems to be more productive (Shiah et al. 2000a).

Though it is recognized that the feedback mechanisms are probably complicated, it is nevertheless worth noting that after an El Niño event, the freshwater outflow and the fish catch in the ECS are both reduced. For instance, after the strong 1982–1983 El Niño event, the yield of a major commercial fish, gunther (*Navodon Sepient*), was reduced by over 60% when coastal rainfall was reduced by 50%. This is in agreement with the above estimate (Chen 2000).

The major rivers bring in carbon in the form of dissolved inorganic carbon (DIC), dissolved organic carbon (DOC), particulate inorganic carbon (PIC) and particulate organic carbon (POC). A mass-balance calculation (Table 3.2) gives the downslope contemporary particulate car-

Table 3.2. The fate of organic carbon produced by the primary production on the East China Sea Shelf (mmol m^{-2} of shelf area per year)

In	(mmol m^{-2} yr^{-1})
Primary production	13322
Net POC influx	652
Total in	13974
Out	**(mmol m^{-2} yr^{-1})**
Denitrification	132
Mn reduction	10
Fe reduction	70
Sulfate reduction	730
CH_4 reduction	7
POC deposit on shelf	667
POC transported offshore	772
Net DOC export	1144
Total out	3531
Aerobic regeneration	10443

bon transport rate as 7.72 ±3.9 mmol C m^{-2} d^{-1} of which 27% is organic (Fig. 3.3). The offshelf transport of POC is only 5.7% of the average primary productivity. It should be mentioned that bacteria production in the ECS also constitutes an important part of the carbon cycle. In terms of carbon turnover, bacterial production is on average about 20% of the primary production (F. K. Shiah, pers. comm.). Since the growth efficiency of bacteria is rather low (approximately 30%), the organic carbon consumed during bacterial growth is much greater than that indicated by the bacteria production. In other words, although it is not known how much of the organic carbon is labile, at least three times more organic carbon may be consumed by bacteria in the ECS.

Bacteria production shows considerable spatial and temporal variations (Kemp 1994; Shiah et al. 1999, 2000b). The inner shelf enjoys a rich supply of organic carbon from river runoff, sediment resuspension and in situ production. In cold seasons, namely winter and spring, bacteria production is predominantly temperature-dependent in the inner and mid-shelves, where water temperature is low. In warm seasons, the inner and mid-shelves are not thermally stressed for bacteria nor substrate-limited, but bacteria production does not rise above a certain limit, perhaps due to enhanced grazing. Since the bacteria production is limited by temperature in cold seasons and reaches a plateau in warm seasons, a significant fraction of the CO_2 uptake by phytoplankton seems to escape bacterial decomposition throughout the year. In the outer shelf, where the intruding Kuroshio Surface Water keeps the temperature high and nutrient-depleted throughout the year, bacteria production is substrate-limited. The optimal thermal condition for bacterial growth in the outer shelf

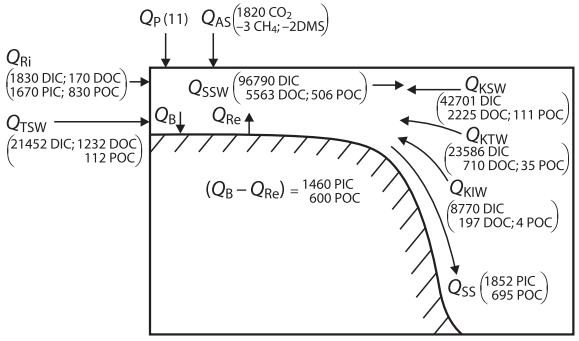

Fig. 3.3. Schematic diagram for the annual carbon budget in the East China Sea (numbers in 10^9 mol C yr^{-1}) (taken from Chen and Wang 1999). Subscripts as in Fig 3.2

results in the rapid oxidation of organic carbon. Little fixed carbon from primary production may escape bacterial degradation, except in areas with strong shelf break upwelling or subsurface water intrusion. A seaward export of organic carbon has been observed in these areas (Liu et al. 1995; Hung et al. 2000).

Continental shelf waters are generally high in total alkalinity (TA) because of river discharge and in situ generation due to the oxidation of organic material. If we formulate the particulate organic materials as $(CH_2O)_{106}(NH_3)_{16}H_3PO_4$, then the aerobic oxidation of organic material in seawater by oxygen can be represented by the Eq. 3.1 which reduces TA by 17 moles for the regeneration of 106 moles of organic carbon. (Chen et al. 1982). Accordingly,

$$(CH_2O)_{106}(NH_3)_{16}(H_3PO_4) + 138O_2 \longrightarrow 106CO_2 + 122H_2O + 16HNO_3 + H_3PO_4 \qquad (3.1)$$

When the dissolved oxygen is exhausted, the system turns to the next most abundant source for the oxidation of organic material, NO_3^-. Afterwards, the manganese, iron, sulfate and methane reductions occur.

Based on the water fluxes after taking into account the above reactions, the alkalinity budget is given in Table 3.3 and Fig. 3.4. The order of 3.9 ±3.9 mmol m^{-2} d^{-1} of alkalinity is generated on the shelf, mainly the the result of iron and sulfate reductions (Chen and Wang 1999).

The ECS has a net export of 64 ±32 mg C m^{-2} d^{-1} organic carbon offshelf, which is the equivalent of 15% of primary productivity. Results from the SEEP-II program on the eastern US continental shelf also indicate that most of the biogenic particulate matter is remineralized over the shelf. Only a small proportion (<5%) is exported to the adjacent slope (Biscaye et al. 1994). In the North Sea, only 1.5% of the primary production is accumulated on the shelf as organic carbon, and 2–3% of the primary production is exported over the margin (de Haas et al. 1997). The ECOMARGE and OMEX projects have also led to similar conclusions (Monaco et al. 1990; Antia et al. 1999).

Table 3.3.
Processes affecting alkalinity on the East China Sea Shelf (per m^2 of shelf area per year)

Process	Source	Quantity (mmol in TA)
Input	Ri	2 444 plus 3 711 from PIC
	KSW	56 204
	KTW	30 138
	KIW	10 173
	TSW	27 808
	Aerosol	24 from PIC
Output	SSW	124 214
	Net burial	3 246 from PIC
	S.S.	4 117 from PIC
Water column production	New production	310
	New production that supports anaerobic processes	152
Anaerobic reduction in sediments	Denitrification	104
	Mn reduction	42
	Fe reduction	559
	Sulfate reduction	723

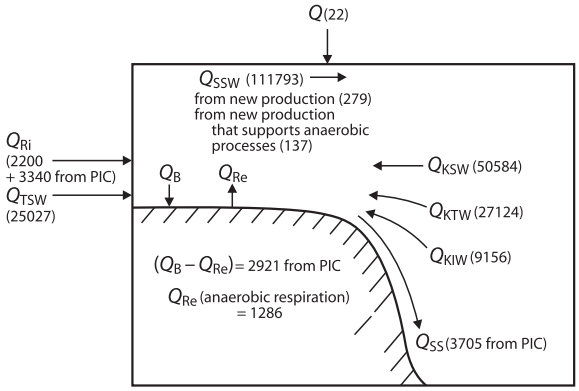

Fig. 3.4. Schematic diagram for the annual alkalinity budget (numbers in 10^9 mol yr^{-1}) in the East China Sea (taken from Chen and Wang 1999). Subscripts as in Fig 3.2

It is also not yet possible to directly measure the offshore transport of particulate matter due to large spatial and temporal variabilities. Again mass-balance calculations reveal an offshore flux at $7.9 \pm 4 \times 10^9$ mol yr^{-1} of particulate organic phosphorus for the ECS. Independent calculations give a downslope flux of contemporary particulate organic and inorganic carbon at 2.12 ± 1.1 and 5.64 ± 2.8 mmol m^{-2} d^{-1}, respectively. At least 20% of this is old, refractory material which accounts for the relatively old ^{14}C ages obtained from core tops (up to 8 000 years old). A similar situation has been found elsewhere (Jahnke and Shimmield 1995).

The ECS shelf is probably saturated with the anthropogenic, excess CO_2. Between the shelf break and Ryukyu Island is a deep trench. The hydrography is such that there is upwelling toward the west, bringing older deep waters upward. As a result, excess CO_2 penetrates to only about 600 m. The entire ECS contained 0.07 (±0.02) Gt C excess carbon in 1992. Since the waters on the ECS shelf are highly supersaturated with respect to calcite and aragonite, sediments on the ECS shelf are not expected to neutralize excess CO_2 in the coming century. The high productivity, nevertheless, causes a large portion of the ECS inner and mid-shelf waters to be undersaturated with respect to CO_2 near the surface all year round. As a result, the flux of CO_2 into the ECS is large. The outer shelf and the Kuroshio region (east of 126° E) are depleted in PO_4 and the surface water pCO_2 is near saturation.

3.3 Export Systems

Export systems are continental margins with effective processes to export materials to the open ocean. For practical reasons, all continental margins with narrow shelves (less than 100 km in width) are considered as export systems. In continental margins with wide shelves, 200 m isobaths may be used to define the outer boundaries of the margins (Gordon et al. 1996). In coastal zones with very narrow shelves, highly active biogeochemical processes are not confined to the shelves but occur in the boundary current systems, which are distinct from the adjacent open ocean and often poorly represented by the coarsely gridded ocean models or databases. Therefore, we need to treat the coastal zone beyond the boundary of the shelf as a part of the continental margin.

Among the 85 continental margins listed in Appendix 3.1, 30 are narrow margins. Many of them are bordered by eastern boundary currents. In fact, most of the eastern coast of the Pacific Ocean, from Vancouver Island to the Central Chilean Shelf, belongs to this category. So does most of the eastern coast of the Atlantic Ocean from the western Iberian Coast to Cape Town. Many of the eastern boundary current systems are characterized by coastal upwelling. Another important coastal upwelling system with narrow shelves is the northwestern coast of the Arabian Sea driven by the monsoons. Essentially all major coastal upwelling systems are export systems.

There are also other types of export systems where the river delta systems extend near the shelf edge; for

example, the Mississippi Delta, the East African Coast, the eastern coast of the Bay of Bengal, the southeastern coast of Australia, the northern coast of New Guinea and the eastern coast of Brazil. Yet another type of export system includes many tropical watersheds that discharge a high volume of water and sediments to the ocean due to frequent floods caused by torrential rains. More than half of the total runoff and land-derived sediments are discharged to the oceans from tropical coasts, especially the Indo-Pacific Archipelago (Nittrouer et al. 1995). The narrow shelves and weak Coriolis force favor cross shelf transport of sediments, which may carry a significant amount of carbon, to the deep ocean. This type of continental margin is especially vulnerable to human perturbation, which causes up to ten fold increase of sediment production rate in a typical Oceania watershed (Kao and Liu 1996). The extra sediment transport to the ocean may result in non-negligible change in the carbon cycle, but the available information is not sufficient for quantitative estimation of the associated carbon fluxes.

The most important biogeochemical activities within the export systems are associated with upwelling in the coastal provinces. Therefore, we devote most of this section to describe these systems. One way to define these margins is to use the Rossby deformation radius as the width of the coast zone (Barber and Smith 1981; Hall et al. 1996). Here we adopt the coastal provinces defined by Longhurst (1998) to represent these continental margins. The Coastal Domain is further defined as the system bounded by the continental shelf and the coastline on the landward side and by the vertical surface at the edge of the coastal provinces and the horizontal surface at 200 m depth in regions beyond the shelf.

3.4 Coastal Upwelling Systems

Coastal upwelling is mainly induced by the along shore wind, which drives water across the upwelling front, producing surface divergence near the coast and convergence offshore (Csanady 1990). Upwelling brings subsurface nutrient-rich water to the surface, where it fuels blooming of phytoplankton and enhances primary productivity (Barber and Smith 1981). The upwelling condition has a direct impact upon new production (Kudela and Chavez 2000) and also the air-sea exchange of CO_2 (Torres et al. 1999), which are crucial to the understanding of the marine carbon cycle.

Before the onset of upwelling, the coastal water is usually stratified and low in nutrient. As the wind intensifies, upwelling and offshore surface Ekman transport occurs (Brink 1998). The mass balance in the upper water column is maintained by an indirect circulation cell with upward advection of the subsurface water and the subduction of surface water. The coastal water becomes enriched in nutrients, which is often separated from the warm nutrient-poor offshore water by an upwelling front. When the wind is uniform and sustained, the front tends to be parallel to the coast. When the wind weakens, the front tends to intensify and become unstable. The instability of the current may cause meandering of the along shore flow and produce filaments of upwelled water (Fig. 3.5). These filaments have strong influence over the biological activities and offshore transport of organic carbon (Brink and Cowles 1991).

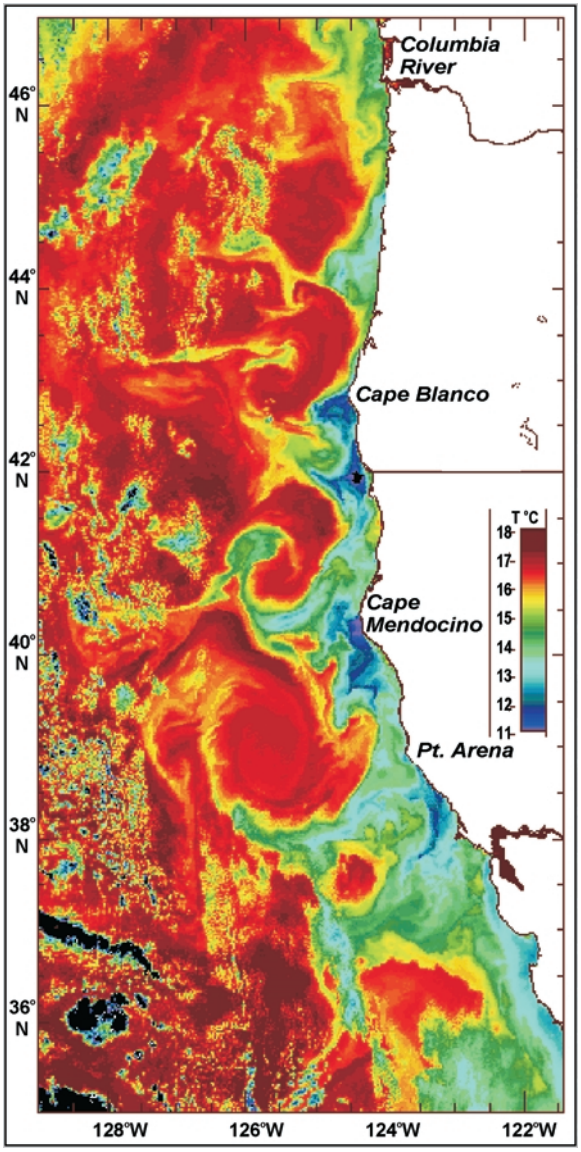

Fig. 3.5. Sea surface temperature along the coast of Oregon and northern California, USA, on September 5, 1994 as measured by satellite-borne AVHRR of NOAA (courtesy of Oregon State University). Upwelling filaments were manifested as offshore-shooting tongues of low temperature waters, which were usually associated with high concentrations of Chl *a*

During intense upwelling, primary production may reach as high as 10 g C m^{-2} d^{-1} (Barber and Smith 1981). However, the spatial and temporal variability is rather high due to the very dynamic nature of the upwelling system. Nitrogen is often the limiting nutrient in upwelling ecosystems due to their juxtaposition with denitrifying zones (e.g., Codispoti and Christensen 1985). Nevertheless, phosphate limiting could also occur in some of the upwelling systems, where the source waters have high N/P ratio, such as in the North Atlantic (Fanning 1992, Michaels et al. 2000). The rich supply of nutrients enhances phytoplankton growth, which in turn may sustain a considerable biomass increase at the higher trophic levels. What fraction of the new production may go into fish harvest is a question of interest.

3.5 California Current System

The west coast of North America from Vancouver Island to the tip of Baja California is bordered by the California Current System (CCS). Major currents in the system include the California Current, the Davison Current and the California Undercurrent (Hickey 1998). The California Current is an equatorward surface current. In winter, there is a poleward surface flow shoreward of the California Current along the coastline north of Southern California Bight, which is the major bend in the otherwise pretty straight coastline. The undercurrent is the poleward return flow. Upwelling is strongest in summer at most places along the northern half of the coast. In the Southern California Bight, upwelling is strongest in winter and early spring. Coastal upwelling, subduction and filaments (Fig. 3.5) make the coastal zone a highly variable and dynamic zone (Brink and Cowles 1991). The primary production and new production are closely related to the upwelling and other dynamic processes in the coastal transition zone (Chavez et al. 1991). Estimates of the transport across the filaments are in the range of 1.5–3.6 Sv (Korso and Huyer 1986)

In the CCS, the sea surface Chl *a* concentrations shows a summer maximum in most locations near the coast (Thomas et al. 1994). The strongest seasonal variation in the CCS within 100 km of the coast occurs at 34–45° N and at 24–29° N. The maximum Chl *a* concentration exceeds 3.0 mg m^{-3} in May–June. The seasonal variation is weaker in the Southern California Bight. In winter, the Chl *a* concentrations in the offshore extension patches reach 0.5–1 mg m^{-3}. The primary production in the CCS was estimated to be 740–1 240 mg C m^{-2} d^{-1} based on shipboard observations (Chavez et al. 1991). The estimation based on CZCS pigment concentrations yields a mean PP of 1 060 mg C m^{-2} d^{-1} (Longhurst et al. 1995).

Notable inter-annual variation is coupled with El Niño conditions (Fig. 3.6). During ENSO events, the trade wind is weakened in the western Pacific. The Chl *a* in the CCS is reduced during El Niño events. The primary production seems to be less affected by the ENSO condition probably due to a more efficient recycling of nutrients, while the new production is much reduced as the upwelling flux of nutrients is reduced due to the intrusion of nutrient-poor water in the source layer of the upwelling water (Kudela and Chavez 2000).

The pCO_2 off Oregon coast varied in a wide range from 150 to 690 µatm in summer, which is attributable to large spatial variation of upwelling intensity (van

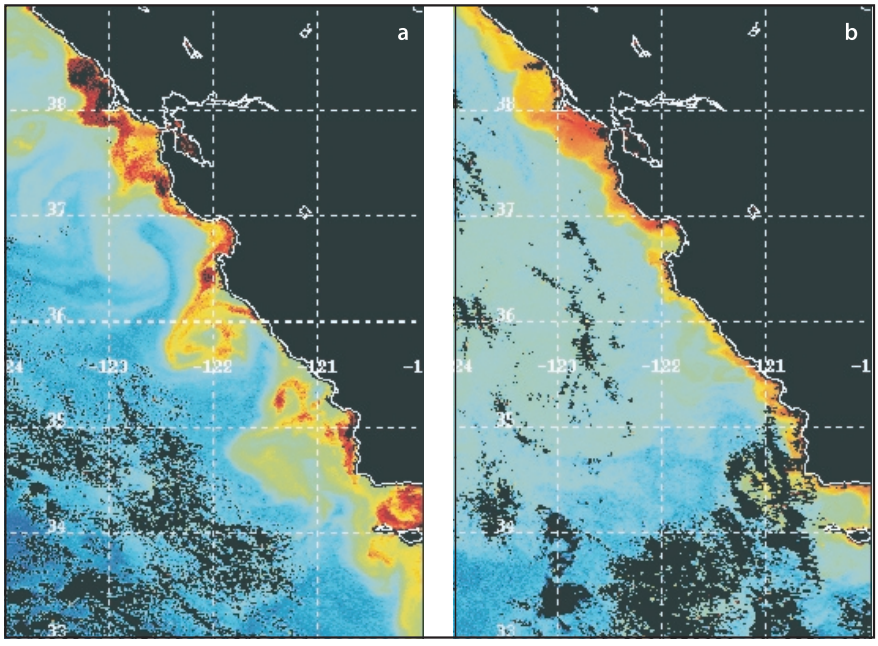

Fig. 3.6.
Imagery of chlorophyll concentration (mg m^{-3}) derived from SeaWiFS data for the central California Current Coastal Province (courtesy of Monterey Bay Aquarium Research Institute, *http://www2.mbari.org/kura/seawifs_share/images/index.htm*). **a** February 9, 1998 during intense El Niño condition; **b** May 17, 1998, when the El Niño condition weakened

Geen et al. 2000). Although TCO_2 accounts for much of the large pCO_2 variation, the temperature and salinity effects may cause a 25% shift of pCO_2. The strong CO_2 uptake is associated with a coastal bloom of phytoplankton dominated by large diatoms (Chavez et al. 1991). Up to 200 mg C kg^{-1} of TCO_2 may be removed by the phytoplankton bloom. One important factor controlling phytoplankton growth and, thereby, pCO_2 in surface seawater is the availability of iron from contact of the upwelled water with the shelf sediments (Johnson et al. 1999). In spite of the active upwelling off California, the observed mean pCO_2 values at the sea surface along an onshore-offshore transect throughout the year in 1993 were below the atmospheric partial pressure of CO_2 in most cases (Friederich et al. 1995), suggesting that the CCS may not be a net source of CO_2.

The VERTEX experiment carried out a direct measurement of the export flux of particulate organic carbon from the euphotic zone off Point Sur, California (Martin et al. 1987). Because of the coupling between offshore advection and high primary production (Chavez et al. 1991), phytodetritus may be transported offshore advectively and settle to the deep water. The POC and PON fluxes depend on the primary production and decreases as a power function of depth (Pace et al. 1987):

$$F_{POC} = 3.523\, Z^{-0.734}\, PP \tag{3.2}$$

$$F_{PON} = 0.432\, Z^{-0.743}\, PP^{1.123} \tag{3.3}$$

where F is the flux in mg m^{-2} d^{-1}, Z is in units of metres and PP is primary production in the same unit as the flux. The observed POC fluxes were 42–85 g C m^{-2} yr^{-1} (Martin et al. 1987). The high POC flux near the continental margin is obviously related to the high upwelling-induced primary production (250~420 g C m^{-2} yr^{-1}). The f-ratio is about 0.17–0.2.

Denitrification occurs in both the water column and the sediments beneath the CCS. The annual mean flux of denitrification in the sediment column on the Washington Shelf has been estimated to be 0.18 mol N m^{-2} yr^{-1} from porewater profiles of nitrate (Christensen et al. 1987), but observations of N_2 evolution using benthic chamber suggest a mean flux almost twice as high as the previous estimate (Devol 1991). The difference is attributed to ammonia oxidation to N_2 during denitrification, which had been neglected in the previous estimation. Denitrification in the water column occurs only in the southern part of Baja California (Gruber and Sarmiento 1997) and within basins on the continental borderland off California (Liu and Kaplan 1982, 1989). The latter are much deeper than the upper water column addressed in this section and, therefore, excluded from consideration.

3.6 Humboldt Current System

The Peru-Chile Coast is bordered by the Humboldt Current System between 4° S and 45° S (Longhurst 1998). The upwelling system is determined by the presence of upwelling favorable winds and the pattern of coastal ocean circulation (Strub et al. 1998). The continental shelf along this coast is generally rather narrow and, in some areas practically non-existent. In many places, the shelf width is less than the Rossby radius of deformation, which depends on the Coriolis force, and therefore on latitude. It changes from about 270 km at 4° S, to 46 km at 24° S, and to about 29 km at 40° S (Chavez and Barber 1987).

The Humboldt Current System is the counterpart of the California Current System in the southern hemisphere. It is characterized by a generally equatorward flowing current, but the whole system is quite complex with interleaving currents and countercurrents, which may be separated into the coastal and the oceanic branches (Longhurst 1998). Upwelling favorable winds are seasonal, and coastal divergence and cyclonic wind-stress curl cause extensive upwelling from 4° S latitude to about 40° S (Thomas et al. 1994; Strub et al. 1998). Satellite images show upwelling occurs mainly along the Peruvian Coast from 5–15° S (Fig. 3.7) and the Chilean Coast from 25 to 40° S. The South Pacific high that drives the long-shore winds strongly affects the amount of nutrient upwelled (Strub et al. 1998). The strongest upwelling favorable winds are found during July–August (austral winter) off Peru and during December–January (austral spring and summer) off Chile (Thomas et al. 1994, Strub et al. 1998). It is noteworthy that poleward

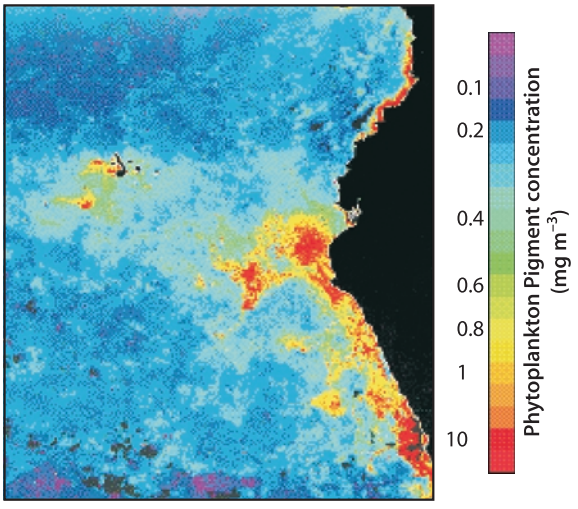

Fig. 3.7. The CZCS composite image of phytoplankton pigment concentration around the Peruvian upwelling centers covering the periods from 16–26 January, 1980 (modified, courtesy of NASA). The equatorward current brought the upwelled nutrient-laden water to the northwest

currents, as undercurrent over the shelf and countercurrent offshore, are dominant off Peru and can continue as far as middle latitudes off Chile. The dynamics responsible for such a feature is not clear, but the wind system and the shelf topography have been suggested to contribute to this special feature (Strub et al. 1998).

Very high concentrations of Chl *a* (10–20 mg Chl m^{-3}) associated with large size phytoplankton (>20 μm) have been observed during intense upwelling in the austral spring (Chavez 1995; Morales et al. 1996). Off Peru between 6 and 17° S, there is a minimum in Chl *a* in fall. Between 17 and 40° S, maximum Chl *a* values occur in austral winter (Thomas et al. 1994). North of 20° S, the maximum Chl concentration reaches 1.5 mg m^{-3} or higher during the austral spring, summer and fall. The primary production for the Peruvian upwelling region was estimated to be as high as 3 200 mg C m^{-2} d^{-1} (Chavez et al. 1989). The estimated *f*-ratio ranges between 0.21 and 0.75 (Minas et al. 1986; Chavez et al. 1989). The upper limit represents the potential export fraction under strong upwelling conditions. The annual average primary production is estimated to be 833 g C m^{-2} yr^{-1} for the coastal zone (Chavez and Barber 1987), but the mean PP drops to 270 g C m^{-2} yr^{-1} for the broad Humboldt Current System (Longhurst et al. 1995). Under El Niño conditions, the sinking flux of foraminifera off the Chilean coast decreased by about 30%, but the flux is still higher than those in other upwelling systems under normal conditions (Marchant et al. 1998). This implies that the export production in this upwelling system could be much higher than other upwelling systems, which is consistent with the fact that the South American fisheries are the most productive among all upwelling systems. Apparently the ecosystem performance is the result of intricate interplay among physical forcing, shelf width, bottom topography and biological responses (Walsh 1977), that is yet to be unveiled.

Very large fluctuations of air-sea CO_2 exchange fluxes have been observed around the upwelling center at 30.7° S off the Chilean coast in January (Torres et al. 1999). During the upwelling period, the surface pCO_2 reached as high as 900 μatm. The maximum outgasssing flux reached 25 mmol C m^{-2} d^{-1}, but there was still uptake of atmospheric CO_2 in the Tongoy Bay where the uptake flux was around –4 mg C m^{-2} d^{-1}. During the relaxation period, the maximum outgasssing flux at the upwelling center dropped to 3 mmol C m^{-2} d^{-1}, while the maximum uptake flux was enhanced slightly to –6 mg C m^{-2} d^{-1}.

Denitrification occurs in the suboxic water off Peru extending from 10° S to 25° S. The suboxic water in the coastal zone off Peru covers an area of 326×10^9 m^2. The average denitrification flux is 3.2 mol N m^{-2} yr^{-1} (Codispoti and Packard 1980). Denitrification in the surface sediments off Peru reaches as high as 1.4 mol N m^{-2} yr^{-1} (Codispoti and Packard 1980), which is apparently caused by the high flux of sinking organic particles.

3.7 Benguela Current System

The Benguela Current System, which forms the eastern limb of the South Atlantic gyre circulation, consists of a series of coastal jets and wind-induced upwelling cells (Shillington 1998). There are four groups of major coastal upwelling centers (Longhurst 1998). In northern and central Namibia, upwelling is strong throughout the year with the highest intensity in the austral winter from June to August. From Luderritz to Walvis Bay, upwelling is most vigorous with intensity peaking in the austral spring (Nelson and Hutchings 1983). In the Hondeklip Bay, maximum upwelling occurs from October to December. In the southern part around Cape Columbine and Cape peninsula, upwelling is largely restricted to the austral summer. The lateral output of the upwelled water is about 1.7 Sv (Shannon 1985). The upwelling water in the offshore region has a mean nitrate concentration around 19 μM and a mean N/P ratio (by atom) around 11 (Chapman and Shannon 1985).

No extensive suboxic water mass has been observed in the Atlantic Ocean (Deuser 1975). However, localized oxygen-deficient waters do exist on the Namibian Shelf around Walvis Bay in the Benguela Current System (Chapman and Shannon 1985). Oxygen concentration in the bottom water on the shelf may be reduced to less than 0.5 ml l^{-1} (Chapman and Shannon 1985). A secondary nitrite maximum often occurs in the bottom water, indicating denitrification in the suboxic bottom layer of the inner shelf (Calvert and Price 1971; Chapman and Shannon 1985). The low N/P ratio and the raised $\delta^{15}N$ values of nitrate (above 6.5‰, K. K. Liu unpublished data) in the upwelling water also indicate the occurrence of denitrification.

3.8 Monsoonal Upwelling Systems

The most famous monsoonal upwelling system is that along the northwest coast of the Arabian Sea (Longhurst 1998). Analogous to the Arabian Sea, the South China Sea also exhibits monsoon-driven upwelling off northwestern Luzon in winter (Shaw et al. 1996) and off the coast of central Vietnam in summer (Wu et al. 1999). Both areas have very narrow shelves. Satellite observations and model predictions suggest enhanced phytoplankton biomass in these upwelling areas, but little direct observations are available to assess the carbon fluxes reliably. Therefore, we focus on the Northwest Arabian Upwelling System below.

The African and the Arabian coasts of the Arabian Sea have very narrow shelves, usually less than 10 km in width (Longhurst 1998). The Arabian Sea experiences two monsoons every year. The more energetic south-

west monsoon blows from June to September, and the weaker northeast monsoon blows from December to February (Burkill 1999). During the SW monsoon, the wind maximum is the low level Findlater Jet that peaks in July as it blows along the Somali and Oman coast. Wind stress curl is anti-cyclonic seaward of the jet and cyclonic landward of the jet. The Somali Current occurs shortly following the onset of the jet and upwelling is induced in the northwestern Arabian Sea.

The total volume transport of coastal upwelling in the Arabian Sea is estimated to be 10–15 Sv (Chavez and Toggweiler 1995). The mean nitrate concentration in the source water is probably around 10 μM (Chavez and Toggweiler 1995). The observed N/P ratio is 12.2 (Woodward et al. 1999). In nearshore waters a mixed community of diatoms and *Synechococcus* dominate during the southwest monsoon (Tarran et al. 1999). However, very high concentration of Chl *a* (13 mg m^{-3}) have been found associated with small size (0.2–2 μm) phytoplankton (Savidge and Gilpin 1999), which is quite different from the diatom dominated population in the coastal upwelling systems. Towards the late stage of the SW monsoon, the phytoplankton biomass may reach as high as 69 mg Chl m^{-2} and the production may reach 3 800 mg C m^{-2} d^{-1}.

The total organic carbon (TOC) concentration in the surface water varies between 60 and 100 μM, while the concentration variation in the subsurface water below 100 m is much reduced with a mean concentration around 45 μM (Hansell and Peltzer 1998). The TOC concentration drops abruptly just below the surface mixed layer. The TOC production probably accounts for 6–8% of the total primary production (Hansell and Peltzer 1998). Since a major fraction of the TOC is dissolved organic carbon (DOC), the distribution is probably controlled mostly by the DOC dynamics.

The Arabian Sea has been observed as a persistent CO_2 source to the atmosphere (Fig. 3.8) with the highest fluxes during southwest monsoon in summer (Goyet et al. 1998). The strongest CO_2 outgassing occurs in the coastal zone along the Arabian Peninsula. The monthly mean of ΔpCO_2 in the coastal zone peaks in August (Fig. 3.8), but much higher local maximum up to 400 μatm has been reported (Kortzinger et al. 1997), indicating the high temporal and spatial variability. The outgassing flux of CO_2 shows a much stronger peak during the southwest monsoon than the corresponding ΔpCO_2 peak due to the wind enhanced gas transfer velocity. The estimated annual average of CO_2 outflux in the Arabian Sea is 0.46 mol C m^{-2} yr^{-1} (Goyet et al. 1998). The low N/P ratio in the upwelling water indicates denitrification in the Arabian Sea. The oxygen minimum zone extends from the northern coast of the Arabian Sea towards the central part of the basin (Wyrtki 1971). Along the northwest coastal zone of the Arabian Sea, suboxic condition occurs mainly in the northern and central Arabian Sea and around the northern tip of the Omani coast.

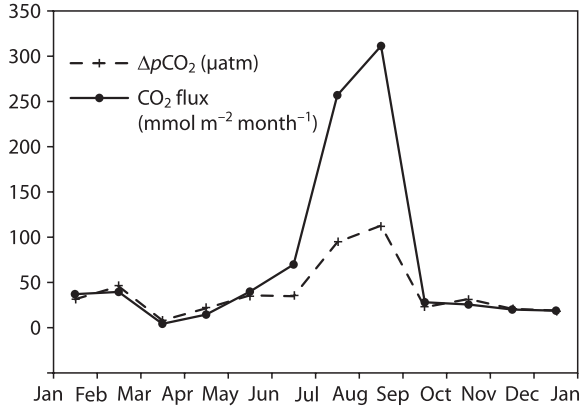

Fig. 3.8. The monthly mean values of ΔpCO_2 (μatm) and the flux of CO_2 (mmol m^{-2} $month^{-1}$) along the Arabian Peninsula (data taken from Goyet et al. 1998)

3.9 Biogeochemical Budgeting

The budget of carbon, nitrogen and phosphorus fluxes in six upwelling systems are given in Table 3.4. As stated above, the domains considered are not restricted to the shelf region. Instead, the domains of study consist of the upper 200 m in the coastal provinces, which are defined following Longhurst et al. (1995) or Longhurst (1998) except one. The one exception is the Portugal-Morocco Coastal Province, which is defined following Walsh (1988) and Barton (1998). Slightly modified is the definition of the Northwest Arabian Upwelling Province, which does not extend as far south as that of Longhurst (1998). Instead, it extends only to the northern Somali Coast where the upwelling is significant (Hill et al. 1998).

The major fluxes are the upwelling of nutrients and the export of organic carbon. Also considered are the river runoff, the burial of biogenic matter and denitrification in shelf sediments and water column. For the calculation of water column processes, the areas of the coastal provinces are used; for that of benthic processes, the areas of the shelves are used. The shelf areas are taken from either Appendix 3.1 or Table III of Walsh (1988).

The upwelling volume transport has been estimated for a few locations by integrating the offshore transport along the coast (e.g., Korso and Huyer 1986). In upwelling regions without such estimates, a mean upwelling index of 100 (in units of m^3 s^{-1} per 100 m or Sv per 1 000 km) of coastline is assumed for calculation (Huthnance 1995). It is cautioned that the upwelling index does show considerable variability, and, therefore, the assumption only represents a ballpark value. The reported mean upwelling index off northwest Africa is as high as 270

(Barton 1998). The length of the coastline for each upwelling system is listed in Table 3.4. The nitrate fluxes are calculated from the volume transports and nitrate concentrations in the source waters. The phosphate fluxes are calculated from the nitrate fluxes and the observed N/P ratios. In four out of the six cases, the N/P ratio is less than the normal Redfield ratio of 16, indicative of denitrification in the upwelling systems. However, in the North Atlantic the N/P ratio in the upwelling source water is slightly above the normal N/P ratio, apparently resulting from the prevalent nitrogen fixation (Michaels et al. 2000).

Most of the upwelling systems receive little runoff from land. Among the few major rivers that discharge into these systems is the Columbia River. The total runoff within the coastal upwelling systems accounts for only 3% of the total global runoff (Walsh 1988). In the six upwelling systems considered here, the total river runoff amounts to 522 $km^3\,yr^{-1}$ (0.017 Sv), which is less than 1% of the total upwelling volume transport. The inputs of C, N and P from river discharge are negligible in the upwelling systems.

The primary productivity data are taken from Longhurst et al. (1995) except for the Portugal-Morocco Coastal Province whose PP value is taken from Walsh (1988). The area-integrated primary production is calculated from the PP data and the area of the coastal provinces (Table 3.4). The total primary production amounts to 273×10^{12} mol C yr^{-1}, which represents 6.6–7.3% of the global ocean primary production of $3\,800–4\,200 \times 10^{12}$ mol C yr^{-1} (Longhurst et al. 1995). From the primary productivity several important variables are derived. Most important of all is the export production or new production. By definition, the export systems readily export a significant fraction of primary production to the deep water. Only a small fraction is buried on the shelves. The carbon burial fluxes are listed in Table 3.4. The sum represents less than 0.4% of the total primary production. The export production is derived from the reported *f*-ratios and further constrained by the available nitrate or phosphate, which is provided by upwelling. However, a significant fraction of the upwelled nitrate may be removed during denitrification in the coastal zone.

Since denitrification in the suboxic water column often occurs in the subsurface layer of coastal upwelling systems, the fluxes of nitrate removal during denitrification are derived from primary production data. Liu and Kaplan (1984), based on then available data, suggested that the rate of denitrification was proportional to the availability of organic carbon. This notion was later substantiated with additional data (e.g., Naqvi 1987). The availability of organic carbon may be calculated from the change of the sinking flux of particulate organic carbon within the water column of the denitrifying layer. Using the relationship between the sinking flux of POC and the primary production observed in the California Current upwelling system (Pace et al. 1987), we calculated the available fluxes of sinking POC in the subsurface layer of 100–200 m (Table 3.5). It is noted that the denitrifying zone was assumed to be 150–200 m for the Northwest Arabian Upwelling Province. The relationship reported by Liu and Kaplan (1984) indicates that ¼ to ½ of the available sinking POC flux may be consumed by denitrifying bacteria. For this study, we assume 40% of the available organic carbon flux consumed during denitrification in the water column (0–200 m) of the coastal provinces discussed in this section. We also assume nitrogen gas as the only final product of all nitrogen species reacted. Results of the calculation are listed in Table 3.5. The area-integrated denitrification fluxes are calculated by multiplying the denitrification flux by the area of the denitrifying waters in the coastal provinces. In the California Current and Humboldt Current Coastal Provinces, the suboxic water covers 30% of the coastal provinces, which is indicated by the distribution of negative N* at 200 m depth (Gruber and Sarmiento 1997); in the Northwest Arabian Upwelling Province, the suboxic water covers 60% as indicated by the distribution of the oxygen deficient water (Wyrtki 1971); in the Benguela Current Coastal Province, we assume one half of the shelf regions covered by suboxic waters, based on chemical hydrography (Chapman and Shannon 1985); for the Portugal-Morocco and the Canary Coastal Provinces, we assume no water column denitrification. The total removal of fixed nitrogen sums up to 0.97×10^{12} mol N yr^{-1}.

Since denitrification in the sediment column is directly related to the organic carbon content (Liu and Kaplan 1984), it is assumed for this calculation that the denitrification flux is proportional to the organic carbon burial flux with a C/N ratio of 4:1. The results are listed in Table 3.5. The calculated denitrification flux for the shelf off the western American Coast bordering the California Current is 0.25 mol N $m^{-2}\,yr^{-1}$, which falls in the range of previous estimates, 0.18–0.37 mol N $m^{-2}\,yr^{-1}$ (Christensen et al. 1987; Devol 1991). The sum is 0.24×10^{12} mol N yr^{-1}, which is about 24% of the total rate of denitrification in the water column in these domains. Denitrification as a whole removes fixed nitrogen from these coastal domains at a rate equivalent to 10% of the total upwelling flux of nitrate.

The subsurface circulation patterns in the upwelling systems are complicated. It is not clear whether the upwelling waters would pass the suboxic zones, both in the water column and at water-sediment interface, and experience denitrification. To make a conservative estimate, we subtracted the denitrification fluxes from the upwelled fluxes in the calculation of the net inputs of nitrate to the coastal provinces (Table 3.5). For nitrate-limiting waters which have N/P ratios lower than Redfield ratio, the potential new production can be cal-

Table 3.4. Transports of water and biophilic elements (C, N, P) and their transformation in coastal upwelling provinces. All areas are in units of 10^9 m^2; fluxes in mol m^{-2} yr^{-1}; total transports of C, N and P in 10^{12} mol yr^{-1}

Coastal provinces	Shelf area[q]	Coastal zone area[n]	Coastal length (km)	Water transport (Sv)		Primary production[m]		New production	Organic C burial[d]		Source waters		Total upwelled nutrients	
				Upwelling	Runoff[q]	Flux	Total	Total	Flux	Total	NO_3^- (mM)	N/P	NO_3^-	PO_4^{3-}
California Current	270	960	3 000	1.5–3.6[m]	0.0080	32.3	31.0	6.2	1.00[c,e]	0.270	20[h]	14.2[k]	0.95–2.27	0.067–0.16
Humboldt Current	100	2610	4 000	4.0	0.0035[o]	22.4	58.5	12.3	0.23[i]	0.023	25[g]	12.0[k]	3.15	0.263
Northwest Arabian Upwelling	166	2500	3 000	15.0[h]		37.8	94.6	26.5	0.40	0.066	10[h]	12.2[r]	4.73	0.388
Portugal-Morocco	80	600	1 300	1.3	0.0038	14.6[q]	8.8	1.9	0.05	0.004	8[a]	17.9[a]	0.33	0.018
Canary Current	100	810	1 000	2.7[b]	0.0009	61.0	49.4	8.0	0.05	0.005	15[j]	17.0[k]	1.28	0.075
Benguela Current	144	1130	2 700	1.7[p]	0.0004[f]	26.9	30.4	5.5	4.00	0.576	19[f]	11.0[f]	1.02	0.093
Sum	860	8610	15000	27.3	0.017		272.7	60.4		0.94			12.23	0.96

Data sources: [a] Alvarez-Salgado (1997); [b] Barton (1998); [c] Berelson et al. (1996); [d] Berner (1982); [e] Carpenter (1987); [f] Chapman and Shannon (1985); [g] Chavez et al. (1989); [h] Chavez and Toggweiller (1995); [i] Codispoti and Christensen (1985); [j] Codispoti and Friederich (1978); [k] Fanning (1992); [l] Hall et al. (1996); [m] Korso and Huyer (1986); [n] Longhurst et al. (1995); [o] Milliman et al. (1995); [p] Shannon (1985); [q] Walsh (1988); [r] Woodward et al. (1999).

Table 3.5. Nitrogen budget and export fraction in coastal upwelling systems

Coastal provinces	Water column denitrification				Benthic denitrification		Available nitrate (Tmol N y^{-1})	Maximum export fraction	Reported *f*-ratio	Export fraction
	ΔF_{OrgC} (g C m^{-2} y^{-1})	F_N (mol N m^{-2} y^{-1})	Area (10^9 m^2)	Total rate (Tmol N y^{-1})	F_N (mol N m^{-2} y^{-1})	Total rate (Tmol N y^{-1})				
California Current	1.55	0.64	288	0.19	0.250	0.068	1.39	0.30	0.20[b]	0.20
Humboldt Current	1.07	0.45	783	0.35	0.058	0.006	2.80	0.32	0.21[c] 0.75[d]	0.21
Northwest Arabian Upwelling	0.64	0.27	1500	0.40	0.100	0.017	4.31	0.31	0.28 ±0.12[e]	0.28
Portugal-Morocco	0.70	0.29	0	0.00	0.013	0.001	0.33	0.22[a]	0.25[c]	0.22
Canary Current	2.92	1.22	0	0.00	0.013	0.001	1.28	0.16[a]	0.64[c]	0.16
Benguela Current	1.29	0.54	72	0.04	1.000	0.144	0.84	0.18		0.18
Sum			2643	0.97		0.236	10.94			

[a] Value based on phosphate limitation (see text).
Data sources: [b] Martin et al. (1987), [c] Minas et al. (1986), [d] Chavez et al. (1989), [e] Watts and Owens (1999).

culated from the net nitrate input under the assumption of 100% nitrate utilization (Chavez et al. 1989). The maximum export fraction e_{max} may be calculated from the total potential new production and the total primary production (Table 3.5). The potential new production is calculated under the assumption of nitrate limitation for all provinces except the two in the North Atlantic, where the high N/P ratio makes these upwelling systems P-limiting. The calculated e_{max} values for the California Current Coastal Province and the Northwest Arabian Upwelling Province are in reasonable agreement with reported *f*-ratios. The discrepancy is probably attributed to the much bigger area of the provinces defined in this study than the traditional coastal zone. For those provinces where there are reported *f*-ratios, we adopt the minimum among the *f*-ratios and the e_{max} values as the export fraction; for those provinces where there are no available *f*-ratios, we adopt the calculated e_{max} values as the export fraction (Table 3.5). The total new production is 60×10^{12} mol C yr^{-1}, which yields a mean export fraction of 0.22.

If DOC production accounts for 5–7% of the total primary production (based on Hansell and Peltzer 1998) in the upwelling systems, the total DOC production is $14–19 \times 10^{12}$ mol C yr^{-1}. The difference between the DOC concentrations in the surface and the subsurface layers was about 20 μM as observed off the Northwest Arabian Coast. If this represents the mean difference between the input and the output fluxes in coastal upwelling systems, the total export of DOC would be 17×10^{12} mol C yr^{-1}, which is in good agreement with the estimated DOC production.

A major fraction of the fish catch comes from the coastal upwelling systems. The world catch of marine fishes varies from 25.9 to 92.7 Mt yr^{-1} between 1953 and 1993 with a mean of 61 Mt yr^{-1} (FAO 1996). Assuming a carbon content of 6% of wet weight of fish (Walsh 1981), we get an average carbon removal rate of 0.3×10^{12} mol C yr^{-1} by marine fishing. If the coastal provinces discussed in this section provide 50% of the total fish catch in the world, fishing would result in a mean carbon removal rate of 0.15×10^{12} mol C yr^{-1} from these systems, which accounts for only 0.25% of the new production.

Whether the upwelling systems act as a source or sink of atmospheric CO_2 depends on the origin of the upwelling water (Watson 1995). The higher the content of deep ocean water in the upwelling water, the stronger it tends to release CO_2 to the atmosphere; the higher the content of the intermediate water ventilated in the subpolar region, the stronger it tends to absorb atmospheric CO_2. Among the provinces discussed in this section, the Arabian Sea (10–25° N) is a persistent source of CO_2 (Goyet et al. 1998), whereas the eastern North Atlantic Ocean off the Iberian Peninsula (40–43° N) is a sink of CO_2 in spite of coastal upwelling (Perez et al. 1999). It is likely that the closer to the equator the upwelling area, the higher is the tendency of releasing CO_2. However, the air-sea CO_2 exchange fluxes in some of the other upwelling systems have extremely high spatial and temporal variability (e.g., Torres et al. 1999), which prevents any meaningful estimation of the net fluxes. Since strong upwelling occurs mostly at relatively low latitudes, it is reasonable to assume the upwelling systems are a net source of CO_2.

3.10 The Arctic Shelves

3.10.1 Introduction

The Arctic Ocean differs from all others by virtue of the combination of sea ice, large volumes of runoff from land, and enormous continental shelves. Furthermore, the Arctic Ocean is a mediterranean sea surrounded by a drainage basin that exceeds the size of the ocean and has only restricted passages through which it exchanges water with the Pacific and Atlantic Oceans (Fig. 3.9). Arctic shelves undoubtedly behave in many ways the same as other shelves; for example, runoff from the land will stratify shelf surface water and produce estuarine circulation, winds will force exchange and upwelling at the shelf margins, and the shelves will generally have higher primary production and greater terrestrial influence than the interior ocean. However there are also vital differences. Exceptionally strong seasonality in runoff and light intensity occur synchronously around the entire Arctic Basin. Seasonal ice formation has a bipolar impact on the freshwater cycle. In summer, melting ice provides a broadly-distributed source of stratification, but in winter, ice formation destroys stratification by rejecting salt to the water column and thereby enhances mixing or produces convection (Fig. 3.10). Particularly in the flaw leads and polynyas that are widely distributed over the central shelves (Macdonald 2000), intense ice formation can produce convecting water which then flows across the bottom to spread as descending plumes into the interior ocean transporting material with them (see for example, Kämpf et al. 1999; Melling and Lewis 1982). The coupling of shelves to the interior ocean in the Arctic is, therefore, unique because it is so strongly affected by the oscillating cycle of ice formation and melting (Fig. 3.10). On one hand, the ice restricts air-sea interaction reducing wind mixing, sediment resuspension and upwelling. On the other hand, ice produces upwelling at its edge, provides an additional transient habitat for biota, and is an exceptionally powerful medium for material transport either directly in the ice itself or indirectly though thermohaline circulation (Cota et al. 1990; Eicken et al. 2000; Pfirman et al. 1989). The combination of the above seasonally modulated processes has no parallel in any other ocean.

Fig. 3.9.
View of the Arctic Ocean showing the drainage basin, major rivers, the shelves and the major passages connecting the Arctic with the Pacific and Atlantic Oceans

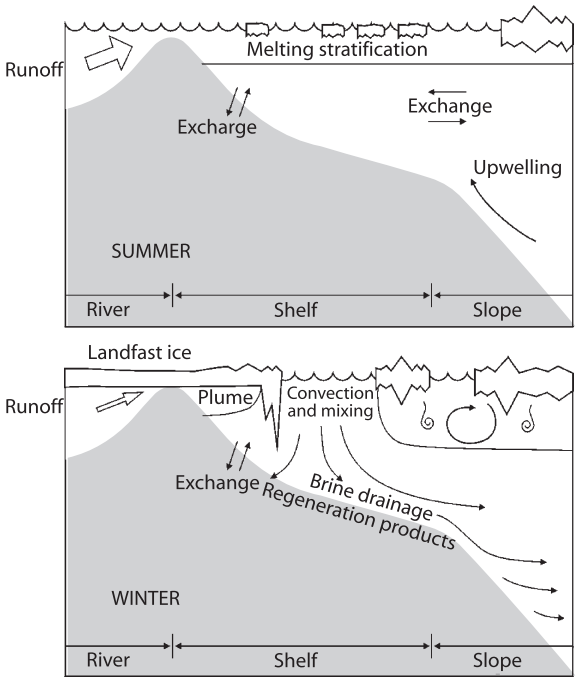

Fig. 3.10. A simplified scheme of the Arctic shelves showing the strong bipolarity produced by the alternation between ice melting and clearing in summer and ice formation during winter. Ice production produces two exchange pathways in ice export and brine export

The Arctic is thought to be particularly sensitive to global climate change (Cuffey et al. 1995; Fyfe et al. 1999; Walsh J. E. 1991a) and recent evidence suggests that, for reasons that remain unclear, the Arctic Ocean is now undergoing significant change in its ice climate and in its water-mass composition and distribution (Dickson 1999; Macdonald 1996; Macdonald et al. 1999; McLaughlin et al. 1996). An alteration in the sea ice climate will inevitably lead to large changes in the biogeochemistry of the shelves where seasonal clearing of ice already occurs. And so, in the world oceans we can expect global change to manifest itself first in the Arctic and, within the Arctic, first in the marginal seas. It has been suggested recently that the Arctic Ocean may be two or three times more important for anthropogenic CO_2 sequestration than its size implies (Bauch et al. 2000). However, the critical question is not how important the Arctic Ocean is presently in global elemental cycles, but, rather, how important it might be in contributing to change in these cycles. It seems likely in view of the size of the shelves and the vulnerability to drastic change from ice cover to open water that the Arctic Ocean will factor well above its relative size in the equation of global change.

Here, we start with a view of the Arctic Ocean as a large, shelf-dominated semi-enclosed sea (Fig. 3.9). We then

survey the shelves within the Arctic, outlining their characteristics, and eventually focus on the Mackenzie Shelf where recent material budgets have been constructed for organic carbon, nitrogen and phosphorus. We then construct a preliminary budget for Arctic Ocean treating the shelves as a single box. Finally, we speculate on how global change might affect the marginal Arctic seas.

3.10.2 The Arctic Ocean As a Mediterranean, Shelf-Dominated Sea

The potential to construct budgets for the entire Arctic Ocean by viewing it as a semi-enclosed sea has long been recognized (Aagaard and Carmack 1989; Aagaard and Coachman 1975; Anderson et al. 1983; Anderson et al. 1998; Codispoti and Lowman 1973; Goldner 1999b; Wijffels et al. 1992). Although constraining such budgets is made difficult by recirculation in Fram Strait, which obscures the estimate of net flow, it may be easier to close material budgets for the entire Arctic Ocean than it is for any one of the shelves within the Arctic. All Arctic Ocean budgets have depended first on estimating the volumetric flows of water and sea ice into and out of the Arctic. The assignment of salinity to exchanging water masses together with freshwater runoff and precipitation estimates allow the construction of reasonably accurate freshwater (Fig. 3.11a) and salt budgets (Fig. 3.11b). Once volumetric flows and exchanges have been established, budgets can be constructed for any property for which there are appropriate concentration data. Examples of such budgets include silicate (Anderson et al. 1983; Codispoti and Lowman 1973; Walsh et al. 1989), inorganic carbon (Anderson et al. 1998; Lundberg and Haugan 1996), organic carbon (Anderson et al. 1998; Opsahl et al. 1999), hexachlorocyclohexane (Macdonald et al. 2000), Cd (Macdonald 2000; Yeats and Westerlund 1991) and Al (C. Measures, unpublished). There is considerable variation in the estimates of volumetric flow used in budget constructions and there is considerable variability in the current flows themselves. Despite these variations, reasonable closure on budgets for the entire Arctic Ocean seems presently attainable (Goldner 1999a).

In the context of carbon and nutrients, Anderson and co-workers (Anderson et al. 1998) have undoubtedly produced one of the most detailed budgets to date. They considered the Arctic Ocean as two basins (Canada and Eurasian Basins), amalgamated the shelves into three main boxes (Laptev Sea, Chukchi/East Siberian/Beaufort Seas, Barents and Kara Seas) and, because the vertical stratification is so important in the Arctic Ocean in terms of property exchanges between the shelves and interior oceans, they sectioned the basins vertically into 6 boxes in the Canada Basin and 5 boxes in the Eurasian Basin. Inflows from the Atlantic and Pacific Oceans cross the Barents/Kara Shelves and the Chukchi and East Siberian Shelves before entering the interior ocean. Importantly, the shelves are incorporated into their box

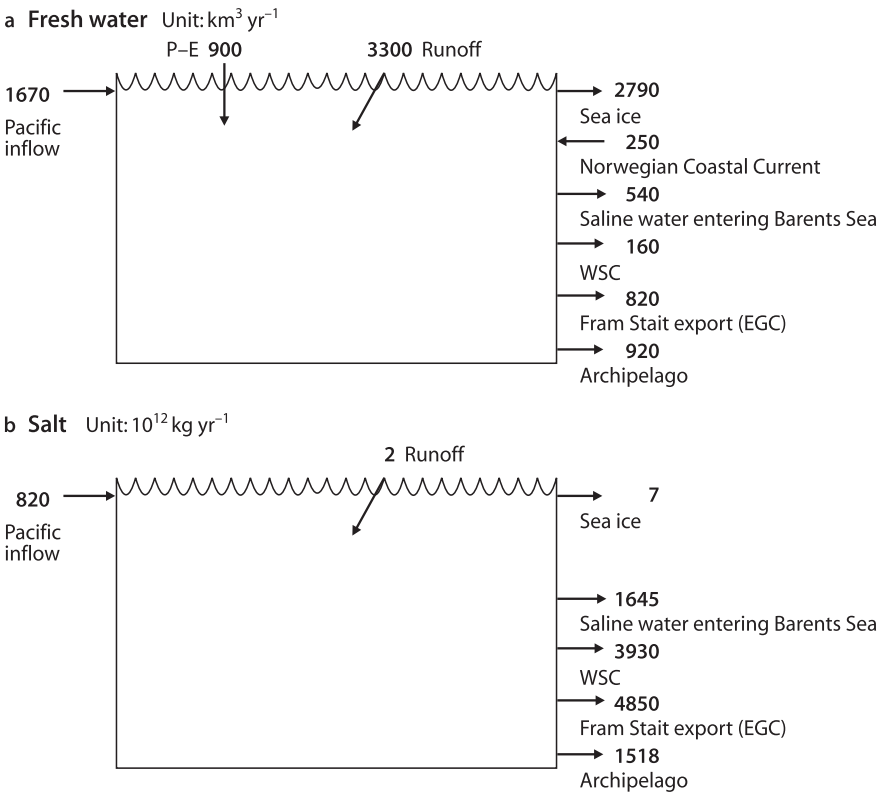

Fig. 3.11.
a A schematic diagram showing the freshwater budget for the Arctic Ocean constructed by Aagaard and Carmack (1989). The freshwater budget has been calculated using a foundation salinity of 34.8 which explains why saline water entering the Barents Sea and in the West Spitzbergen Current (WSC) are entered as freshwater losses to the Arctic Ocean. Each component was calculated independantly with the result that this budget is unbalanced to amount of net accumulation of 890 $km^3 yr^{-1}$ which the authors suggest is well within the uncertainties. **b** A schematic diagram showing the salt budget for the Arctic Ocean adapted from (Goldner 1999b). The original budget, presented relative to a median salinity of 34.4 has been converted and simplified to make it comparable to the freshwater budget in Fig. 3.11a

model so as to allow exchanges with the interior ocean at surface and at depth. This latter exchange process, illustrated in Fig. 3.10, is mediated by the ice formation/brine production over the shelves which nourishes the Arctic halocline (Aagaard et al. 1985). One of the problems identified both by Anderson et al. (1998) and Lundberg and Haugen (1996) is that the Arctic Ocean is not at steady state with respect to CO_2 due to increased atmospheric CO_2 pressure over the past two centuries. They estimate the current vs. the pre-industrial CO_2 budget considering only the altered air-sea exchange (i.e., effects on the biological pump are not considered).

Their budget for inorganic carbon (C_T), simplified in Fig. 3.12a, shows that the exchanges between the Arctic Ocean and the Atlantic dominate. The Pacific provides an important source of C_T for the Arctic Ocean whereas rivers and sea ice play only a minor role. While Anderson et al. (1998) have made significant progress in identifying the major components of the carbon budget and sensitivity to error, Fig. 3.12a underscores the difficulty in using differences between large fluxes to estimate relatively small net fluxes. Furthermore, the error estimates provided by the authors are fairly large and caution is warranted in drawing too many conclusions. As pointed out by Anderson et al. (1998), water that supplies input has been in contact more recently with the atmosphere (younger) than water supplying the output. Since atmospheric CO_2 concentrations have been increasing during that time, the ocean is not in steady state and the output reflects historical conditions whereas the input reflects impacted conditions. In this budget, the present input of C_T to the Arctic Ocean exceeds output

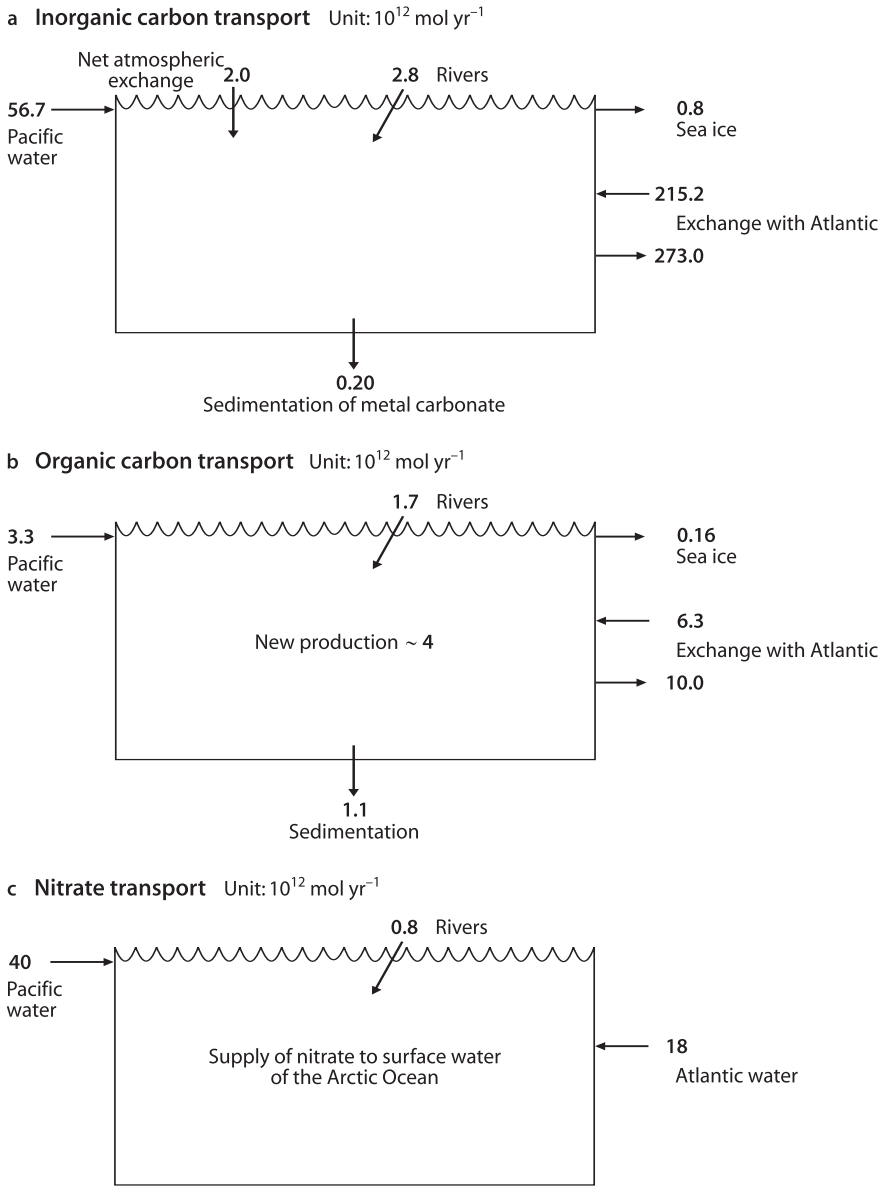

Fig. 3.12.
A simplified schematic of the budget for the Arctic Ocean based on (Anderson et al. 1998) for **a** inorganic carbon, **b** organic carbon and **c** nitrate inputs that support new production in surface water

by $0.75 \pm 0.50 \times 10^{12}$ mol C yr^{-1}. The carbonate burial flux was estimated to be small (0.02×10^{12} mol C yr^{-1}) and, considering both the C_T and organic carbon (OC) budgets (Fig. 3.12b), air-sea flux of CO_2 was estimated from the budget imbalance to be $2.0 \pm 1.4 \times 10^{12}$ mol C yr^{-1} into the Arctic Ocean.

The OC budget (Fig. 3.12b) shows that rivers and sedimentation contribute more significantly than they did in the case of C_T. The burial of OC in sediments is estimated from the Arctic Ocean new production which is supported by nitrate inputs primarily from the Pacific and Atlantic Oceans with only very minor additions from rivers (Fig. 3.12c), and by considering that 80% of the new carbon production is regenerated and therefore does not get captured in sediments. These authors caution that dissolved organic nitrogen may be an important but as yet unconsidered component of the system especially for river waters (and see Gordeev et al. 1996). Based on the denitrification estimate for western Arctic Shelf sediments (0.7 mol m^{-2} yr^{-1}; Devol et al. 1997) the loss of nitrate collectively by the total shelf area would be about 3×10^{12} mol yr^{-1}, which would far outweigh any input of nitrate from rivers (Table 3.7).

The first estimation of the silicate budget for the Arctic Ocean (Codispoti and Lowman 1973) concluded that this ocean was not a major source for reactive silicate and could even be a sink. A subsequent budget (Anderson et al. 1983) estimated net outputs (1.89×10^{12} mol yr^{-1}) to exceed slightly the net inputs (1.78×10^{12} mol yr^{-1}) and, finally, a re-estimation by Walsh et al. (1989) gave a balanced budget but suggested that, depending on the silicate concentration in water entering at Bering Strait, there could be a burial loss of as much as 0.4×10^{12} mol yr^{-1}. Unfortunately, the major term in these budgets, the silicate-rich Pacific inflow, was overestimated because flows of 1.3–1.5 Sv were used compared to the more probable 0.83 Sv determined recently by (Roach et al. 1995). The question of whether or not the Arctic Ocean is a sink for silicate has by no means been convincingly demonstrated.

Opaline silicate sequestration in the Arctic Ocean is of more than academic interest. Carbonate oceans (nutrient poor surface water, coccolith dominated) can be contrasted with silicate oceans (nutrient rich surface water, diatom dominated). In the former, little net carbon dioxide uptake by the ocean occurs whereas in the latter, diatoms are more effective in supporting net CO_2 uptake from the atmosphere because they sediment organic carbon decoupled from carbonate (Honjo 1997; Nozaki and Oba 1995). The surface (0–200 m) of the Arctic Ocean comprises two domains – the Pacific-dominated water in the Canada Basin and the Atlantic-dominated water in the Eurasian Basin which have traditionally been separated by a front over the Lomonosov Ridge. Because Pacific water is rich in silicate we might expect regions of the Arctic Ocean where water of Pacific origin dominates to be more productive of diatom assemblages; this would include especially the Chukchi and East Siberian Seas, but also large portions of the Canada Basin and the Canadian Archipelago. Recent observations show that one manifestation of change in the Arctic Ocean is the displacement of the front between Atlantic and Pacific water (McLaughlin et al. 1996). Large-scale change in the size of the Pacific (silicate) Domain could be an effective, but as yet unquantified, way to alter CO_2 sequestration on a large scale for the Arctic Ocean without even necessarily altering the primary production.

3.10.3 The Shelves of the Arctic Ocean

Of the Arctic Ocean total area ($\sim 10 \times 10^6$ km^2), over 30% is shelf (Table 3.6; Fig. 3.13). The predominant shelf area forms a continuous circumpolar band over 7 000 km long and up to 1 000 km wide. Figure 3.13 and Table 3.6 suggest that each of the identified shelves is unique and that there really is no 'representative' Arctic Shelf. Since the last ice age, many of the coastal regions in the Arctic have undergone relative sea-level rise and, consequently, have drowning coastlines. This process which is ongoing suggests that Arctic shelves continue to adjust to the new sea level. Many coastal regions in the Arctic are flat, do not extend much above present sea level, and are composed of poorly bonded soils sensitive to permafrost destruction. Therefore, coastal erosion for many of the regions is an important component of the coastal sediment budget (Are 1999; Kassens et al. 1998; Macdonald et al. 1998). Coastal inputs of freshwater and solids are now reasonably well estimated for most Arctic shelves (Table 3.6) as are their general physical characteristics. However, the exchanges at the shelf edge have not been directly quantified and models do not constrain them particularly well (e.g., see Björk 1990; Goldner 1999b). These latter, which probably dominate C, N and P cycles, are complicated in the Arctic by transport processes mediated by ice and brine production on the shelves (Fig. 3.10).

It is important to clarify how ice effects transport. The ice itself is not a particularly efficient transporter of conservative water properties like salt or nutrients because these tend to be excluded from the ice during formation (e.g., Fig. 3.11b). In contrast, sea ice often provides an important vehicle for the transport of sediment through suspension freezing (Eicken et al. 2000) and organic carbon (Mel'nikov and Pavlov 1978). Ice exerts its greatest influence on conservative property exchange by forcing thermohaline circulation through brine rejection. It is estimated that, for the entire Arctic, as much as 1–1.4 Sv on average is involved in such transport from shelf to basin (Goldner 1999a) which rivals the estimated strength of Arctic shelfbreak upwelling (3.8 Sv; Goldner 1999a).

Table 3.6. Characteristics of the Arctic shelves and inputs from land

Shelf	Shelf area (10^3 km^2)	Freshwater inflow (km^3 yr^{-1})	Sediment (10^6 t yr^{-1})	Ice export (km^3 yr^{-1})	Residence time (yr)	TOC (10^9 mol yr^{-1})	DIC (10^9 mol yr^{-1})	DIN (10^9 mol yr^{-1})	DIP (10^9 mol yr^{-1})	$Si(OH)_4$ (10^9 mol yr^{-1})	Primary production (g C m^{-2} yr^{-1})
Barents	600	463	22	560		442	510	4.7	0.28	43	150 (nearshore) 40 – 80 (deep)
Kara	880	1478	33	340	2.5	725	1180	59	1.9	184	?
Laptev	504	745	25	480–660	3.5 ± 2	433	600	4.1	0.16	47	12 – 27
E. Siberian	890	250	34	Import	3.5 ± 2	150	100	1.4	0.05	13	60 – 360
Chukchi	570	~100	<5	Import	0.2 – 1.2	~15	3	~0.8	~0.1	~8	60 – 360
Beaufort	180	>330	130	450	0.5 – 1	~280	360	1.0	~0.03	~15	20 – 40
Archipelago	300	~60	?	?	~0.5	?	?	<0.5	<0.05	?	12 – 27
Total	3924	3426	~250	1920		~2000	2750	~71.5	~2.6	310	

Data sources include Barrie et al. (1998), Dethleff (1995), Gordeev (2000), Gordeev et al. (1996), Hanzlick and Aagaard (1980), Macdonald et al. (1998), Pavlov and Pfirman (1995), Rigor and Colony (1997), Sakshaug et al. (1994), Schlosser et al. (1994), Walsh (1989).

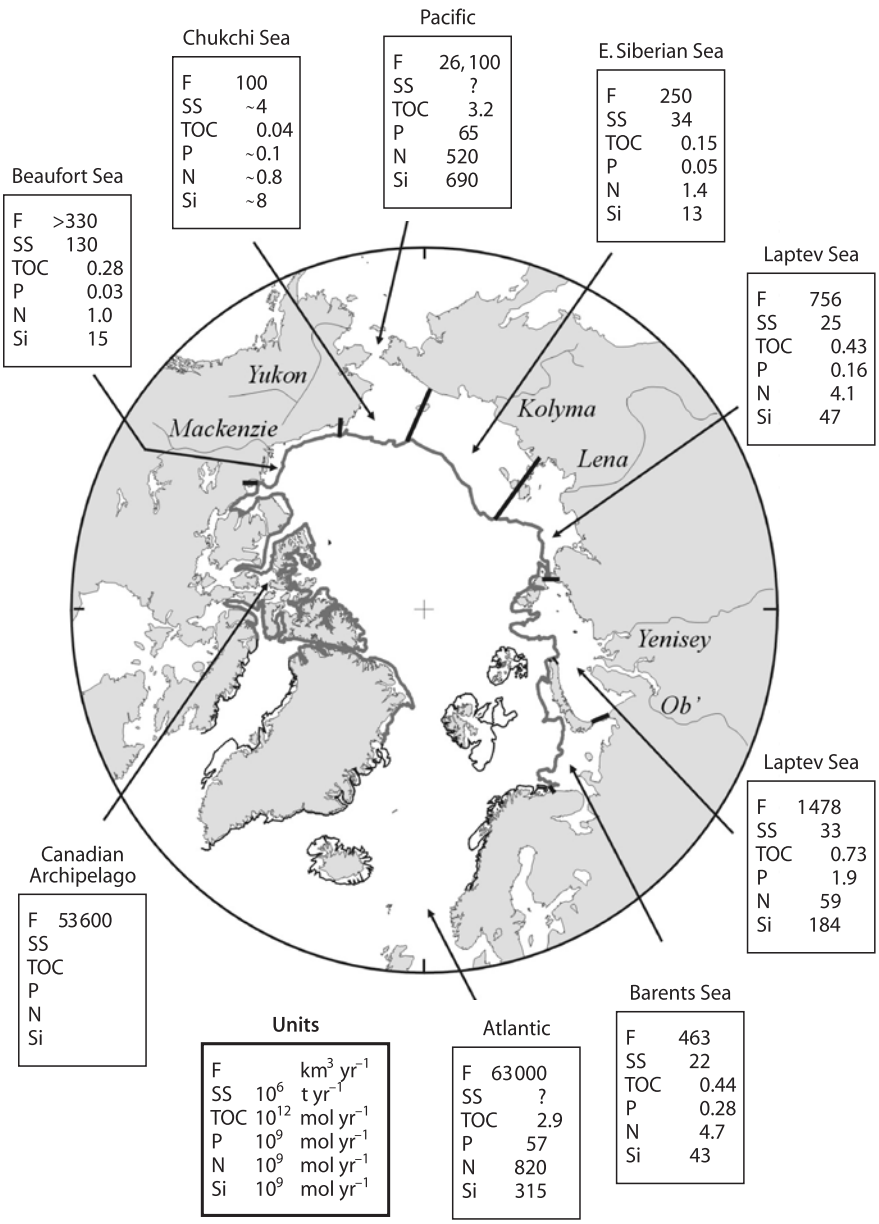

Fig. 3.13.
The Arctic Shelves and coastal inputs. Data have been collated from (Barrie et al. 1998; Gordeev 2000; Macdonald et al. 1998; Sharma 1979; Walsh et al. 1989) and references therein. Shown also is the inflow to the Chukchi from the Pacific Ocean. *F* refers to water and *SS* is the suspended solids. Symbols represent fresh water (*F*), suspended sediment (*SS*), total organic carbon (*TOC*), dissolved inorganic phosphorus (*P*), dissolved inorganic nitrogen (*N*) and reactive silicate (*Si*)

3.10.4 Barents Shelf

This shelf (Fig. 3.13) receives moderate inputs of runoff, small amounts of terrestrial particulate matter and has a relatively high productivity (Table 3.6). The Barents Sea branch of Atlantic water enters over this shelf to undergo seasonal modification by ice formation (Gerdes and Schauer 1997). The polar front results in a migrating and melting ice edge that can be both a contributor to productivity and source of material from the melting ice (cf. Sakshaug and Slagstad 1992). Salinification and cooling is crucial for the production of lower halocline waters which is reflected by the fairly large ice export from this region.

3.10.5 Kara Shelf

The Kara Sea has been relatively well studied because of the radioactive wastes disposed there (Eicken et al. 2000; Pavlov and Pfirman 1995; Pfirman et al. 1997). As an extension of the Barents Sea, the Kara Sea is strongly influenced by Atlantic water which has been cooled and modified while travelling over the Barents Shelf (Loeng et al. 1997). It receives large amounts of runoff from two of the Arctic major rivers, the Yenesey and the Ob, and exports substantial amounts of ice (Pfirman et al. 1997). The circulation and hydrology are highly variable due to winds, runoff and the sea ice cycle (Harms and Karcher 1999). Like all of the shelves on the Russian side

of the Arctic, large amounts of freshwater runoff are not accompanied by much sediment. For these shelves, therefore, the burial rate must be small due to the lack of a supply of inorganic terrestrial material. Of all the shelves, the Kara appears to have the greatest nutrient impact from human activities as reflected by large inputs of nitrate and phosphate from the rivers (Table 3.6, Fig. 3.13).

3.10.6 Laptev Shelf

The Laptev Sea is remarkable as one of the greatest ice exporting regions in the Arctic Ocean. Ice produced over this shelf can transit the ocean to Fram Strait within only a couple of years and carries with it substantial quantities of sediment. Eicken et al. (2000) estimated that a total ice-bound sediment export from the Laptev Sea of 18.5×10^6 t resulted from one entrainment event alone in 1994. This sediment export rivals the annual delivery of sediments to the Laptev Sea by rivers (Table 3.6) and illustrates the potential for ice to extend the influence of Arctic shelves over long distances, at least in terms of particle transport. Within only a few years, the sediment entrained in Laptev Sea ice will have been released when the ice melts either along the Transpolar Drift track or, more likely, in the Greenland Sea. Coastal erosion has been estimated to contribute about as much sediment to the Laptev Sea as the rivers (Are 1999) with local retreat rates for the Siberian coast of up to 40 m yr^{-1} (Weller and Lange 1999). Taken together, coastal erosion, river input and ice export of sediments probably result in net accumulations of sediment near the coast but net losses over the central to outer shelf. The net supply of terrestrial sediment, however, is low and implies similarly low average burial rates on this shelf. In addition to the local inputs from rivers, the Laptev Sea receives much of the runoff that first enters the Kara Sea and then follows coastal currents into the Laptev Sea before exiting to the interior ocean (Olsson and Anderson 1997). Although this would transport mainly conservative properties, it would have a strong influence on the freshwater balance in the Laptev Sea. The characteristic formation of a flaw lead in the Laptev Sea at the end of the landfast ice in winter suggests that the substantial ice production and export is mirrored by brine additions to the water with consequent enhancement of mixing and, potentially, convection of dense plumes as illustrated in Fig. 3.10. Despite the low supply of terrestrial solids, the Laptev Sea margin sediment is dominated by terrigenous material as reflected in its organic matter composition (Stein et al. 1999). The terrestrial appearance of Laptev sediments is probably due to the relative stability of terrestrial organic compounds and the rapid remineralization of marine organic carbon in surface sediments (Olsson and Anderson 1997) since marine organic carbon in the form of algal material is abundant at times in the surface water (Peulvé et al. 1996).

3.10.7 East Siberian and Chukchi Shelves

This East Siberian Shelf is the largest in the Arctic Ocean and has the most persistent ice cover (Barrie et al. 1998). In contrast to the other shelves, the East Siberian is a net importer of ice (Table 3.6). However, it does form a flaw lead at the end of the landfast ice (~25 m isobath) suggesting that ice and salt production must occur over the central shelf in winter. The shelf is characterized by relatively low freshwater inputs for its size, has a long water residence time, and can support only low sedimentation rates due to the large area and small supply of sediments from land. A discontinuity occurs in the oceanography of this shelf toward its eastern end. Nutrient rich Pacific water (0.83 Sv; Roach et al. 1995) enters through Bering Strait especially in the Anadyr current on the west side of the strait to leave its imprint on shelf waters of both the Chukchi and East Siberian Seas (Codispoti and Richards 1968). The import of these nutrients supports one of the most productive areas in the world ocean (Walsh et al. 1989). This region, which receives little runoff from land, is instead influenced by slightly fresh Pacific water which is seasonally modulated through ice production and cooling.

3.10.8 Beaufort Shelf

The Beaufort Shelf is distinguished by a narrow, sediment-starved shelf along the Alaskan north slope but, moving further to the east, the shelf widens and becomes completely dominated by the Mackenzie River (Macdonald et al. 1998). The Mackenzie Shelf portion of the Beaufort Shelf is unique by virtue of the yield of fresh water (over 5 m yr^{-1}) and terrestrial sediment supply (~130×10^6 t yr^{-1}). Indeed, this shelf receives as much terrestrial sediment as all of the Russian shelves together. Furthermore, like its Russian counterparts, this shelf is subject to substantial coastal retreat (up to 10 m yr^{-1}) which provides a further 7×10^6 t yr^{-1} of terrestrial sediment. Despite the enormous input of freshwater, which continues at 5 000 $m^3 s^{-1}$ in winter under the landfast ice, this shelf produces convecting water over the middle shelf through salt rejection from ice (Melling and Lewis 1982). Because of its rich supply of inorganic terrestrial sediments, this shelf can sustain reasonable rates of burial.

The shelves of the Archipelago are somewhat disconnected from one another by channels (Fig. 3.9). Many of these shelves, especially the outer ones facing the Arctic Ocean, have not been studied. There is probably little freshwater runoff in the Archipelago, most of it coming from widely distributed small streams that have an exceptionally brief period of flow. Over the outer shelf the Arctic Ocean attains its thickest pack ice (Bourke

and Garrett 1987) which probably limits primary production. Within the Archipelago, strong tidal mixing in passages can supply nutrients to support greater production (Cota et al. 1987). The net flow of water is out of the Arctic Ocean through the Archipelago (1.7 Sv) with much of that water originating in the Pacific. As a result the Archipelago forms a mirror image of the Chukchi and net exchange is from the interior Arctic Ocean, across the shelf and, eventually, down into Baffin Bay. Although the Archipelago channels form an important outflow for Arctic Ocean surface water (0–200 m), they cannot be viewed simply as 'pipes'. For much of the Archipelago, the Rossby radius (~10 km) is exceeded by the channel width and the channels, therefore, behave like a series of connected seas.

Although there are common features for all Arctic shelves in terms of seasonal ice cover, inputs from land, and exchange at the shelf edge, this brief survey of the shelves emphasizes how different they all are in terms of freshwater and sediment supply, ice production, source of nutrients and source of saline water (Pacific vs. Atlantic).

3.10.9 The Mackenzie Shelf of the Beaufort Sea as a Case Study

Budgets have been estimated previously for the Mackenzie Shelf for freshwater, sediments and organic carbon (Macdonald et al. 1995; Macdonald et al. 1998). Here, we build on those budgets, adding dissolved inorganic nitrogen (DIN) and dissolved inorganic phosphorus (DIP) using the terms and methods for box-modeling outlined by Hall et al. (1996) and Gordon et al. (1996). With this method, the shelf is viewed as a single box between land and interior ocean.

Within the Arctic Ocean, the Mackenzie Shelf provides one of the best opportunities to construct material budgets because: (*1*) inputs can be reasonably well constrained; (*2*) a large amount of data exist with which to estimate water and sediment properties over the shelf; and (*3*) the important processes are known qualitatively if not quantitatively. Despite many oceanographic studies of this shelf, there remain uncertainties in closing budgets for non-conservative properties including sediments and nutrients. The common feature of all Arctic shelves, the exchange or export of ice (Table 3.6) and brine (Fig. 3.10), creates difficulties not anticipated in Gordon et al. (1996) and Hall et al. (1996).

The Mackenzie Shelf comprises about one third of the Beaufort Shelf area (65 000 km^2, Fig. 3.13, Table 3.6). In the freshwater budget, the Mackenzie inflow by far dominates (Fig. 3.14a) but export of ice, directly or as ice melt, contributes significantly with precipitation minus evaporation only a minor component. The export of fresh water to the interior ocean is shown as two major components – one deriving from meteoric processes (V_R: runoff plus net precipitation), the other from the internal distillation inherent in ice production (V_I). This ice distillation process differs from the meteoric

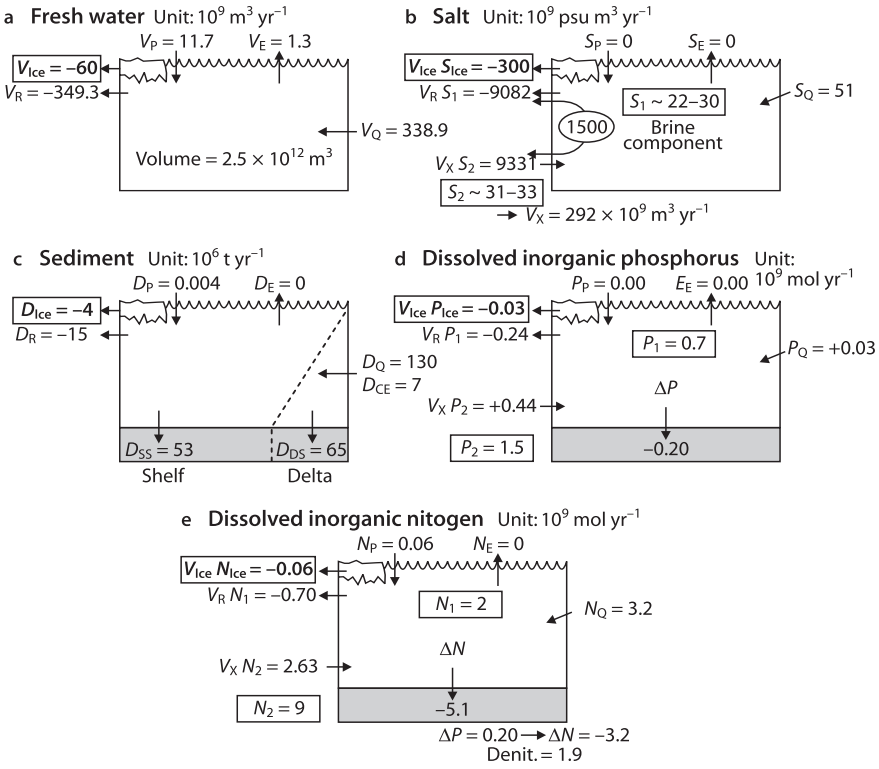

Fig. 3.14.
Budgets for the Mackenzie Shelf for **a** freshwater; subscripts refer to *Q* (inflow), *E* (evaporation), *P* (precipitation) and *R* (meteoric water); **b** salt; subscripts as in Fig. 3.14a and *X* (calculated volume exchange), and the brine component is estimated from the exported ice volume; **c** sediment; *SS* is shelf sedimentation, *CE* is coastal erosion and *DS* is sedimentation in the delta; **d** inorganic phosphorus and; **e** inorganic nitrogen

freshwater supply in that conservation of salt requires that it be mirrored elsewhere in the system by the brine rejected during ice growth. How this ice export affects budgets and/or stratification depends crucially on whether the brine is separated from the ice by penetrative convection or whether it remains coupled with the ice in the polar mixed layer (Macdonald 2000).

From the freshwater budget, salt exchanges (Fig. 3.14b) can be estimated using representative salinity distributions. The budget shows that shelf-edge exchange dominates. Although the transport of ice, with salinity of about 5 psu, is only a minor part of the salt budget ($\sim 300 \times 10^9$ kg yr^{-1}), the brine rejected from the ice is likely very significant ($\sim 1\,500 \times 10^9$ kg yr^{-1}). This brine will be exported near the surface if, for example, the water fails to convect deeply in winter. When sufficiently dense water is formed, the brine may sink and transit the shelf bottom picking up other properties (e.g., regenerated nutrients) to be exported into deeper waters of the interior ocean (Fig. 3.10). Although either route will satisfy salt balance, they differ drastically in where they will transport other components carried by the transport (nutrients, inorganic and organic carbon). If 60 km^3 of ice is exported (Fig. 3.14a), a further $1\,500 \times 10^9$ kg of salt must also be exported in surface or deeper water to maintain salt balance. It is difficult to close the ice/brine budget because both ice export and brine export are difficult to measure directly (Macdonald et al. 1995). The lack of certainty in how much salt is involved in convection, discussed above, makes it difficult to estimate other parameters (nitrate, phosphate) transported with the brine.

The sediment budget (Fig. 3.14c) is a crucial foundation for constructing budgets of other geochemical properties for this shelf as it provides the master control for burial flux on the shelf and slope. Although the Mackenzie loadings are well constrained (Macdonald et al. 1998), it is less certain what portion of this load stops in the delta which leads to uncertainty in other sedimentary components for the shelf.

Because we have no direct measurements of particle export, the quantity of sediment escaping the shelf is estimated as the difference between input and sedimentation which leads to an uncertainty of the same order as the estimate itself. For this shelf ice may be an important way to export particles but we have no direct observations to support an estimate of the quantities involved.

The DIP budget (Fig. 3.14d) shows that shelf-edge exchange dominates and that very little DIP enters in runoff. Using concentrations based on salinity-DIP relationships to estimate shelf-edge exchanges implies a loss (–P) to shelf sediments if the budget is to be balanced. This may partly explain high sediment P observed over the central shelf (Ruttenberg and Goñi 1996) but it is also likely that DIP is removed to sediments in the estuary by flocculation and particle settling (cf. Macdonald et al. 1987). In Mackenzie Shelf sediments, there is a close relationship between solid-phase Fe and P and a decrease in solid-phase P with depth (Gobeil et al. 1991). Phosphorus, therefore, is clearly linked to Fe geochemistry and a portion of the P must undergo regeneration back to the water column. It is difficult to use sediment measurements of total P to estimate the fraction of P actively cycling (Fig. 3.12) because the Mackenzie River supplies large amounts of solid phase P (~ 870 μg g^{-1}), some of which may be bioavailable, carried by a large and variable background sediment flux (Ruttenberg and Goñi 1996).

An important component of the DIN budget is supplied by the Mackenzie River (Fig. 3.14e). There is a significant sink (ΔN) in sediments which, compared to ΔP, exceeds the Redfield ratio ($\Delta N : \Delta P = 26 : 1$ – Redfield = 16 : 1) suggesting a preferential loss of DIN.

Porewater profiles clearly show that nitrate and ammonia both diffuse out of sediments into bottom water (Gobeil et al. 1991) and therefore sediments act as a source of regenerated nitrogen. However, the budget suggests a net loss of DIN over the shelf, most likely due to denitrification in sediments (cf. Christensen 1994). This loss (1.9×10^9 mol yr^{-1}) implies a denitrification rate of 0.1 mmol m^{-2} d^{-1} which is about a factor of 10 lower than rates measured in Bering and Chukchi sediments (Devol et al. 1997). This discrepancy may be partly explained by organic nitrogen which is often an important component of pristine rivers, equalling or exceeding DIN (Gordeev 2000).

The above budget for a small Arctic shelf dominated by terrestrial inputs is reasonably well constrained for the input terms due to a long time series of measurements both for the Mackenzie River and for the shelf properties. Nevertheless, dissolved organic nutrients could be a significant component of bioavailable nutrient supply and yet they are rarely quantified. The challenge provided by ice and brine to constrain the shelf budget is well illustrated and endemic to all shelves in the Arctic. The shelf-edge exchanges remain the largest and most uncertain component in this shelf budget, and will certainly provide the greatest challenge for Arctic shelves in general.

3.10.10 Shelf to Basin Sediment Transport in the Arctic

The slopes and basins of the Arctic Ocean cover an area of about 6×10^6 km^2. Evidence from Eurasian and Canadian Basin sediment cores supports the notion that much of the supply of sediment comes from the shelves either by ice rafting or by turbidity currents (Grantz et al. 1999; Stein et al. 1994b). Compositional and biomarker measurements of the sediments suggest that terrestrial, or shelf, material contributes strongly to both the inor-

ganic and organic components of these basin sediments (Schubert and Stein 1996). As previously discussed, sea ice is recognized as an important transporting agent for sediments and, in some cases may remove sediments from shelves at a rate comparable with riverine supply. Nevertheless, evidence from the basin cores suggests that ice rafting is not the only, and probably not the major, source of sediments to basins (Stein et al. 1994a) and that the dominant transporting mechanism is probably turbidity currents initiated at the margins. It seems likely, therefore, that an important but poorly quantified export process for shelf particulates is slumps or turbidity flows at the shelf edge. Ice rafting, also an important export mechanism, probably delivers most of the sediments it carries to regions where the ice melts – either in the Barents Sea or in the Greenland Sea.

3.10.11 CH_4, DMS (Dimethyl-Sulphide) Production in the Arctic

Methane and DMS, produced in marine environments, are important contributors to greenhouse gases (Houghton et al. 1995) and pathways for organic carbon. In the case of methane, shelf sediments are likely to be the most important source to Arctic surface waters (Kvenvolden et al. 1993), whereas for DMS it will be open water and biological production that supplies the flux to air (Sharma et al. 1999). Based on measurements in the Beaufort Sea, Kvenvolden et al. (1993) estimated that Arctic shelves collectively could contribute a seasonal CH_4 source of about 0.1 Tg yr^{-1} (~0.006×10^{12} mol yr^{-1}). Clearly, in view of the inorganic and organic carbon budgets given in Fig. 3.11a,b, CH_4 is a negligible component. Likewise for DMS, Sharma et al. (1999) estimated a flux equivalent to 0.004×10^{12} mol C yr^{-1}, also clearly a minor component of the OC budget.

3.10.12 A Budget for the Arctic Shelves

Arctic shelves vary so widely that no one shelf – for example, the Mackenzie – can reliably be used as a proxy for the others or by extrapolation to provide estimates for the entire Arctic Shelf. Furthermore, the differences between the shelves imply that they will each respond independently to change and each will have to be monitored to understand how change is manifested over the entire Arctic Shelf. With these cautions, we provide here a budget that builds on previous budgets and models of the Arctic Ocean. A primary difficulty in preparing such a budget, is that various authors use different boxes, assume different flows, and usually treat only selected components of the biogeochemical system (e.g., carbon or silicon). Here, we start with the terrestrial input data listed in Table 3.6 and Fig. 3.13. We build the budget using recent measured flows where available (e.g., Roach et al. 1995, for Bering Sea inflow) or model results where not available (e.g., Goldner 1999b) for upwelling and shelf-edge exchange. For organic and inorganic carbon, we rely heavily on the fluxes estimated by Anderson et al. (1998) recognizing that these authors did not use exactly the same water flows given in Fig. 3.15.

Although the budget (Fig. 3.15) cannot presently be closed, it captures important components of cycling on Arctic Shelves and reveals key weaknesses. The input of nutrients from land to sea is generally not the most important component of shelf cycling: shelf-edge ex-

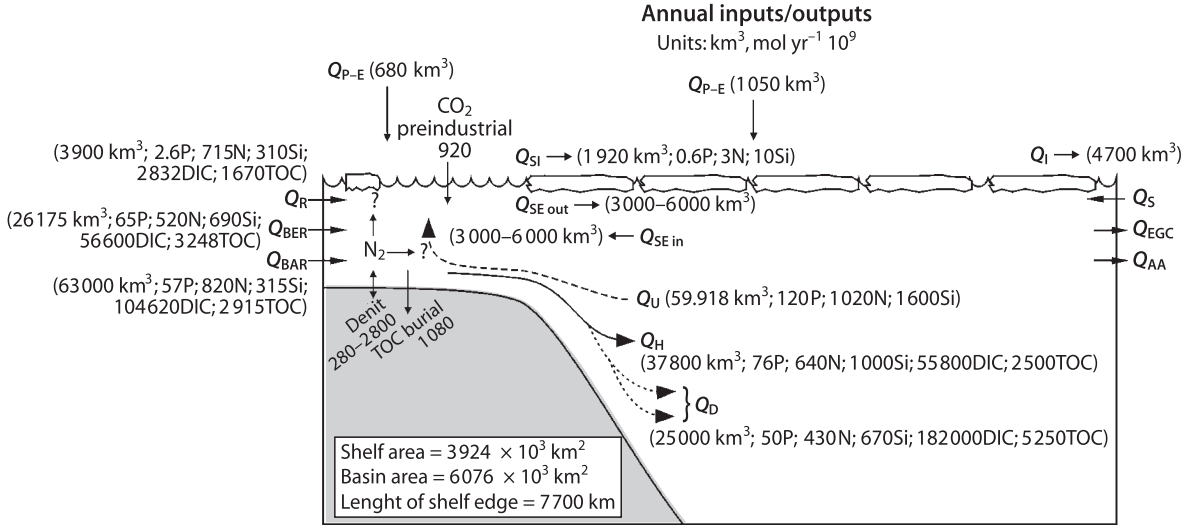

Fig. 3.15. A budget for the Arctic shelves. Q_R (river inflow, Table 3.6); $Q_{P\text{-}E}$ (moisture flux – Walsh et al. 1994); Q_{Ber} (Bering Strait inflow – Roach et al. 1995); carbon fluxes (DIC, TOC (Anderson et al. 1998); Q_U, Q_H, Q_D (upwelling, halocline nourishment, deep water formation, Anderson et al. 1998; Goldner 1999b; Melling 1993); Q_{SI} (shelf ice export, Table 3.6). Fluxes of carbon were taken directly from Anderson et al. who used slightly different volumetric flows in their budget

changes appear to have far greater potential fluxes. Two key shelves, the Chukchi and Barents stand out because they are supported by throughflow from the Pacific or Atlantic Oceans respectively. These two regions, therefore, have the greatest potential for export production into the interior ocean. Denitrification over the shelves could, potentially, be a very large component of biogeochemical cycling and well exceeds whatever nitrogen the rivers supply to the shelves. This remains true even if we have underestimated the nitrogen input from rivers by a factor of two by neglecting the organic nitrogen. Clearly, it is crucial to refine our estimate of denitrification either by direct measurements in shelf sediments or by looking for the its 'integrated' signature of N_2O in halocline water. A shelf budget for the Arctic Ocean can be constructed without considering the Arctic Archipelago, as is done in Fig. 3.15, because this latter region is essentially an outflow. However, similar to the Chukchi and Barents Seas, the Archipelago is a flow-through shelf which accepts biogeochemical components from the Arctic Ocean, processes them within the broad channels and basins (mixing, primary production, decay, air-sea exchange, sedimentation), and discharges products into Baffin Bay. The Archipelago, therefore, is another location where strong biogeochemical cycling can occur and which is vulnerable to change especially in its ice climate and it deserves more intensive study.

Shelf-edge exchange remains very problematic in the Arctic Ocean budget. We envision three separate exchange processes (Fig. 3.15) which together with advection of ice and water must balance property fluxes: (*1*) surface mixed-layer exchange (Q_{SE}); (*2*) halocline and deep-water formation (Q_H, Q_D); and (*3*) upwelling (Q_U). Goldner's model (Goldner 1999b) without $\delta^{18}O$ constraint suggests that surface exchanges are of the order of 5 Sv (160 000 $km^3\,yr^{-1}$) but the model is consistent with exchanges as high as 72 Sv. Clearly, these rates of exchange are far larger than those implied by the budget for the Mackenzie Shelf (Fig. 3.14; $V_x \sim 300\ km^3\,yr^{-1}$ for about 7% of shelf edge in the Arctic Ocean). Using $\delta^{18}O$ distribution as a constraint produces more reasonable-appearing surface exchanges (0.1–0.2 Sv) but even these imply large, as yet undetermined, elemental fluxes (Fig. 3.15). Of equal, or greater concern, are the potentially large fluxes in Goldner's model for upwelling (up to 3.8 Sv; Fig. 3.15 uses half this value) and halocline nourishment (1.4 Sv). The latter value is supported by other estimates (Anderson et al. 1998; Melling 1993) suggesting it to be a reasonable estimate. However, an upwelling flux that equals or exceeds halocline nourishment seems highly improbable. Nevertheless, the model suggests that upwelling ought not to be neglected and measurements of its intensity are needed. Finally, although ice can be an important player in forcing transport through thermohaline circulation, Fig. 3.15 implies that the direct transport of soluble nutrients is small.

Permanent burial of organic carbon in Arctic shelf sediments is estimated to be about $1\,000 \times 10^9\ mol\ yr^{-1}$ by Anderson et al. (1998) which, on an aerial basis, is about ¼ the burial rate estimated for the Mackenzie Shelf. This seems reasonable given that the Mackenzie Shelf is strongly supplied with terrestrial sediments and can therefore support a relatively large burial flux. For the enormous Russian shelves, sediment supply is small and, in some cases, may be less than sediment loss from the shelf making these shelves poor sites for burial but potentially good sites for denitrification. For much of the Arctic Ocean, the shelf slope and basins may provide the most important burial sites.

Recently, Bauch et al. (2000) have inferred from stable isotope ($\delta^{13}C$) measurements that the Arctic Ocean with only 2% of the global ocean area accounts for 4–6% of the global ocean's anthropogenic CO_2 uptake. This anthropogenic carbon (4–7 Gt C or 0.3–0.6 Pmol C) probably entered the ocean through direct ventilation of shelf waters and river inflow, and was subsequently exported to the interior ocean in the halocline either directly or via a growth-decay cycle on the shelf.

3.10.13 Global Change; Speculation on Consequences for Arctic Shelves

The changes most easy to visualize for the Arctic Ocean in the upcoming decades relate to alteration in the Arctic ice cover which has recently shown surprising rapid manifestations of change (Macdonald et al. 1999; Maslanik et al. 1996; Rothrock et al. 1999). With warming, we expect the shelves to have longer periods of little or no ice cover and, therefore, to become more 'temperate' in their behavior. More open water for longer periods would enhance wind mixing, shelf-edge upwelling and shelf-edge exchange. Primary production would also be enhanced from an average total production of about 50 g C $m^{-2}\,yr^{-1}$ to perhaps 100 g C $m^{-2}\,yr^{-1}$ or more. The location and timing of primary production could also change as could the relative importance of ice vs. pelagic primary production and with this the pelagic – benthic coupling would alter (Grebmeier and Whitledge 1996; Walsh 1989). If reduced amounts of ice are produced in winter and enhanced amounts of runoff enter the sea, the convective engine of the shelves (Fig. 3.10) could stall. However, the effect of length of ice growth season on water convection is not easy to predict because more open water in late summer may help to clear shelves of freshwater inventories and so enhance the possibility of producing dense water (Macdonald 2000).

Longer periods of open water, continued relative sea-level rise and a higher incidence of storms (Everett et al. 1997) will accelerate coastal erosion. In some locations, for example the coasts of the Siberian and western

Canadian Arctic, enhanced coastal erosion could provide significant added supply of terrestrial material to the shelf which would be further augmented by sediment and carbon from rivers which have enhanced flow (Miller and Russell 1992) and which carry more sediments due to breakdown of permafrost in the drainage basins. The delivery of DOC by rivers to the coastal sea could further be affected by changes in the drainage basin including the drying out of peat or increase in fire.

Potentially the most significant changes facing the Arctic could originate from shifts in atmospheric pressure fields (e.g., the Arctic Oscillation, Thompson and Wallace 1998). Such shifts alter the Arctic Ocean surface circulation pattern (Proshutinsky and Johnson 1997) leading to rapid change in the ice climate (Macdonald et al. 1999), water-mass distribution and circulation (Carmack et al. 1997) and thence potentially large-scale change in primary production. In particular the Pacific/Atlantic front is prone to change its location (McLaughlin et al. 1996) which clearly may alter the large-scale distribution of silicate in surface waters. As discussed above, a change like this could alter the way this ocean takes up CO_2 from the atmosphere – smaller areas dominated by $Si(OH)_4$ imply less CO_2 flux into the water due to biological flux of sinking particles (Honjo 1997; Nozaki and Oba 1995). Although polar oceans are not reported to have widespread coccolithophore populations (Tyrrell et al. 1999), recent unprecedented blooms of these carbonate phytoplankton in the Bering Sea (Weller and Lange 1999) should serve as a warning.

Ozone depletion in the upper atmosphere is a concern in the Arctic because it would enhance the incident UV radiation to the surface (Weatherhead and Morseth 1998). DOC – especially highly-coloured terrestrial DOC – strongly attenuates UV in aquatic systems (Schindler et al. 1997) and, in fact, changing its concentration provides a potentially far greater effect on aquatic environments than the projected change to incident UV from ozone depletion. Terrestrial DOC contributes a much larger component of DOC in Arctic surface water than it does in the Atlantic and Pacific Oceans and appears presently to survive transport to Fram Strait which takes between 1–6 years (Opsahl et al. 1999). One of the reasons why allochthonous DOC survives in Arctic surface waters may be that it is protected from photochemical degradation by ice cover (Opsahl et al. 1999). If so, reduced ice cover could not only enhance incident UV to the water surface but, more importantly, it could allow greater destruction of terrestrial DOM further exacerbating the exposure. The above comments underscore the need to construct budgets independently for the terrestrial and marine carbon components as they have different sensitivities to change.

Taken together, the primary forcing for Arctic Ocean change is most likely to come from change in the ice climate which can be effected by increased temperature and by change in the wind fields which provide both thermal and mechanical forcing. Furthermore, the loss of ice cover enhances the penetration of solar radiation leading to further melting – i.e., positive feedback. It is easy to envisage that reduced ice will lead to direct changes in shelf productivity through enhanced upwelling and mixing, for example, and enhanced air-sea exchange (e.g., heat, moisture, DMS). The greatest impact on global climate and carbon, however, may come from displacements or bifurcations in biogeochemical and physical pathways of the Arctic. Examples include: (*1*) The pathways of freshwater and other terrestrial inputs from the Russian Shelves (amount entering the Canadian Basin vs. the amount entering the Eurasian Basin); (*2*) The amount and source of surface water exiting through the Archipelago vs. Fram Strait; (*3*) The amount of primary production from pelagic vs. ice algae (which also may affect the particle flux); (*4*) The amount of primary production supported by silicate phytoplankton vs. carbonate phytoplankton; and (*5*) The amount of organic carbon regenerated in sediments to CO_2 vs. CH_4.

We are presently far from a sufficient understanding of the Arctic Ocean system that would allow us to predict these changes except that the shelves will likely be the first and most important locations for change.

3.11 Marginal Seas

Marginal seas form the linkage between the continents and the oceans, and as such, receive much land runoff, ventilate the deep oceans and exchange much material with the open oceans. The roles of these marginal seas in the context of carbon and nutrient cycles are briefly discussed here, with special emphasis on the CO_2 sink.

3.11.1 High Latitude Marginal Seas

High latitude marginal seas, such as the Bering Sea, the Sea of Okhotsk and the Baltic Sea are relatively nutrient-rich compared with the open oceans, and not surprisingly, enjoy higher productivity. Diatoms often dominate in these waters and because their skeletons are silicious and their soft tissues consume CO_2, the biological pump in these marginal seas continuously removes CO_2 from the atmosphere.

The Bering Sea, with an area of 2.3×10^6 km^2, is the third largest marginal sea in the world. Half of the sea is less than 200 m in depth, and the shelf waters frequently have a pCO_2 of 100 ppm or more below saturation as a result of the cooling effect in winter and primary productivity in spring and summer. Near the shelf break, pCO_2 is frequently supersaturated because of vertical

mixing, but overall the shelf ecosystem serves as a sink for atmospheric CO_2 (Codispoti et al. 1986; Chen 1993; Walsh and Dieterle 1994). Primary productivity on the shelf is on the order of 165 (50–300) g C m^{-2} yr^{-1}. Although most of it is consumed on the inner shelf, just slightly less than half is exported northward to the Arctic Ocean through the Bering Strait or southward to the Aleutian Basin. The *f*-ratio is 49% on the outer shelf and 17% at mid-shelf (Wollast 1998; Takahashi 1998). In the surface water, dimethylsulfide and N_2O have concentrations of about 50 ng S l^{-1} and 313 ppb, respectively (Nojiri et al. 1997; Uzuka et al. 1997).

The shelf water is probably supersaturated with anthropogenic, or excess CO_2, unlike the deep basin waters which are not. Overall, the Bering Sea contained about 0.21 (±0.05) Gt excess carbon around 1980. Albeit small in value, the carbonate deposits in the vast Bering Sea and the Sea of Okhotsk shelves may well be capable of providing a large sink for excess CO_2 in the near future. It would follow that a doubling of the current CO_2 level in the atmosphere by the latter part of the next century would bring about the dissolution of the calcites on the shelves, which in turn would provide another large sink for CO_2 (Chen 1993).

The surface water in the Sea of Okhotsk is also generally below saturation for pCO_2, except near the Kashevarou Bank and the Boussole Strait where tidal mixing is strong (Rogachev et al. 1997). The dense intermediate water is believed to be an important source of the North Pacific Intermediate Water (NPIW). Kurashina et al. (1967) estimated the gross exchange of water between the North Pacific and the Sea of Okhotsk is about 15 Sv. The present authors have estimated that excess CO_2 totaling 0.18 ±0.08 Gt has already penetrated to at least 1 000 m in the Sea of Okhotsk, and that there is an export value of (0.011–0.18 Gt C yr^{-1}) to the North Pacific (σ_θ = 27.35–27.5; Chen and Tsunogai 1998; Andreev et al. 2001).

The Baltic Sea, at 0.42×10^6 km^2, is essentially an estuary with a large runoff; moreover, precipitation exceeds evaporation. As a result, very fresh water flows out of the Baltic Sea through the Kattegat and Danish Straits mainly in the surface layer, while the saltier North Sea water mainly enters near the bottom. With its shallow depth, the entire Baltic Sea is thought to be saturated with respect to excess CO_2, but the total amount is actually only 0.011 ±0.002 Gt C. Most C, N and P are recycled, with little being exported to the North Sea.

3.11.2 Semi-Enclosed Marginal Seas

The South China Sea (SCS), the largest marginal sea in the world (3.5×10^6 km^2), the Mediterranean Sea (2.5×10^6 km^2), the second largest in the world, the Sea of Japan (1×10^6 km^2), the eighth largest and the Red Sea (0.44×10^6 km^2), the 13th largest are all deep basins with narrow shelves. They are characterized by a unique homogeneity in their subsurface waters with only narrow and shallow straits connecting them to the outside. The Red and Mediterranean Seas are unique in the sense that evaporation is greater than precipitation plus runoff. Consequently, there is an inflow of warm, nutrient-poor surface water and an outflow of cooler, nutrient-rich deep waters through the Straits of Gibraltar and Babel Mandeb, respectively.

Since the deep waters in some semi-enclosed marginal seas are formed inside a closed basin, they provide a unique opportunity to estimate the Redfield ratios based on the mass-balance method and a 1-D model (Chen et al. 1996a). For instance, the isolated basins in the Sea of Japan provide a clear indication that the bottom water has become stagnated at least since the 1940s, perhaps because of global warming. Meanwhile, nitrogen and phosphorous concentrations in the deep waters have increased. Similar results have been reported for the Mediterranean (Bethoux et al. 1998a,b; Chen et al. 1999) where the paucity of rivers and upwelling results in low productivity, and P is probably a key factor in the control of the bacterial and phytoplankton growth rates and in the export of carbon (Thierry et al. 2000).

Many marginal seas have deep water formation and, in the process, take up atmospheric CO_2 and transport it to the deep waters. Most phytoplankton also absorbs CO_2 from the surface layer and carries carbon to the deep waters. However, with their coral formations marginal seas in the tropics may release CO_2 to the atmosphere because the formation of coral skeletons results in higher pCO_2. Additionally, the growth of *coccolithophorids* can change the roles of sinks and sources of CO_2 depending on the inorganic vs. organic carbon ratio. The calculated vertical profiles of excess CO_2 indicate that the entire Sea of Japan, Red Sea and the Mediterranean Sea have been penetrated by excess CO_2, amounting to 0.31 ±0.05 Gt C for the Sea of Japan in 1992 (Chen et al. 1995a), 0.07 ±0.02 Gt C for the Red Sea in 1978 (Krumgalz et al. 1990; Chen and Tsunogai 1998) and 1.3 ±0.3 Gt for the Mediterranean in 1990. Owing to its shallow sills, the Sea of Japan does not transport excess CO_2 to the interior of the North Pacific. In contrast, the Mediterranean Sea transports 0.012 ±0.006 Gt yr^{-1} of excess CO_2 to the intermediate waters of the North Atlantic. The *f*-ratio in the Mediterranean Sea ranges from 0.15–0.44, yet the POC flux represents even less than 5% of primary production. This suggests that a large fraction of the carbon export is in the form of DOC, though this is still unquantified (Miquel et al. 2000). There is also deep water formation in the northern Gulf of California in winter, but the newly-formed deep water, along with the

excess CO_2 it carries, seems to be confined to only the northern gulf which is also shallow.

The ratio of $CaCO_3$ dissolution and organic carbon decomposition varies from 0.05 at 300 m to about 0.17 below 2 000 m in the Sea of Japan (Chen et al. 1996a). These values are lower than the ratios of 0.14 and 0.36 found in the South and North Pacific, respectively (Chen et al. 1982; Chen 1990), or 0.54 in the Bering Sea (Chen 1993) because diatom and silicoflagellates dominate the phytoplankton in the Sea of Japan (Hong et al., pers. comm.). Another result is that the vertical gradient of SiO_2 is several times higher than that of calcium or alkalinity (Chen et al. 1995a). Carbonates do not seem to be dissolved in the Red Sea because calcite and aragonite are already supersaturated by as much as 300% and 100%, respectively.

The shelves of the SCS occupy an area of about 1.2×10^6 km^2. There is considerable seasonal variation in productivity, with the highest value in winter and the lowest during the inter-monsoon periods. A 3-D numerical model gave an annual mean productivity of 370 mg C m^{-2} d^{-1}, almost identical to the observed value. Further, the model also predicted an *f*-ratio of 0.14 (Liu et al. 2000). Much of the new production is supported by upwelling because the nutrient supply from rivers and that in the surface seawaters through the Luzon and Mindoro Straits and the Sunda Shelf (Fig. 3.16) are only a small fraction of what is required to support new production. In fact, the upwelling of the SCS deep waters conveys nutrients to the intermediate and surface layers. Only a portion of the upwelled nutrients is transported to the ECS shelf through the shallow Taiwan Strait. Further, the outgoing SCS surface water in the Luzon Strait contains many more nutrients than the incoming Kuroshio surface water. The outflowing SCS surface and intermediate waters turn northward, therefore also transporting nutrients to the ECS shelf. It is evident that the SCS acts as a pump sending nutrients away from the deep waters into the euphotic zones in the SCS and the ECS (Chen and Wang 1999; Chen et al. 2001b).

Because of strong upwelling, the deepest excess CO_2 penetration (the depth where the excess CO_2 is at 5 μmol kg^{-1}) is only around 1 500 m, a depth shallower than that in the Northwestern North Pacific. The entire SCS probably contained 0.6 (±0.1) Gt of anthropogenic carbon back in 1994. The saturation horizon of calcite is deeper than 2 000 m in the SCS; thus little enhanced dissolution is expected due to excess CO_2 penetration (Chen and Huang 1995). The saturation horizon of aragonite is 600 m, shallower than the depth of excess CO_2 penetration, but deeper than the saturation horizon found in the Bering Sea (350 m). The upward migration of the saturation horizon (Feely and Chen 1982) would not affect the calcareous deposits on the SCS shelf to the degree that it does the Bering Sea deposits.

There are several other marginal seas, but regrettably, relatively little information is available. The Black Sea, at 0.46×10^6 km^2, connects to the Mediterranean Sea through the very narrow and shallow Straits of Bosphorus and Dardanelles. There is a large excess of precipitation plus runoff relative to evaporation; hence, the fresher surface water flows out of the straits on top of the incoming saltier Mediterranean water. The shallow Persian Gulf (0.24×10^6 km^2), on the other hand, has more evaporation than precipitation plus runoff. As a result, subsurface water flows out at the same time that the outside surface water flows in through the Straits of Hormuz. The oxidation of organic matter is mainly by sulfate (Goyet et al. 1998), and it is expected that the old, anoxic water in the Black Sea below the depth of about 100 m does not contain much excess CO_2. Unlike the Sea of Japan or the Mediterranean Sea that have warmed, the Black Sea has shown a decrease in temperature, perhaps because of decreased freshwater input (Murray et al. 1991). The nutrient supply, however, has actually increased. Indeed, in the last three decades its ecosystem has transformed from a once highly diverse, healthy state in the 1960s to its present eutrophic state charactized by low biodiversity (Oguz et al. 2001).

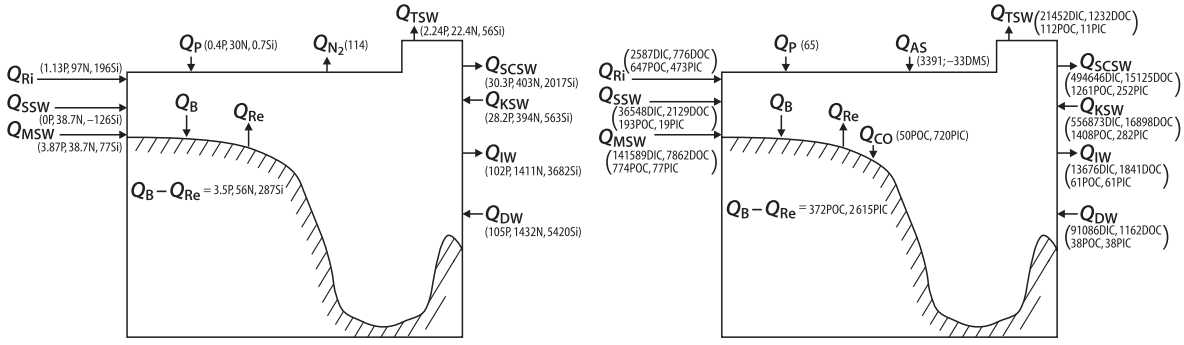

Fig. 3.16. Schematic diagram for the annual (**a**) nutrient and (**b**) carbon budgets (numbers in 10^9 mol yr^{-1}) in the South China Sea. Symbols are the same as Fig. 3.1 except that *SCSW*, *KSW*, *DW*, *MSW*, *SSW* and *CO* denote South China Sea Surface Water, Kuroshio Surface Water, Kuroshio Deep Water, Mindoro Strait Water, Sunda Shelf Water and coral reefs

3.11.3 Initial Synthesis

Almost without exception, the observed data and budget calculations for the continental shelves suggest that although a small fraction of carbon is exported across the shelf-slope break, the principal fate of the carbon which is produced on the shelf is, in fact, oxidation on the shelf. Upwelling seems to support most of the nutrients that are required for new production and denitrification. The global mean dissolved N/P ratio for river outflow is 23 (18–31) according to Bolin and Cook (1983). It is natural to suggest that P is the limiting factor, especially when considering that nitrogen fixation occurs. It is the upwelled seawater, with normally an inorganic N/P ratio close to 16, that supplies DIP to the shelves.

Recently, Nixon et al. (1996) and Galloway et al. (1996) studied the outcome of N and P at the land-sea margin (5.7×10^6 km^2) of the North Atlantic Ocean. They concluded that riverine N is only transported to the open ocean in a few areas, with the flow mostly coming from a few major rivers. This is because net denitrification in most estuaries and continental shelves exceeds the amount of N supplied to the shelves by rivers and requires a supply of nitrate from the open oceans. Their denitrification flux is equal to 12 times the amount deposited on the shelf and slope. Results for the ECS (Fig. 3.2) give a denitrification flux of less than half of the shelf and slope deposit. Another discrepancy is that the P budgets of Nixon et al. and Galloway et al. indicate that there is a net export of DIP to the open oceans in the water column, whereas the opposite holds true in the ECS (Fig. 3.2). The net export from the ECS is mostly supported by upwelling. Extrapolating the ECS value to the global shelves gives an upwelling rate of 4.2×10^{12} mol N yr^{-1}. Brink et al. (1995) gave 7.5×10^{12} mol N yr^{-1}, but J. J. Walsh (1991) gave 40×10^{12} mol N yr^{-1} which seems to be too high as upwelling is probably seldom that strong. The true value is probably on the order of 10×10^{12} mol N yr^{-1} (Fig. 3.17).

J. J. Walsh (1991) and Wollast (1998) gave a net denitrification flux for the world ocean shelf zone (26×10^6 km^2) of 3.6×10^{12} and 2.5×10^{12} mol N yr^{-1}, respectively. Middelburg et al. (1996) gave 7×10^{12} mol N yr^{-1} occurring in shelf sediments. Had the ECS value been extrapolated in this study to cover the world shelves, the flux would be 2.77×10^{12} mol N yr^{-1}, which is in good agreement with the results of Wollast. However, Wollast estimated a net preservation of 0.71×10^{12} mol N yr^{-1} for shelves globally compared with the extrapolated value of 2.17×10^{12} mol N yr^{-1} based on the ECS studies. The offshore transport of organic N was estimated to be 28×10^{12} mol N yr^{-1} by Wollast vs. the extrapolated ECS value of 3.64×10^{12} mol N yr^{-1}. Extrapolating the value of Galloway et al. (1996) would yield a value of only 0.12×10^{12} mol N yr^{-1} for the sum of shelf deposits and offshelf transport of organic N. Despite such a large discrepancy, it is obvious that upwelling is by far the dominant source of nitrogen necessary to sustain organic N production, and hence, burial and offshore transport on the continental shelf. A denitrification value of 2.5×10^{12} mol N yr^{-1} is adopted in this study (Fig. 3.17).

J. J. Walsh (1991) used a primary productivity of 430×10^{12} mol yr^{-1}. He assumed that all upwelled nitrate is taken up by phytoplankton, and he went on to estimate

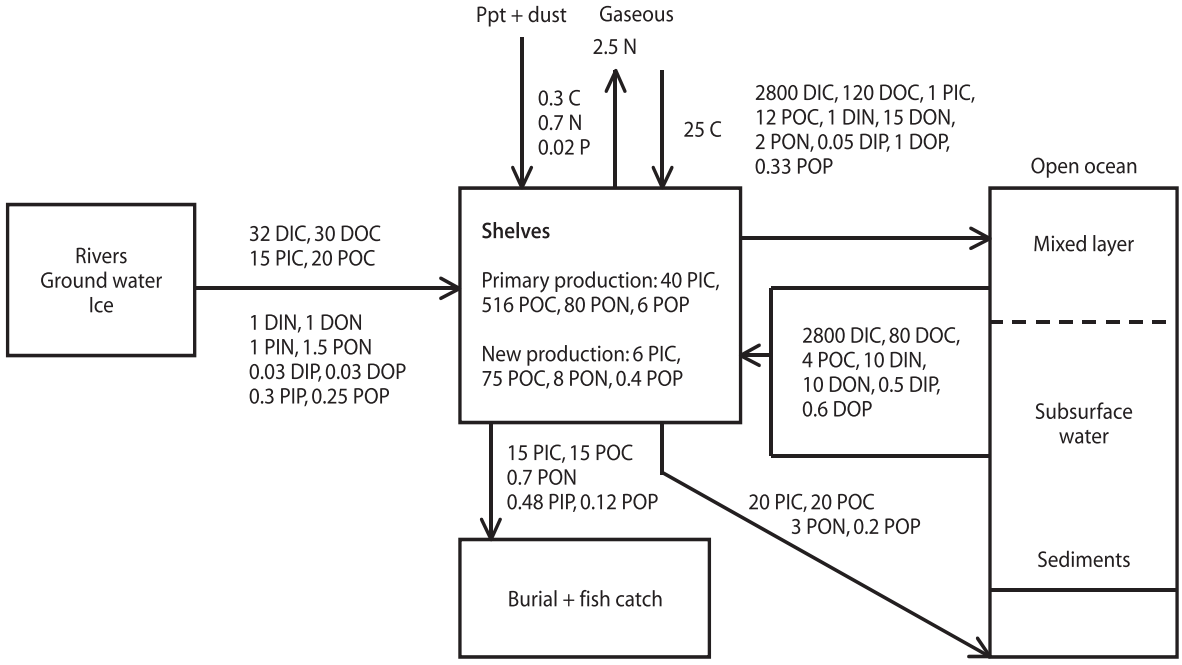

Fig. 3.17. Schematic diagrams for the annual carbon and nutrient budgets (in 10^{12} mol yr^{-1}) for the continental margins

Table 3.7. Non-conservative fluxes in the continental margins

Name	(*p*–*r*)	IC air/sea	POC/PIC sed.	DOC/POC offshore	DIC/PIC offshore	IP dust	POP/PIP sed.	DOP/POP offshore	DIP/PIP offshore	IN dust/rain	Net denit	PON/PIN sed.	DON/PON offshore	DIN/PIN offshore	Ref.
Amazon Shelf		–	+/+	–/–	+/–	+	+/+	–/–	+/–	+	–	+/+	–/–	+/–	1,5
Baltic Sea	+	+	–/–	–/0		+	–/–	–/0	0/0	+	–	–/–	–/0	0/0	1,7,11
Barents Sea		+	+/												1,8
Beaufort Sea			+/												
Benguela Current	+	+	–/–	0/0	+/–	+	–/–		+/–	+	–	–/–		+/–	1,2
Bering Sea Shelf, summer	+	+	–/–	–/–	+/–	+	–/	?/–	+/–	?	+	–/	–/–	+/–	1–5
Bering Sea Shelf, winter	?	0	–/–	–/–	+/–	+	–/	?/	+/–	?	?	–/	–/–	+/–	1–6
Brazil Shelf		–				+				+	–				1,9,10,12
Buenos Aires Shelf	+	+				+				+	0				1,9,12
Californian Shelf		+	0	–/–	+/–	+	0/	?/–	+/–	+	–	0/	–/–	+/–	1,5,12
Canadian Archipelago Shelf															
Caribbean Sea						+				+	0				1,12
Chukchi Shelf		+	–/–		+/–		–/–		+/–			–/–		+/–	1,5,8
E. China Sea Shelf	+	+	–/–	–/–	+/–	+	–/	–/	+/–	+	–	–/	–/–	+/–	1,4–6,12
E. Canadian Shelf			–/–								–				2,10
E. Siberian Shelf			+/												
Equatorial W. African Shelf		–				+				+					1,9
Great Barrier Reef	+	–	–/–	?	?	0	–/–	0/0	0/0	0	0	–/–	0/0	0/0	1,2
Gulf of St. Lawrence						+				+	–				1,10
Gulf of Thailand	–	0	–/–	–/–	+/–	0	–/	?/–	+/–	?	–	?/	?	+/–	2
Iberia Shelf		+				+				+					1,9
Irish Sea	+	+	?	?		+	?		+/–	+	–	?		+/–	1,2
Kara Sea		+													1,8
Laptev Sea		+	–/–		+/–		–/?		+/–				–/?	+/–	1,8,13
Mackenzic Shelf	–	–	–/–	+/+	+/–	+	–/–	–/–	+/–	+	–	–/–	–/–	+/–	1,2
Mediterrean Sea		+	–/–		–	+	–/–			+	–	–/–			1
Mid Atlantic Bight			–/–	–/–		+				+	–				2
N. Chile Coast	+	?	?	–/–	+/?	+	?	–/–	+/–		–	?	–/–	+/–	1,2
North Sea	+	+	–/–	–/–	+/–	0	–/–	–/–	+/–	+	–	–/–	–/–	+/–	1,2,5
NW African Shelf		+				+				+	–				1,9,12
NW American Shelf		+	–/–	–/–	+/–	+	–/	?/–	+/–	+	–	–/	–/–	+/–	1,5,12
Patagonia Shelf		+				+				+	–				1,9,12
Red Sea			–		+	+				+	–				1,12
Sea of Japan Basin			–/–			+	–/					–/			1
Sea of Okhotsk Basin			–/–			+	–/					–/			1
S. Atl Bight						+				+	–				1,2
South China Sea Basin	+	+	–/–	?		+	–/	?		+	–	–/	?	–/+	1
Sulu Sea			–/–			+				+		–/–			1
Upper Gulf of Thailand	+	–	–/–	0	0	0	–/	?/–	?/–	+	–	–/	?/–	?/–	2
Weddell Sea		–	–/–												1,12
Western Canadian Shelf			0	–/–	+/–	+	0/	?/–	+/–	+	–	0/	–/–	+/–	1,5

1: This study; *2:* JGOFS (1997); *3:* Walsh (1995); *4:* Walsh et al. (1981, 1989); *5:* de Haas (1997); *6:* Chen (1985, 1988, 1993); *7:* Gordon et al. (1996); *8:* Semiletov (1997); *9:* Bakker (1998); *10:* Seitzinger and Giblin (1996); *11:* Thomas and Schneider (1999); *12:* Weiss et al. (1992); *13:* Stein et al. (1999); *14:* Walsh et al. (1992)."+" means entering the shelf system;"–" means leaving the system.

a global shelf new productivity of 240×10^{12} mol yr^{-1}, which gave an *f*-ratio (new/total production) of 0.54. Wollast (1998) also estimated primary productivity at 500×10^{12} mol yr^{-1} (230 g C m^{-2} yr^{-1}) on the shelf globally, but he claimed that 16.5×10^{12} mol yr^{-1} (7 g C m^{-2} yr^{-1}) is preserved in the sediments and that 180×10^{12} mol yr^{-1} (83 g C m^{-2} yr^{-1}) is exported offshelf in organic form. Mackenzie et al. (1998b) chose to use primary productivity, organic carbon accumulation and offshore transport as 766, 20 and 32×10^{12} mol yr^{-1}, respectively, in their global continental shelf carbon cycle budget calculations. J. J. Walsh (1991) pointed to an offshelf export of 240×10^{12} mol yr^{-1} without shelf deposit although Mackenzie et al. reported only a small offshelf export. In this study, the global shelf productivity is taken to be 516×10^{12} mol yr^{-1} (214 g C m^{-2} yr^{-1}), while the organic C preservation and the downslope offshelf POC export is 15×10^{12} mol yr^{-1} (7.9 g C m^{-2} yr^{-1}) and 20×10^{12} mol yr^{-1} (9.2 g C m^{-2} yr^{-1}), respectively (Fig. 3.17).

In terms of the PIC, Milliman (1993) obtained a preservation value of 7.5×10^{12} mol yr^{-1} for all shelves other than coral reefs in the world. The export is 2.5×10^{12} mol yr^{-1}, again excluding coral reefs. In this study, the preservation value of PIC is taken to be 15×10^{12} mol yr^{-1}, and the export is 20×10^{12} mol yr^{-1}, much higher values than those reported by Milliman. Mackenzie et al. (1998b) chose an accumulation rate of 21×10^{12} mol yr^{-1}. Though they did not report on the PIC export rate, they did use an air-to-sea flux of 0.03×10^{12} mol yr^{-1} which Wollast (1998) ignored. The extrapolated global air-to-sea flux on the shelf based on the ECS data would be 53×10^{12} mol yr^{-1}. Tsunogai et al. (1997) gave an even larger value of 83×10^{12} mol yr^{-1}. In contrast, Holligan and Reiners (1992) and Ver et al. (1999) gave an opposing direction, sea-to-air flux of 33 and 17×10^{12} mol yr^{-1}, respectively. Clearly, large uncertainties and discrepancies exist here, but data for the Sea of Okhotsk, the North Sea and the Arctic Ocean, among others, also show an air-to-sea flux of CO_2 (Table 3.7). It seems that a global air-to-sea transfer rate of 25×10^{12} mol yr^{-1} of CO_2 for the shelves is not unreasonable. In terms of POC, the global net offshelf export data is 28×10^{12} mol yr^{-1}. The net offshelf DOC export is larger, at 40×10^{12} mol yr^{-1} (Fig. 3.17). These values are larger than the riverine inputs thus the shelves are autotrophic.

The above budget calculations, however, are all under the assumption of a steady state. Interannual variations, such as those from an ENSO event, affect the runoff a great deal. As a result, the upwelling rate and all associated fluxes should likely be subject to change. Further, slumping and turbidity currents may wash away the shelf deposit and reduce the reservoir. These possibilities have not been considered. Another point of concern is the reduced freshwater outflow due to irrigation and the damming of rivers. For instance, the Nile, Colorado and the Yellow Rivers now discharge little water. Reduced freshwater input to the shelves reduces the buoyancy effect and diminishes upwelling and the nutrient supply, not to mention productivity as well.

Table 3.7 summarizes the systems studied above to exemplify the similarities and differences in terms of the general typological characteristics explored. These include allocating systems on the basis of positive or negative estimates for a number of processes and fluxes, where the symbol is taken as gains (+) or losses (–) with respect to the shelf. Key processes are ($p - r$), (*nfix* – *denit*), air-to-sea transfer of C, shelf-to-ocean particle transfers and burial, where p is production, r is respiration, *nfix* is nitrogen fixation, and *denit* is denitrification.

One growing concern from these considerations of cross-shelf exchange and regionalization in the construction of some of the models for the various budgets is the constraint of the boundary conditions, particularly in the complexity of physical oceanography which affects upwelling and offshore advection. Another concern is the common use of C and N as currencies of metabolism when P may be a better choice as it exhibits no change in speciation. Phosphorous essentially behaves as a conservative tracer with respect to system-level metabolic processes – except where sediment-loading and riverine input may cause inorganic reactions to dominate P-cycling processes. A case in point is denitrification which is clearly an important process in continental margins, where N/P flux ratios offer the opportunity to explore DIN deficits due to denitrification.

Notwithstanding the uncertainties, the following scenario seems to emerge once all of the available information is summarized and studied (Table 3.8): On the present day shelves, the *f*-ratio is only about 0.15, with most external inorganic nutrients supplied by upwelling. About 97% of the organic matter introduced onto the shelves from terrigenous sources and by primary production remineralize in the water column and in the sediments. Thus, under present day conditions, it can be asserted that shelves do not play an important role in the preservation of organic carbon although the shelves do absorb 0.3 Gt C from the atmosphere each year. Periods with low sea level during the ice ages probably resulted in the exposure and erosion of sediments, thereby reducing the role of the shelves in the preservation of organic carbon and the sequestration of atmospheric CO_2 even more.

3.11.4 Future Research

Global warming is likely to result in increased stratification but decreased productivity in the upper layer of the open ocean. On the other hand, warming is likely to be accompanied by a stronger pressure gradient between

the land and the oceans. The stronger pressure gradient will strengthen alongshore geostrophic wind, causing enhanced offshore Ekman transport and amplified coastal upwelling. Whether this may cause the already 'turbulent' upwelling system to become less productive or instead, cause the increased supply of nutrients to generate higher productivity needs to be investigated. The effects of ENSO, known to affect the physical and biological properties of near coast waters, are less known in the marginal seas and the polar regions. The existence or absence of teleconnections must be determined.

Total groundwater discharge and associated chemical fluxes to the coastal zones are also a question of debate, especially over lengthy periods of time and in large areas. The total groundwater discharge is probably about 5 to 10% of the total surface discharge (36 000 to 38 000 $km^3\,yr^{-1}$) that reaches the oceans. However, the total flux of dissolved solids in groundwaters may make up a higher proportion of the riverine flux and may even represent as much as 50%. Although the input of DIP via groundwaters is not expected to be higher than that via surface waters because of the poor solubility of mineral phosphates and the tendency of dissolved phosphorus to be adsorbed on solid particles, nitrate loading of groundwaters may result in a substantial input to the coastal zones. DIC concentrations in groundwaters are elevated owing to the dissolution of limestone and the bacterial oxidation of organic matter. Thus, the DIC flux via groundwaters to the coastal oceans may amount to as much as 25% of the riverine flux. Dissolved organic fluxes of carbon, nitrogen and phosphorus associated with groundwater discharge to the coast are poorly known, but they probably do not make up a very substantial portion of the surficial inputs. The global depositional fluxes of nitrogen (NO_y) and reduced nitrogen (NH_3) are known over large areas of the world and, to a first approximation, over certain regions of the oceans. Less well constrained are the depositional fluxes of organic carbon, nitrogen and phosphorus. It is also unknown whether increasing anthropogenic C, N and P inputs from rivers, but maintaining a relatively constant Si supply would affect the relationship between siliceous and calcareous organisms. More siliceous organisms, of course, would lead to larger CO_2 draw down. Si-depleted nutrient loading, however, yields *Phaeocystis* which are neither siliceous nor calcareous, but are major dimethyl sulfide producers in areas such as the North Sea.

It has been hypothesized that the atmospheric delivery of major nutrients (N, P and Si) plus some trace nutrients (e.g., Fe) would affect coastal and ocean biological production, and in some cases, limit production. For instance, inputs of nitrogen via atmospheric deposition to coastal areas may constitute on a local scale as much as 50% of the total river plus atmospheric input. In the North Atlantic, atmospheric delivery of elemental carbon comprises about one third of the total tropospheric anthropogenic carbon flux to the sea surface, a result of biomass burning and fossil fuel combustion. Atmospheric deposition of both organic carbon and nitrogen is substantial, and world-wide, the atmospheric deposition of organic nitrogen is about the same as inorganic nitrogen.

Dissolved organic nitrogen and, for that matter, dissolved organic phosphorus have been little studied. These components are not included in most, if not all, box model calculations. Further, high rates of DON release have been reported for *Trichodesmium*, and DOP may be a major source of P supporting nitrogen fixation. Clearly DON and DOP ought to be measured along with DOC, the latter of course having thus far received more attention. Further, the possibility that excess CO_2 may be stored in an ever increasing DOC pool also requires investigation (Gorshkov 1995). Corals reefs, although covering only 1.12×10^5 km^2 of surface area, are very productive. Whether most material is recycled, however, needs to be evaluated.

In the past few centuries, human activities on land have become an important factor greatly affecting the coastal environment and its exchanges with the atmosphere and the open oceans. A word of caution is that historical records give us only estimates as to the short-term potential responses of ocean margin systems to natural perturbations. Hsu (1991) maintains that if we want to evaluate the consequences of very large anthropogenic perturbations, much longer geological records must be studied so that extreme, catastrophic events can be taken into account. In fact, Hsu postulated that the present rate of species extinction might have already exceeded that which occurred at the end of the Cretaceous. The fluxes of material and energy across ocean margin boundaries will possibly reach just as catastrophic rates as those that prevailed during that critical time in Earth's history. Aeolian flux of material, notably Fe, may have also been much higher during the ice ages because of the exposed shelves. Enhanced Fe influx could increase oceanic productivity but exactly how much of it might be offset by reduced productivity on the shelves is not known. Fortunately, the International Marine Past Global Changes Study (IMAGES) program has obtained cores in several marginal seas. These should broaden our knowledge of cross-shelf exchange processes over a time span of about 300 000 years.

Another issue that deserves further study is the role of the western Bering Sea and the Sea of Okhotsk in the formation of the North Pacific Intermediate Water (NPIW). The accumulation and redistribution of anthropogenic and greenhouse gases, such as CO_2, CH_4 and freons, in the North Pacific are limited and controlled by the lower boundary of the NPIW. It has been shown that the bottom shelf water with density up to 27.05 σ_θ is formed in the coastal polynyas in the Sea of Okhotsk as a result of cooling and brine rejection un-

Table 3.8. Fluxes relevant to continental margins (all values except *f* are in 10^{12} mol yr^{-1}; numbers in parentheses are reference numbers)

C				N				P			
River plus ground water and ice											
32	(1,3, DIC)	17	(1, DOC)	0.265	(1, DIN)	0.7	(1, DON)	0.012	(1,3, DIP)	0.022	(1, DOP)
14	(1, PIC)	14	(1, POC)	2.4	(1, PON)	4.3	(2, DIN)	0.25	(1, PIP)	0.38	(1, POP)
66.7	(2, DOC)	34	(2a, OC)	3.6	(2, DON)	0.32	(3, DIN)	0.03	(1, excess DOP)	1.32	(3, total)
29.6	(3, POC)	31.8	(3, PIC)	3.43	(3)	4.3	(4)	0.22	(5)	0.053	(13, DIP)
18	(3,DOC)	60	(7,IC)	2.7	(5)	0.5	(1, excess DON)	0.047	(13, PIP)	0.05–0.125	(15, DP)
51	(7,OC)	8	(1, excess OC)	0.5	(14, excess par.)	0.9–2.8	(15)	0.53	(15, par.)	0.14	(24, dis.)
42	(15, DIC)	42	(15, DOC)	5.3	(24)	0.32	(25, DIN)	0.55	(24, par.)	0.025	(25, DIP)
16.7	(15, PIC)	29.2	(15, POC)	0.7	(25, DON)	1	(25, excess dis.)	0.038	(1, DOP)	0.013	(25 excess DIP)
25	(15, glacial)	37.8	(16, DIC)	1.5	(25, par.)	0.42	(25, excess par.)	0.019	(25, excess DOP)	0.25	(25, POP)
10.3	(16, DOC)	5.5	(16, POC)	2.9	(26)			0.38	(25, PIP)		
35	(17, POC)	9.2	(17, DOC)								
39.7	(24, dis.)	15	(24, par.)								
Air-to-sea (gaseous)											
8	(2a)	6	(3)	−3.6	(2)	−1.47	(3)	–			
52.6	(6)	0.03	(7)	−2.5	(4)	−2.74	(6)				
83	(11)	−33	(12)	−3.9	(14)	−0.046	(27, N_2O)				
Precipitation plus dust											
0.3	(6, PIC)	0.008	(16*, DIC)	0.7	(4)	0.59	(5)	0.02	(6)	0.022	(15*)
0.45	(16*)			0.87	(6)	0.64	(14)	0.022	(18*)		
				0.68	(26)						
Net burial plus fish catch											
9	(2a,POC)	15	(4,POC)	40	(2, IN)	0.22	(3)	0.59	(3)	0.109	(5, POP)
24	(3)	15	(4, PIC)	0.71	(4, PON)	0.69	(5, PON)	0.165	(6, POP)		
16.5	(4, POC)	42.2	(6, PIC)	2.17	(6, PON)	1.4	(14)				
17.3	(6, POC)	21	(7, IC)	0.4	(20, PON)						
20	(7, POC)	11	(8, POC)								
7.5	(10, PIC)	4.7	(15)								
2.2	(20, POC)	2.5–5	(22)								
Upwelling plus surface inflow											
467	(3)	2 788	(6, DIC)	40	(2)	10.76	(3)	0.44	(3)	0.353	(6, DIP)
126	(6, DOC)	7.6	(6, POC)	26.1	(4, DIN)	3.7	(5, DIN)				
459	(7, IC)	9	(7, OC)	4.93	(6, DIN)	14	(14)				
3 330	(15, DIC)			32	(20, DIN)	7.5	(22, DIN)				
				19	(23, DIN)	4.5	(26)				
Down-slope export of particulates											
167	(2)	2	(3,PIC)	2.64	(3, PON)	3.64	(6,PON)	0.15	(3, POP)	0.227	(6, POP)
18	(3,POC)	3.3	(4, PIC)								
53	(6, PIC)	20	(6, POC)								
25	(10, PIC)										
Surface water outflow											
75	(2, DOC)	500	(3)	12.9	(2, DON)	9	(3)	0.38	(3)	0.029	(6, DIP)
2 796	(6, DIC)	161	(6, DOC)	0.15	(6, DIN)	15	(20, DIN)				
14.6	(6, POC)	502	(7, IC)								
32	(7, OC)										
Gross offshelf export (down-slope + surface outflow)											
75	(2, DOC)	167	(2, POC)	12.9	(2, DON)	27.8	(2, PON)	0.53	(3)	0.029	(6, DIP)
520	(3)	2 796	(6, DIC)	11.64	(3)	0.12	(5, ON)	0.227	(6, POP)		
161	(6, DOC)	53.5	(6, PIC)	3.64	(6, PON)	0.15	(6, DIN)				
34.7	(6, POC)	502	(7, IC)	14	(14)	2.67	(20, DON)				
32	(7, OC)			27	(20, PON)						
Net offshore export (down-slope + surface outflow – upwelling + surface inflow)											
18	(2a, OC)	53	(3)	27.9	(4, ON)	0.7	(2)	0.09	(3)	−0.152	(5)
180	(4, OC)	3.3	(4, PIC)	0.88	(3)	−4.78	(6, DIN)	0.324	(6, DIP)	0.227	(6, DOP)
8	(6, DIC)	35	(6, DOC)	3.64	(6, PON)	−16.9	(20,DIN)				
53.5	(6, PIC)	27.1	(6, POC)	2.67	(20,DON)	27	(20, PON)				
43	(7, IC)	23	(7, OC)								
50	(20, DOC)	71	(20, POC)								

Table 3.8. *Continued*

C				N				P	
Primary productivity									
433	(2, POC)	350	(2a, POC)	90.7	(3)	75.4	(4)	5.66	(3)
600	(3, POC)	25	(4, PIC)						
500	(4, POC)	766	(7, POC)						
750	(19, POC)	658	(20, POC)						
132	(20, DOC)	516	(21)						
New productivity									
242	(2, POC)	195	(4)	48	(2)	51.8	(4)	0.39	(6, POP)
20.5	(6, DOC)	29.8	(6, POC)	7.2	(6, PON)	7.5	(22)		
125	(19, POC)	123	(20)						
75	(21)	50	(22)						
225	(23)								
f-ratio									
0.54	(2)	0.4	(4)	0.54	(2)	0.7	(4)	0.12	(6)
0.15	(6)	0.17	(19)	0.14	(6)	0.12	(20)		
0.16	(20)	0.15	(21)						
N-fixation									
–				2.37	(3)	1.07	(4)	–	
				0.09	(5)				
Denitrification									
–				3.57	(3,4)	6.39	(5)	–	
				7	(9)				
Net denitrification									
–				3.6	(2)	1.2	(3)	–	
				2.5	(4)	6.3	(5)		
				2.74	(6)	2.88	(20)		

Note: *1:* Meybeck 1982, 1993; *2:* Walsh (1991) and references therein; *2a:* Smith and Hollibaugh 1993; *3:* Mackenzie et al. 1998a, total P; *3a:* Mackenzie et al. 1998a, total P, mostly particulates; *4:* Wollast 1998; *5:* extrapolated from Galloway et al. (1996); *6:* extrapolated from Chen et al. (1999) for the ECS; *7:* Mackenzie et al. 1998b; *8:* Berner 1982; *9:* Middelburg et al. 1996; *10:* Milliman 1993; *11:* Tsunogai et al. 1997; *12:* Holligan and Reiners 1992; *13:* Fox 1991, soluble PIP; *14:* Wollast et al. 1993; *15:* Bolin and Cook 1983; *16:* Kempe 1983; *17:* Michaelis et al. 1986; *18:* Mackenzie 1995; *19:* Knauer 1993; *20:* extrapolated from Walsh (1994) for the Atl. Bight; *21:* Liu et al. (2000); *22:* Brink et al. (1995), net burial and upwelling only; *23:* Chavez and Toggweiler (1995); *24:* Martin and Whitfield (1983); *25:* Berner and Berner (1996); *26:* extrapolated from Seitzinger et al. 2000, for the N. Atl.; *27:* Seitzinger and Kroeze (1998).
* Assuming that half of the dust that falls on the oceans deposits on the shelves.

der ice. This water directly ventilates the surface and upper intermediate waters (Talley and Nagata 1995). Another important process is the import of cold and relatively saline water with σ_θ up to 27.25 from the Sea of Japan (Takizawa 1982).

Recent data further indicate that these high density waters underfeed intensive diapycnal mixing induced by strong tidal currents near the Kuril Islands and accelerate the penetration of anthropogenic gases to the lower part of the intermediate water with a σ_θ as high as 27.6 (Riser et al. 1996; Andreev et al. 1999). Strong, cold winds coupled with intensive vertical mixing and interleaving in the winter enhance the oceanic penetration of excess CO_2 in the Bering Sea, as well as the Sea of Okhotsk. Despite the availability of winter carbonate data for the eastern Bering Sea, no corresponding data are available for the western Bering Sea near the Kamchatka Peninsula and in the Sea of Okhotsk, where surface seawater is below –1.5 °C in winter at a time when vertical penetration is enhanced, and at the location where subsurface water is believed to be formed.

Such winter data are essential to obtain complete information on the excess CO_2 penetration in the western Bering Sea and in the Sea of Okhotsk. Similarly, winter data for the Barents and Weddell Sea are also lacking because of their precondition of waters important for the Great Conveyor Belt and deep water formation. Although these seas have only a limited capacity to store excess CO_2, they serve as conveyer belts which transport excess CO_2 to the deep oceans. The excess CO_2 budgets can not be studied adequately without knowledge of source water chemistry (Chen 1993). In view of the large capacity of the NPIW and the North Atlantic Deep Water in storing greenhouse gases, these regions must be studied in much detail.

However, even by pulling all available resources together, it is still not possible to measure all parameters in all seasons everywhere. Simplified, worldwide budg-

eting is still necessary. One basic requirement for budgets and processes is to clearly define the objectives of the whole budgeting exercise. The LOICZ program has emphasized the following points: extrapolation of budgets and global integration as a validation check; regional distribution of differences between production (p) and respiration (r); and regionalization and global integration of the difference between nitrogen fixation and denitrification.

The optimal exploitation of the existing budgets needs to be related to the rates derived from process studies. Internal and external validations should be performed whenever possible. The first step in the treatment of budgets should be in the selection of the most promising budgets on the basis of certain criteria; these include: a well-defined morphology with either restricted or open boundaries, or with appropriate information on open-boundary exchanges from other sources, such as dynamic models or direct field observations; adequate monitoring for salinity, nutrients, input and output, and; in the presence of horizontal gradients in the concentrations of salt or nutrient, greater care must be taken to multiply the incoming and outgoing water fluxes with the appropriate concentrations.

All budgets should be subjected to a sensitivity analysis in which the input parameters are varied within realistic limits and are ideally set through observation. Sensitivity analyses ought to be part of the presentation of budgets. Finalized budgets will then need as much validation as possible measuring them against independent results of biogeochemical process studies such as those from Lagrangian, time-dependent biological and physical-biological models (Hoffman 1991). Budget results will also need to be compared with process results wherever possible.

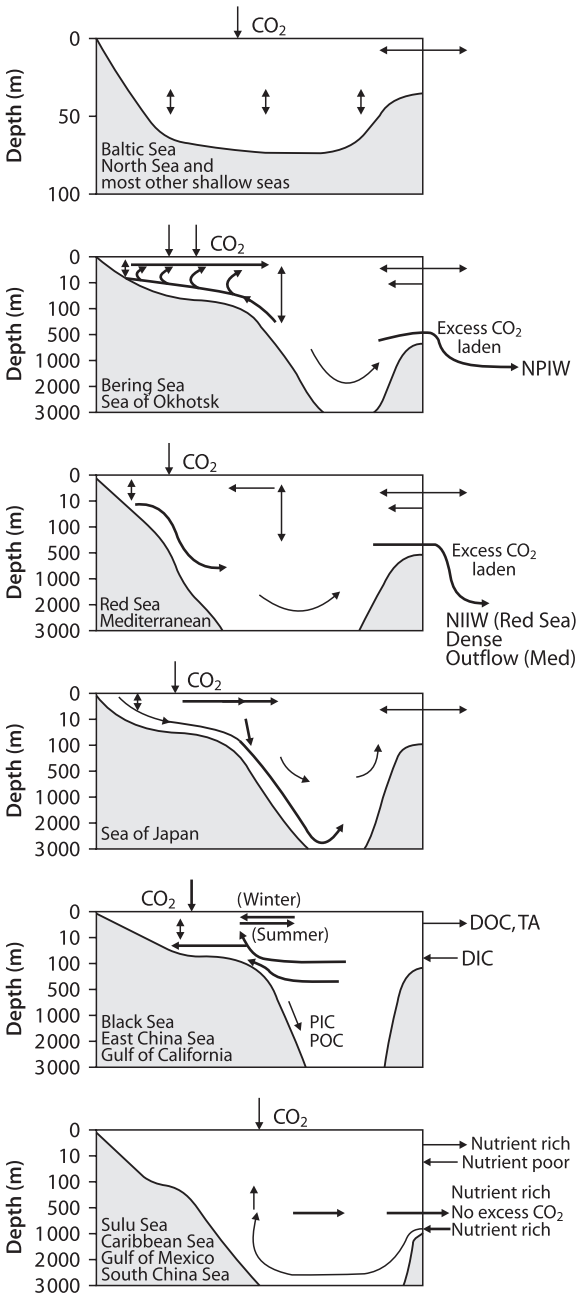

Fig. 3.18. Schematic diagrams of flow patterns in various marginal seas, where *NPIW* denotes the *North Pacific Intermediate Water* and the NIIW the *North Indian Intermediate Water*

3.11.5 Summary

The results of the budget calculations support the conclusions of the SEEP-II study that the hypothesis of the export of a large proportion of the shelf primary productivity is untenable. Only a small fraction of particulate organic carbon, to the order of 5% produced, is exported across the shelf break. The role of DOC is less certain but about 10×10^{12} mol yr^{-1} are exported to the open oceans.

The schematic diagrams of flow patterns of the marginal seas discussed above are given in Fig. 3.18. The Bering Sea and the Sea of Okhotsk do not have very deep water formations but may contribute to the formation of NPIW (Reid 1965, 1973; Talley 1991). The Red and Mediterranean Seas have deep water formations and may contribute to the North Indian Intermediate Water and the dense outflow from the Mediterranean. These processes may thus pump excess CO_2 into the North Pacific, the Indian and the North Atlantic Oceans. The Sea of Japan has deep and bottom water formation but does not export excess CO_2 due to the shallow sills. Sediments in the shelves of these three seas may neutralize excess CO_2 in the latter part of this century when the shelf waters become undersaturated with respect to calcite and aragonite.

The Bering, East China, and North Seas absorb a large amount of CO_2 because of their high productivity which

leads to low pCO_2. Yet the East and South China Seas, and for that matter, the Black Sea, the Gulf of California, the Sulu Sea and the Gulf of Mexico, are not important reservoirs for excess CO_2 owing to their small size and upwelling. It is unlikely the sediments will neutralize excess CO_2 in this century, but carbonate will be regenerated from organic matter at the bottom. This regenerated carbonate will be exported to and stored in the pelagic ocean (Tsunogai et al. 1997).

Another emerging issue will be the large-scale diversion of water and development of hydroelectric power in basins such as the Yangtze and Mekong Rivers. The impact of regulating large river systems is not well understood, and an assessment of the potential impact must be undertaken.

Because of mounting human perturbation in the environment, future coastal zones will become stronger sinks for atmospheric CO_2. Since it is not practical to study each and every estuary or marginal sea in the world, generalizations may suffice. Accordingly, the recommendations made by the CMTT are still valid: there is a need to check, validate and carry out sensitivity analyses on the available budgets. However, all budgets are not equal; some budgets have more precise input data and so have more precise output. This degree of precision must be identified in their descriptions. There is a need to compare budget results with process studies in as many locations as possible. One possibly useful comparison would be with direct measurements of p-r and denitrification, and efforts should be made to explore the finer categorization of different shelf systems based on other globally available parameters, such as shelf width and human impact.

Acknowledgments

The authors wish to thank Prof. S. Smith for his assistance. Professors J. Walsh and M. Fasham provided constructive comments. The National Science Council of the ROC supported the preparation of this manuscript (NSC 89-2611-M-110-001).

References

Aagaard K, Carmack EC (1989) The role of sea ice and other fresh water in the Arctic circulation. J Geophys Res 94, C10:14485–14498

Aagaard K, Coachman LK (1975) Toward an ice-free Arctic Ocean. Eos 56, 7:484–486

Aagaard K, Swift JH, Carmack EC (1985) Thermohaline circulation in the Arctic and Mediterranean Seas. J Geophys Res 90, C3:4833–4846

Alvarez-Salgado XA, Castro CG, Perez FF, Fraga F (1997) Nutrient mineralization patterns in shelf waters of the Western Iberian upwelling. Cont Shelf Res 17:1247–1270

Anderson LG, Dyrssen DW, Jones EP, Lowings MG (1983) Inputs and outputs of salt, fresh water, alkalinity and silica in the Arctic Ocean. Deep-Sea Res 30:87–94

Anderson LG, Olsson K, Chierici M (1998) A carbon budget for the Arctic Ocean. Global Biogeochem Cy 12, 3:455–465

Andreev AG, Bychkov AS, Zhabin IA (1999) Excess CO_2 penetration in the Okhotsk Sea. Extended abstract, 2nd International Symposium on CO_2 in the Oceans. National Institute of Environmental Studies, Tsukuba, January 18–22, 1999, pp 21–05

Andreev A, Honda M, Kumamoto Y, Kusakabe M, Murata A (2001) The excess CO_2 and pH excess in the intermediate water layer of the Northwestern Pacific. J Oceanogr 57:177–188

Antia AN, Bondungen BV, Peinert R (1999) Particle flux across the mid-European continental margin. Deep-Sea Res Pt I 46: 1999–2024

Are FE (1999) The role of coastal retreat for sedimentation in the Laptev Sea. In: Kassens H, Bauch HA, Dmitrenko I, Eicken H, Hubberten HW, Melles M, Thiede J, Tomokhov L (eds) Land-ocean systems in the Siberian Arctic: dynamics and history. Springer-Verlag, Heidelberg, pp 287–295

Bakker DCE (1998) Process studies of the air-sea exchange of carbon dioxide in the Atlantic Ocean. Dissertation, Netherlands Institute of Sea Research, 220 pp

Barber RT, Smith RL (1981) Coastal upwelling ecosystems. In: Longhurst AR (ed) Analysis of marine ecosystem. Academic Press, N.Y, pp 31–68

Barrie L, Falck E, Gregor D, Iverson T, Loeng H, Macdonald R, Pfirman S, Skotvold T, Wartena E (1998) The influence of physical and chemical processes on contaminant transport into and within the Arctic. In: Gregor D, Barrie L, Loeng H (eds) The AMAP assessment. Arctic Monitoring and Assessment Programme, pp 25–116

Barton ED (1998) Eastern boundary of the North Atlantic: Northwest Africa and Iberia. In: Robinson AR, Brink KH (eds) The sea, vol. 11. John Wiley & Sons, New York, pp 633–657

Bauch D, Carstens J, Wefer G, Thiede J (2000) The imprint of anthropognic CO_2 in the Arctic Ocean: evidence from planktic $\delta^{13}C$ data from water column and sediment surfaces. Deep-Sea Res Pt II 47:1791–1808

Bauer JE, Druffel ERM (1998) Ocean margins as a significant source of organic matter to the deep open-ocean. Nature 392:482–485

Berelson WM, McManus J, Coale KH, Johnson KS, Kilgore T, Burdige D, Pilskaln C (1996) Biogenic matter diagensis on the sea floor: a comparison between two continental margin transects. J Mar Res 54:731–762

Berner EK, Berner RA (1996) Global environment. Prentice Hall, Upper Saddle River, N.J., 376 pp

Berner RA (1982) Burial of organic carbon and pyrite sulfur in the modern ocean: its geochemical and environmental significance. Am J Sci 282:451–473

Berner RA (1992) Comments on the role of marine sediment burial as a repository for anthropogenic CO_2. Global Biogeochem Cy 6:1–2

Bethoux JP, Gentili B, Tailliez D (1998a) Warming and freshwater budget change in the Mediterranean since the 1940s, their possible relation to the greenhouse effect. Geophys Res Lett 25: 1023–1026

Bethoux JP, Morin P, Chaumery C, Connan O, Gentili B, Ruiz-Pino D (1998b) Nutrients in the Mediterranean Sea, mass balance and statistical analysis of concentrations with respect to environmental change. Mar Chem 63:155–169

Biscaye PE, Flagg CN, Falkowski PG (1994) The Shelf Edge Exchange Processes experiment, SEEP-II: an introduction to hypotheses, results and conclusions. Deep-Sea Res Pt II 41:231–252

Björk G (1990) The vertical distribution of nutrients and oxygen 18 in the upper Arctic Ocean. J Geophys Res 95, C9:16025–16036

Bolin B (1977) Changes of land biota and their importance for the carbon cycle. Science 196:613–615

Bolin T, Cook RB (1983) The major biogeochemical cycles and their interactions. John Wiley & Sons, New York, 532 pp

Bourke RH, Garrett RP (1987) Sea ice thickness distribution in the Arctic Ocean. Cold Reg Sci Technol 13:259–280

Brink KH (1998) Wind driven currents over the continental shelf. In: Brink K, Robinson A (eds) The sea, vol. 10. John Wiley & Sons, New York, pp 3–20

Brink KH, Cowles TJ (1991) The coastal transition zone program. J Geophys Res 96:14637–14647

Brink KH, Abrantes FFG, Bernal PA, Dugdale RC, Estrada M, Hutchings L, Jahnke RA, Muller PJ, Smith RL (1995) Group Report: How do coastal upwelling systems operate as integrated physical, chemical, and biological systems and influence the geological record? The role of physical processes in defining the spatial structures of biological and chemical variables. In: Summerhayes CP, Emeis KC, Angel MV, Smith RL, Zeitzschel B (eds) Upwelling in the ocean: modern processes and ancient records. John Wiley & Sons, Chichester, pp 103–124

Burkill PH (1999) ARABESQUE: an overview. Deep-Sea Res Pt II 46:529–547

Calvert SE, Price NB (1971) Upwelling and nutrient regeneration in the Benguela Current, October 1968. Deep-Sea Res 18:505–523

Carmack EC, Aagaard K, Swift JH, Macdonald RW, McLaughlin FA, Jones EP, Perkin RD, Smith J, Ellis K, Kilius LK (1997) Rapid changes of water properties and contaminants within the Arctic Ocean. Deep-Sea Res Pt II 44:1487–1502

Carpenter R (1987) Has man altered the cycling of nutrients and organic C on the Washington continental shelf and slope? Deep-Sea Res 34:881–896

Chapman P, Shannon LV (1985) The Benguela ecosystem. Part II. Chemistry and related processes. In: Barnes M (ed) Oceanography and marine biology: an annual review, vol. 23. Aberdeen University Press, Aberdeen, Scotland, pp 183–251

Chavez FP (1995) A comparison of ship and satellite chlorophyll from California and Peru. J Geophys Res 100:24855–24862

Chavez FP, Barber RT (1987) An estimate of new production in the equatorial Pacific. Deep-Sea Res 34:1229–1243

Chavez FP, Toggweiler JR (1995) Physical estimates of global new production. In: Summerhayes CP, Emeis KC, Angel MV, Smith RL, Zeitzschel B (eds) Upwelling in the ocean: modern processes and ancient records. John Wiley & Sons, Chichester, pp 103–124

Chavez FP, Barber RT, Sanderson MP (1989) The potential primary production of the Peruvian upwelling ecosystem, 1953–1984. In: Pauly D, Muck P, Mendo J, Tsukayama I (eds) The Peruvian upwelling system: dynamics and interactions. Instituto del Mar del Peru, Callao, Peru, ICLARM Conference Proceedings 18:50–63

Chavez FP, Barber RT, Kosro PM, Huyer A, Ramp SR, Stanton TP, de Mendiola BR (1991) Horizontal transport and distribution of nutrients in the coastal transition zone off northern California: effect on primary production, phytoplankton biomass and species composition. J Geophys Res 96:14833–14848

Chen CT (1985) Preliminary observations of oxygen and carbon dioxide of the wintertime Bering Sea marginal ice zone. Cont Shelf Res 4:465–483

Chen CT (1988) Summer-winter comparisons of oxygen, nutrients and carbonates in the polar seas. La mer 26:1–11

Chen CTA (1990) Decomposition rate of calcium carbonate and organic carbon in the North Pacific Ocean. Journal of Oceanographical Society of Japan 46:201–210

Chen CTA (1993) Carbonate chemistry of the wintertime Bering Sea marginal ice zone. Cont Shelf Res 13:67–87

Chen CTA (1996) The Kuroshio Intermediate Water is the major source of nutrients on the East China Sea continental shelf. Oceanol Acta 1:523–7

Chen CTA (2000) The Three Gorges Dam: reducing the upwelling and thus productivity of the East China Sea. Geophys Res Lett 27:381–383

Chen CTA, Huang MH (1995) Carbonate chemistry and the anthropogenic CO_2 in the South China Sea. Acta Oceanologica Sinica 14:47–57

Chen CTA, Tsunogai S (1998) Carbon and nutrients in the ocean. In: Galloway JN, Melillo JM (eds) Asian change in the context of global climate change. Cambridge University Press, pp 271–307

Chen CTA, Wang SL (1999) Carbon, alkalinity and nutrient budget on the East China Sea continental shelf. J Geophys Res 104: 20675–20686

Chen CTA, Pytkowicz RM, Olson EJ (1982) Evaluation of the calcium problem in the South Pacific. Geochem J 16:1–10

Chen CTA, Holligan P, Hong HS, Iseki K, Krishnaswami S, Wollast R, Yoder J (1994) Land-ocean interactions in the coastal zone. JGOFS Report No. 15, SCOR, 20 pp

Chen CTA, Wang SL, Bychkov AS (1995a) Carbonate chemistry of the Sea of Japan. J Geophys Res 100:13737–13745

Chen CTA, Ruo R, Pai SC, Liu CT, Wong GTF (1995b) Exchange of water masses between the East China Sea and the Kuroshio off northeastern Taiwan. Cont Shelf Res 15:19–39

Chen CTA, Gong GC, Wang SL, Bychkov AS (1996a) Redfield ratios and regeneration rates of particulate matter in the Sea of Japan as a model of closed system. Geophys Res Lett 23:1785–1788

Chen CTA, Lin CM, Huang BT, Chang LF (1996b) The stoichiometry of carbon, hydrogen, nitrogen, sulfur and oxygen in particular matter of the Western North Pacific marginal seas. Mar Chem 54:179–190

Chen CTA, Bychkov AS, Wang SL, Pavlova GYu (1999) An anoxia Sea of Japan by the year 2200? Mar Chem 67:249–265

Chen CTA, Wann JK, Luo JY (2001a) Aeolian flux of trace metals in Taiwan over the past 2 600 years. Chemosphere 43:287–294

Chen CTA, Wang SL, Wang BJ (2001b) Nutrient budgets for the South China Sea basin. Mar Chem 75:281–300

Christensen JP (1994) Carbon export from continental shelves, denitrification and atmospheric carbon dioxide. Cont Shelf Res 14:547–576

Christensen JP, Smethie WM, Devol AH (1987) Benthic nutrient regeneration and denitrification on the Washington continental shelf. Deep-Sea Res 34:1027–1047

Codispoti LA, Christensen JP (1985) Nitrification, denitrification and nitrous oxide cycling in the Eastern Tropical Pacific Ocean. Mar Chem 16:277–300

Codispoti LA, Friederich GE (1978) Local and mesoscale influences on nutrient variability in the northwest African upwelling region near Cabo Corbeiro. Deep-Sea Res 25:751–770

Codispoti LA, Lowman D (1973) A reactive silicate budget for the Arctic Ocean. Limnol Oceanogr 18:448–456

Codispoti LA, Packard TT (1980) Denitrification rates in the eastern tropical South Pacific. J Mar Res 38:453–477

Codispoti LA, Richards FA (1968) Micronutrient distributions in the East Siberian and Laptev Seas during summer, 1963. Arctic 21:61–83

Codispoti LA, Friederich GE, Hood DW (1986) Variability in the inorganic carbon system over the southeastern Bering Sea shelf during spring 1980 and spring–summer 1981. Cont Shelf Res 5:133–160

Cota GF, Prinsenberg SJ, Bennett EB, Loder JW, Lewis MR, Anning JL, Watson NHF, Harris LR (1987) Nutrient fluxes during extended blooms of Arctic ice algae. J Geophys Res 92:C2, 1951–1962

Cota GF, Anning JL, Harris LR, Harrison WG, Smith REH (1990) Impact of ice algae on inorganic nutrients in seawater and sea ice in Barrow Strait, NWT, Canada, during spring. Can J Fish Aquat Sci 47:1402–1415

Csanady GT (1990) Physical basis of coastal productivity – the SEEP and MASAR Experiments. Eos, Transactions, American Geophysical Union, 71:1060–1061, 36:1064–1065

Cuffey KM, Clow GD, Alley RB, Stuiver M, Waddington ED, Saltus RW (1995) Larger Arctic temperature change at the Wisconsin-Holocene Glacial transition. Science 270:455–458

de Haas H (1997) Transport, preservation and accumulation of organic carbon in the North Sea. Dissertation, University of Utrecht. 149 pp

de Haas H, Boer WD, Van Weering TCE (1997) Recent sedimentation and organic carbon burial in a shelf sea: the North Sea. Mar Geol 144:131–146

Degens ET, Kempe S, Richey JE (1991) Summary: biogeochemistry of major world rivers. In: Degens ET, Kempe S, Richey JE (eds) Biogeochemistry of Major World Rivers. SCOPE Report 42, John Wiley & Sons, Chichester, pp 323–347

Dethleff D (1995) Sea ice and sediment export from the Laptev Sea flaw lead during 1991/92 winter season. In: Kassens H, Piepenburg D, Thiede J, Timokhov L, Hubberton H-W, Priamikov SM (eds) Berichte zur Polarforschung. pp 78–93

Deuser WG (1975) Reducing environments. In: Riley JP, Skirrow G (eds) Chemical Oceanography, vol. 3, 2nd Ed. Academic Press, N.Y, pp 1–37

Devol AH (1991) Direct measurement of nitrogen gas fluxes from continental shelf sediments. Nature 349:319–321

Devol AH, Codispoti LA, Christensen JP (1997) Summer and winter denitrification rates in western Arctic shelf sediments. Cont Shelf Res 17:1029–1050

Dickson R (1999) All change in the Arctic. Nature 397:38–40
Eicken H, Kolatschek J, Lindemann F, Dmitrenko I, Freitag J, Kassens H (2000) A key source area and constraints on entrainment for basin scale sediment transport by Arctic sea ice. Geophys Res Lett 26:1919–1922
Everett JT, Fitzharris BB, Maxwell B (1997) The Arctic and the Antarctic. In: Watson RT, Zinyowera MC, Moss RH (eds) The Intergovernmental Panel on Climate Change (IPCC) special report on the regional impacts of climate change. Cambridge University Press, pp 85–103
Fanning KA (1992) Nutrient provinces in the sea: concentration ratios, reaction rate ratios, and ideal conversion. J Geophys Res 97:5693–5712
FAO (1996) Fishery statistics capture production. vol. 82
Fox LE (1991) Phosphorus chemistry in the tidal Hudson River. Geochim Cosmochim Ac 55:1529–1538
Feely RA, Chen CT (1982) The effect of excess CO_2 on the calculated calcite and aragonite saturation horizons in the northeast Pacific. Geophys Res Lett 9:1294–1297
Friederich G, Sakamoto CM, Pennington JT, Chavez FP (1995) On the direction of the air-sea flux of CO_2 in coastal upwelling systems. In: Tsunogai S, Iseki K, Koike I, Oba T (eds) Global fluxes of carbon and its related substances in the coastal sea-ocean-atmosphere system. M & J International, Yokohama, pp 438–445
Fyfe JC, Boer GL, Flato GM (1999) The Arctic and Antarctic oscillations and their projected changes under global warming. Geophys Res Lett 26:1601–1604
Galloway JN, Schlesinger WH, Levy H II, Michaels A, Schnoor JL (1995) Nitrogen fixation: anthropogenic enhancement – environmental response. Global Biogeochem Cy 9:235–52
Galloway JN, Howarth RW, Michaels AF, Nixon SW, Prospero JM, Dentener FJ (1996) Nitrogen and phosphorus budgets of the North Atlantic Ocean and its watershed. Biogeochemistry 35:3–25
Gerdes R, Schauer U (1997) Large-scale circulation and water mass distribution in the Arctic Ocean from model results and observations. J Geophys Res 102, C4:8467–8483
Gobeil C, Paton D, McLaughlin FA, Macdonald RW, Paquette G, Clermont Y, Lebeuf M (1991) Donnés géochimiques sur les eaux interstitielles et les sédiments de la mer de Beaufort. Institut Maurice-Lamontagne, Rapport statistique canadien sur l'hydrographie et les sciences oceaniques, 101, 92 pp
Goldner DR (1999a) On the uncertainty of the mass, heat and salt budgets of the Arctic Ocean. J Geophys Res 104, C12: 29757–29770
Goldner DR (1999b) Steady models of Arctic shelf-basin exchange. J Geophys Res 104:C12, 29733–29755
Gordeev VV (2000) River input of water, sediment, major ions, nutrients and trace metals from Russian territory to the Arctic Ocean. In: Lewis EL, Jones EP, Lemke P, Prowse TD, Wadhams P (eds) The freshwater budget of the Arctic Ocean. NATO Science Series 2. Environmental Security – vol. 70. Klewer Academic Publishers, pp 297–321
Gordeev VV, Martin JM, Sidorov IS, Sidorova MV (1996) A reassessment of the Eurasian river input of water, sediment, major elements, and nutrients to the Arctic Ocean. Am J Sci 296: 664–691
Gordon DC Jr., Boudreau PR, Mann KH, Ong JE, Silvert WL, Smith SV, Wattayakorn G, Wulff F, Yanagi T (1996) LOICZ biogeochemical modelling guidelines. LOICZ Report and Studies, No. 5, 96 pp
Gorshkov VG (1995) Physical and biological bases of life stability. Springer-Verlag, Berlin, 340 pp
Goyet C, Millero FJ, O'Sullivan DW, Eischeid G, McCue SJ, Bellerby RGJ (1998) Temporal variations of pCO_2 in surface seawater of the Arabian Sea in 1995. Deep-Sea Res Pt I 45:609–623
Grantz A, Phillips RL, Jones GA (1999) Holocene pelagic and turbidite sedimentation rates in the Amerasia Basin, Arctic Ocean from radiocarbon age-depth profiles in cores. GeoResearch Forum 5:209–222
Grebmeier JM, Whitledge TE (1996) Arctic system science ocean-atmosphere-ice interactions biological initiative in the Arctic: shelf-basin interactions workshop. ARCSS/OAII Report No. 4
Gruber N, Sarmiento JL (1997) Global patterns of marine nitrogen fixation and denitrification. Global Biogeochem Cy 11:235–266
Hall J, Smith SV, Boudreau PR (eds) (1996) International Workshop on Continental Shelf Fluxes of Carbon, Nitrogen and Phosphorus. LOICZ Reports & Studies, No. 9. Texel, The Netherlands
Hansell DA, Peltzer ET (1998) Spatial and temporal variations of total organic carbon in the Arabian Sea. Deep-Sea Res Pt II 45:2171–2193
Hanzlick D, Aagaard K (1980) Freshwater and Atlantic water in the Kara Sea. J Geophys Res 85:4937–4942
Harms IH, Karcher MJ (1999) Modeling the seasonal variability of hydrography and circulation in the Kara Sea. J Geophys Res 104, C6:13431–13448
Hickey BM (1998) Oceanography of western North America from the tip of Baja California to Vancouver Island. In: Brink K, Robinson A (eds) The Sea, vol. 11. John Wiley & Sons, New York, pp 273–313
Hill AE, Hickey BM, Shillington FA, Strub PT, Brink KH, Barton ED, Thomas AC (1998) Eastern Ocean boundaries. In: Robinson AR, Brink KH (eds) The Sea, vol 11. John Wiley & Sons, New York, pp 29–67
Hoffman EE (1991) How do we generalize coastal models to global scale? In: Mantoura RFC, Martin JM, Wollast R (eds) Ocean margin processes in global change. John Wiley & Sons, Chichester, pp 401–417
Holligan PM, Reiners WA (1992) Predicting the responses of the coastal zone to global change. Adv Ecol Res 22:211–55
Honjo S (1997) The rain of ocean particles and earth's carbon cycle. Oceanus 40, 2:4–7
Houghton JT, Meira Filho LG, Callander BA, Harris N, Kattenberg A, Maskell K (1995) Climate change 1995: the science of climate change. Intergovernmental Panel on Climate Change, Cambridge, 572 pp
Hsu KJ (1991) Fractal theory and time dependency in ocean margin processes. In: Mantoura RFC, Martin JM, Wollast R (eds) Ocean margin processes in global change. John Wiley & Sons, New York, pp 235–250
Hung JJ, Lin PL, Liu KK (2000) Dissolved and particulate organic carbon in the southern East China Sea. Cont Shelf Res 20:545–569
Huthnance JM (1995) Circulation, exchange and water masses at the ocean margin: the role of physical processes at the shelf edge. Prog Oceanogr 35:353–431
Jahnke RA, Shimmield GB (1995) Particle flux and its conversion to the sediment record: coastal upwelling systems. In: Summerhayes CP, Emeis KC, Angel MV, Smith RL, Zeitzschel B (eds) Upwelling in the ocean: modern processes and ancient records. John Wiley & Sons, New York, pp 83–100
JGOFS (1997) Report of the JGOFS/LOICZ Workshop on non-conservative fluxes in the continental margins. JGOFS Report No. 25, LOICZ International Project Office, Texel, The Netherlands, 25 pp
Johnson KS, Chavez FP, Friederich GE (1999) Continental-shelf sediment as a primary source of iron for coastal phytoplankton. Nature 398:697–700
Kämpf J, Backhaus JO, Fohrmann H (1999) Sediment-induced slope convection: Two-dimensional numerical case studies. J Geophys Res 104, C9:20509–20522
Kao SJ, Liu KK (1996) Particulate organic carbon export from the watershed of a subtropical mountainous river (Lanyang Hsi) in Taiwan. Limnol Oceanogr 41:1749–1757
Kashgarian M, Tanaka N (1991) Antarctic intermediate water intrusion into South Atlantic Bight shelf waters. Cont Shelf Res 11:197–201
Kassens H, Dmitrenko I, Rachold V, Thiede J, Tiimokhov L (1998) Russian and German scientists explore the Arctic's Laptev Sea and its climate system. Eos, Transactions, American Geophysical Union, 79, 27, 317, 322–323
Kemp PF (1994) Microbial carbon utilization on the continental shelf and slope during the SEEP-II experiment. Deep-Sea Res Pt II 41:563–581
Kempe S (1983) Carbon in the freshwater cycle. In: Bolin B, Degens ET, Kempe S, Ketner P (eds) The global carbon cycle. John Wiley & Sons, New York, pp 317–342
Kempe S (1995) Coastal seas: a net source of sink of atmospheric carbon dioxide? LOICZ Report and Studies, No. 1, LOICZ International Project Office, Texel, The Netherlands, 27 pp

Kempe S, Pegler K (1991) Sinks and sources of CO_2 in coastal seas: the North Sea. Tellus 43:224–235
Knauer GA (1993) Productivity and new production of the oceanic system. In: Wollast R, Mackenzie FT, Chou L (eds) Interactions of C, N, P and S biogeochemicaly cycles and global change. Springer-Verlag, Berlin, pp 211–231
Korso PM, Huyer A (1986) CTD and velocity surveys of seaward jets off northern California, July 1981 and 1982. J Geophys Res 93:7680–7690
Kortzinger A, Duinker JC, Mintrop L (1997) Strong CO_2 emissions from the Arabian Sea during south-west monsoon. Geophys Res Lett 24:1763–1766
Krumgalz BS, Erez J, Chen CTA (1990) Anthropogenic CO_2 penetration in the northern Red Sea and in the Gulf of Elat. Oceanol Acta 13:283–290
Kudela RM, Chavez FP (2000) Modeling the impact of the 1992 El Niño on new production in Monterey Bay, California. Deep-Sea Res Pt II 47:1055–1076
Kurashina S, Nishida K, Nakabayashi S (1967) On the open water in the southeastern part of the frozen Okhotsk Sea and the current through the Kuril Islands. Journal of Oceanographical Society of Japan 23:57–71
Kvenvolden KA, Lilley MD, Lorenson TD (1993) The Beaufort Sea continental shelf as a seasonal source of atmospheric methane. Geophys Res Lett 20:2459–2462
Liu KK, Kaplan IR (1982) Nitrous oxide in the sea off Southern California. In: Ernst WG, Morin JG (eds) The environment of the deep sea. Prentice-Hall, pp 73–92
Liu KK, Kaplan IR (1984) Denitrification rates and availability of organic matter in marine environments. Earth Planet Sc Lett 68:88–100
Liu KK, Kaplan IR (1989) Eastern tropical Pacific as a source of ^{15}N-enriched nitrate in seawater off southern California. Limnol Oceanogr 34:820–830
Liu KK, Lai ZL, Gong GC, Shiah FK (1995) Distribution of particulate organic matter in the southern East China Sea: implications in production and transport. Terr Atmos Ocean Sci 6:27–45
Liu KK, Su MJ, Hsueh CR, Gong GC (1996) The nitrogen isotopic composition of nitrate in the Kuroshio Water northeast of Taiwan: evidence for nitrogen fixation as a source of isotopically light nitrate. Mar Chem 54:273–292
Liu KK, Iseki K, Chao SY (2000) Continental margin carbon fluxes. In: Hanson RB, Ducklow HW, Field JG (eds) The changing ocean carbon cycle: a midterm synthesis of the Joint Global Ocean Flux Study. International Geosphere-Biosphere Programme Book Series, Cambridge University Press, Cambridge, pp 187–239
Loeng H, Ozhigin V, Adlandsvik B (1997) Water fluxes through the Barents Sea. Ices J Mar Sci 54:310–317
Longhurst A (1998) Ecological geography of the sea. Academic Press, San Diego, 398 pp
Longhurst AR, Sathyendranath S, Platt T, Caverhill C (1995) An estimation of global primary production in the ocean from satellite radiometer data. J Plankton Res 17:1245–1271
Lundberg L, Haugan PM (1996) A Nordic seas-Arctic Ocean carbon budget from volume flows and inorganic carbon data. Global Biogeochem Cy 10:493–510
Macdonald RW (1996) Awakenings in the Arctic. Nature 380:286–287
Macdonald RW (2000) Arctic estuaries and ice: a positive-negative estuarine couple. In: Lewis EL (ed) The freshwater budget of the Arctic Ocean. NATO Science Series, vol. 70, pp 383–407
Macdonald RW, Wong CS, Erikson PE (1987) The distribution of nutrients in the southeastern Beaufort Sea: implications for water circulation and primary production. J Geophys Res 92:2939–2952
Macdonald RW, Paton DW, Carmack EC, Omstedt A (1995) The freshwater budget and under-ice spreading of Mackenzie River water in the Canadian Beaufort Sea based on salinity and $^{18}O/^{16}O$ measurements in water and ice. J Geophys Res 100:895–919
Macdonald RW, Solomon SM, Cranston RE, Welch HE, Yunker MB, Gobeil C (1998) A sediment and organic carbon budget for the Canadian Beaufort Shelf. Mar Geol 144:255–273
Macdonald RW, Carmack EC, McLaughlin FA, Falkner KK, Swift JH (1999) Connections among ice, runoff and atmospheric forcing in the Beaufort Gyre. Geophys Res Lett 26:2223–2226
Macdonald RW, Barrie LA, Bidleman TF, Diamond ML, Gregor DJ, Semkin RG, Strachan WMJ, Li YF, Wania F, Alaee M, Alexeeva LB, Backus SM, Bailey R, Bewers JM, Gobeil C, Halsall CJ, Harner T, Hoff JT, Jantunen LMM, Lockhart WL, Mackay D, Muir DCG, Pudykiewicz J, Reimer KJ, Smith JN, Stern GA, Schroeder WH, Wagemann R, Yunker MB (2000) Sources, occurrence and pathways of contaminants in the Canadian Arctic: a review. Sci Total Environ 254:93–234
Mackenzie FT (1995) Biogeochemistry. In: Encyclopedia of environmental biology. Academic Press, London, pp 249–276
Mackenzie FT, Lerman A, Ver LMB (1998a) Role of continental margin in the global carbon balance during the past three centuries. Geology 26:423–426
Mackenzie FT, Ver LMB, Lerman A (1998b) Coupled biogeochemical cycles of carbon, nitrogen, phosphrous and sulfur in the land-ocean-atmosphere system. In: Galloway JN, Melillo JM (eds) Asian change in the context of global climate change. Cambridge University Press., pp 42–100
Mantoura RFC, Martin JM, Wollast R (eds) (1991) Ocean margin processes in global change. John Wiley & Sons, New York, 469 pp
Marchant M, Hebbeln D, Wefer G (1998) Seasonal flux patterns of planktonic foraminifera in the Peru-Chile Current. Deep-Sea Res Pt I 45:1161–1185
Martin JM, Whitfield M (1983) The significance of the river input of chemical elements to the ocean. In: Wong CS, Boyle E, Bruland K, Burton JD, Goldberg ED (eds) Trace metals in sea water. Plenum Press, pp 265–296
Martin JH, Knauer GA, Karl DM, Broenkow WW (1987) VERTEX: carbon cycling in the north Pacific. Deep-Sea Res 34:267–285
Maslanik JA, Serreze MC, Barry RG (1996) Recent decreases in Arctic summer ice cover and linkages to atmospheric circulation anomalies. Geophys Res Lett 23:1677–1680
McLaughlin FA, Carmack EC, Macdonald RW, Bishop JKB (1996) Physical and geochemical properties across the Atlantic/Pacific water mass boundary in the southern Canadian Basin. J Geophys Res 101, C1:1183–1197
Melling H (1993) The formation of a haline shelf front in wintertime in an ice-covered Arctic sea. Cont Shelf Res 13:1123–1147
Melling H, Lewis EL (1982) Shelf drainage flows in the Beaufort Sea and their effect on the Arctic Ocean pycnocline. Deep-Sea Res 29:967–985
Mel'nikov IA, Pavlov GL (1978) Characteristics of organic carbon distribution in the waters and ice of the Arctic Basin. Oceanology+ 18:163–167
Meybeck M (1982) Carbon, nitrogen and phosphorus transport by world rivers. Am J Sci 282:401–50
Meybeck M (1993) Natural sources of C, N, P, and S. In: Wollast R (ed) Interactions of C, N, P, and S biogeochemical cycles and global change. Springer-Verlag, Berlin, pp 163–93
Michaelis W, Ittekkot V, Degens ET (1986) River inputs into oceans. In: Lesserre P, Martin JM (eds) Biogeochemical processes at the land-sea boundary. Elsevier, pp 37–52
Michaels AF, Karl DM, Knap AH (2000) Temporal studies of biogeochemical dynamics in oligotrophic oceans. In: Hanson RB, Ducklow HW, Field JG (eds) The changing ocean carbon cycle: a midterm synthesis of the Joint Global Ocean Flux Study. Cambridge University Press, Cambridge, pp 392–416
Middelburg JJ, Soetaert K, Herman DMJ, Heip CHR (1996) Denitrification in marine sediments: a model study. Global Biogeochem Cy 10:661–673
Miller JR, Russell GL (1992) The impact of global warming on river runoff. J Geophys Res 97:2757–2764
Milliman JD (1993) Production and accumulation of calcium-carbonate in the ocean – budget of a nonsteady state. Global Biogeochem Cy 7:927–957
Milliman JD, Rutkowski C, Meybeck M (1995) River discharge to the sea: a global river index (GLORI). LOICZ Reports & Studies, No. 2. LOICZ International Project Office, Texel, The Netherlands, 125 pp
Minas HJ, Minas M, Packard TT (1986) Productivity in upwelling areas deduced from hydrographic and chemical fields. Limnol Oceanogr 31:1182–1206
Miquel JC, Fowler SW, La Rosa J (2000) Seasonal and interannual variations of particle and carbon fluxes in the open NW Mediterranean: 10 years of sediment trap measurements at the Dyfamed station, JGOFS Open Science Meeting, Bergen, 13–18 April, 2000

Monaco A, Biscaye P, Soyer J, Pocklington R, Heussner S (1990) Particle fluxes and ecosystem response on a continental margin: the 1985–1988 Mediterranean ECOMARGE experiment. Cont Shelf Res 10:959–987
Morales CE, Blanco JL, Braun M, Reyes H, Silva N (1996) Chlorophyll-*a* distribution and associated oceanographic conditions in the upwelling regions off northern Chile during the winter and spring 1993. Deep-Sea Res Pt I 43:267–289
Murray JW, Top Z, Ozsoy E (1991) Hydrographic properties and ventilation of the Black Sea. Deep-Sea Res 38, (suppl.) 2:S663–689
Naqvi SWA (1987) Some aspects of the oxygen-deficient conditions and denitrification in the Arabian Sea. J Mar Res 45:1049–1072
Nelson G, Hutchings L (1983) The Benguela upwelling area. Prog Oceanogr 12:333–356
Nittrouer CA, Brunskill GJ, Figueiredo AG (1995) Importance of tropical coastal environments. Geo-Mar Lett 15:121–126
Nixon SW, Ammerman JW, Atkinson LP, Berounsky VM, Billen G, Boicourt WC, Boynton WR, Church TM, Ditoro DM, Elmgren R, Garber JH, Giblin AE, Jahnke RA, Owens NJP, Pilson MEQ, Seitzinger SP (1996) The fate of nitrogen and phosphorus at the land-sea margin of the North Atlantic Ocean. Biogeochemistry 35:141–180
Nojiri Y, Nojiri T, Machida T, Inoue G, Fujinuma M (1997) Meridional distribution and secular trend of atmospheric nitrous oxide concentration over the Western Pacific. In: Tsunogai S (ed) Biogeochemical processes in the North Pacific. Japan Marine Science Foundation, Tokyo, pp 115–118
Nozaki Y, Oba T (1995) Dissolution of calcareous tests in the ocean and atmospheric carbon dioxide. In: Sakai H, Nozaki Y (ed) Biogeochemical processes and ocean flux in the Western Pacific. Terra Scientific Publishing Company, Tokyo, pp 83–92
Oguz T, Ducklow HW, Purcell JE, Malanotte-Rizzoli P (2001) Simulation of recent change in the Black Sea pelagic food web structure due to top-down control by gelatinous carnivores. J Geophy Res 106:4543–4564
Olsson K, Anderson LG (1997) Input and biogeochemical transformation of dissolved carbon in the Siberian shelf seas. Cont Shelf Res, 17, 819–833
Opsahl S, Benner R, Amon RMW (1999) Major flux of terrigenous dissoved organic matter through the Arctic Ocean. Limnol Oceanogr 44:2017–2023
Pace ML, Knauer GA, Karl DM, Martin JH (1987) Primary production, new production and vertical flux in the eastern Pacific Ocean. Nature 325:803–804
Pavlov VK, Pfirman SL (1995) Hydrographic structure and variability of the Kara Sea: implications for pollutant distribution. Deep-Sea Res Pt II 42:1369–1390
Pérez Fiz F, Aida F Ríos, Rosón G (1999) Sea surface carbon dioxide off the Iberian Peninsula (North Eastern Atlantic Ocean). J Marine Syst 19:27–46
Peulvé S, Sicre MA, Saliot A, De Leeuw JW, Baas M (1996) Molecular characterization of suspended and sedimentary organic matter in an Arctic delta. Limnol Oceanogr 41:488–497
Pfirman S, Gascard JC, Wollengurg I, Mudie P, Abelmann A (1989) Particle-laden Eurasian Arctic sea ice: observations from July and August 1987. Polar Res 7:59–66
Pfirman SL, Koegeler JW, Rigor I (1997) Potential for rapid transport of contaminants from the Kara Sea. Sci Total Environ 202:111–122
Proshutinsky AY, Johnson MA (1997) Two circulation regimes of the wind-driven Arctic Ocean. J Geophys Res 102:12493–12514
Reid JL (1965) Intermediate waters of the Pacific Ocean. Johns Hopkins Oceanographic Studies 2, The Johns Hopkins University Press, Baltimore, 85 pp
Reid JL (1973) Northwest Pacific Ocean waters in winter. Johns Hopkins Oceanographic Studies 5, The Johns Hopkins University Press, Baltimore, 96 pp
Rigor I, Colony R (1997) Sea-ice production and transport of pollutants in the Laptev Sea, 1979–1993. Sci Total Environ 202:89–110
Riser SC, Yurasov GI, Warner MJ (1996) Hydrographic and tracer measurements of the water mass structure and transport in the Okhotsk Sea in early spring. PICES Science Report 6:138–143
Roach AT, Aagaard K, Pease CH, Salo SA, Weingartner T, Pavlov V, Kulakov M (1995) Direct measurements of transport and water properties through the Bering Strait. J Geophys Res 100: 18443–18457
Rogachev KA, Bychkov AS, Carmack EC, Tishchenko P Ya, Nedashkovsky AP, Wong CS (1997) Regional carbon dioxide distribution near Kashevarov Bank (Sea of Okhotsk): effect of tidal mixing. In: Tsunogai S (ed) Biogeochemical processes in the North Pacific. Japan Marine Science Foundation, Tokyo, pp 52–69
Rothrock DA, Yu Y, Maykut GA (1999) Thinning of the Arctic sea-ice cover. Geophys Res Lett 26:3469–3472
Rowe GT, Smith S, Falkowski P, Whitledge T, Theroux R, Phoel W, Ducklow H (1996) Do continental shelves export organic matter? Nature 324:559–561
Ruttenberg K, Goñi MA (1996) Phosphorus distribution, C:N:P ratios, and δ^{13}COC in arctic, temperate, and tropical coastal sediments: tools for characterizing bulk sedimentary matter. Mar Geol 139:123–145
Sakshaug E, Bjorge A, Gulliksen B, Loeng H, Mehlum F (1994) Structure, biomass distribution, and energetics of the pelagic ecosystem in the Barents Sea: a synopsis. Polar Biol 14:405–411
Sakshaug E, Slagstad D (1992) Sea ice and wind: effects on primary productivity in the Barents Sea. Atmos Ocean 30:579–591
Savidge G, Gilpin L (1999) Seasonal influences on size-fractionated chlorophyll *a* concentrations and primary production in the north-west Indian Ocean. Deep-Sea Res Pt II 46:701–723
Schindler DW, Curtis PJ, Baylery SE, Parker BR, Beaty KG, Stainton MP (1997) Climate induced changes in the dissolved organic carbon budgets of boreal lakes. Biogeochemistry 36:9–28
Schlesinger WH, Melack JM (1981) Transport of organic carbon in the world's rivers. Tellus 33:172–87
Schlosser P, Bauch D, Fairbanks R, Bönisch G (1994) Arctic river-runoff: mean residence time on the shelves and in the halocline. Deep-Sea Res I 41:1053–1068
Schubert CJ, Stein R (1996) Deposition of organic carbon in Arctic Ocean sediments: terrigenous supply vs. marine productivity. Org Geochem 24:421–436
Seitzinger SP, Giblin AE (1996) Estimating denitrification in North Atlantic continental shelf sediments. Biogeochemistry 35:235–260
Seitzinger SP, Kroeze C (1998) Global distribution of nitrous oxide production and N inputs in freshwater and coastal marine ecosystems. Global Biogeochem Cy 12:93–113
Seitzinger SP, Kroeze C, Styles RV (2000) Global distribution of N_2O emissions from aquatic systems: natural emissions and anthropogenic effects. Chemosphere Global Change Science 2:267–279
Semiletov IP (1997) On global change in the north-east Asia and adjacent seas. Reports of the 7th TEACOM Meeting and International Workshop on Global Change Studies in the Far East Asia, Vladivostok, 10–12, November, 1997, Institute of Marine Biology of Far East Branch of Russian Academy of Sciences, Vladivostok, pp 49–88
Shannon LV (1985) The Benguela ecosystem. Part I. Evolution of the Benguela, physical features and processes. In: Barnes M (ed) Oceanography and marine biology: an annual review, vol. 23. Aberdeen University Press, Aberdeen, Scotland, pp 105–182
Sharma GD (1979) The Alaskan Shelf: hydrographic, sedimentary and geochemical environment. Springer-Verlag, New York, 498 pp
Sharma S, Barrie LA, Plummer D, McConnell JC, Brickell PC, Levasseur M, Gosselilin M, Bates TS (1999) Flux estimation of oceanic dimethyl sulfide around North America. J Geophys Res 104:21327–21342
Shaw PT, Chao SY, Liu KK, Pai SC, Liu CT (1996) Winter upwelling off Luzon in the north-eastern South China Sea. J Geophys Res 101:16435–16448
Shiah FK, Liu KK, Gong GC (1999) Temperature vs. substrate limitation of heterotrophic bacterioplankton production across trophic and temperature gradient in the East China Sea. Aquat Microb Ecol 17:247–264
Shiah FK, Gong GC, Liu KK, Kao SJ (2000a) Biological and hydrographic responses to a typhoon in the Taiwan Strait, JGOFS Open Science Meeting, Japan Marine Science Foundation, Tokyo, 13–18 April, 2000
Shiah FK, Liu KK, Gong GC (2000b) The coupling of bacterial production and hydrography in the southern East China Sea north of Taiwan: spatial patterns in spring and fall. Cont Shelf Res 20:459–477
Shillington FA (1998) The Benguela upwelling system off southwestern Africa. In: Robinson AR, Brink KH (eds) The sea, vol. 11. John Wiley & Sons, New York, pp 583–604.

Smith SV, Hollibaugh JT (1993) Coastal metabolism and the oceanic carbon balance. Rev Geophys 31:75–89
Smith SV, Mackenzie FT (1987) The ocean as a net heterotrophic system: Implications from the carbon biogeochemical cycle. Global Biogeochem Cy 1:187–198
Stein R, Grobe H, Wahsner M (1994a) Organic carbon, carbonate, and clay mineral distributions in eastern central Arctic Ocean surface sediments. Mar Geol 119:269–285
Stein R, Schubert C, Vogt C, Futterer D (1994b) Stable isotope stratigraphy, sedimentation rates, and salinity changes in the Latest Pleistocene to Holocene eastern central Arctic Ocean. Mar Geol 119:333–355
Stein R, Fahl K, Niessen F, Siebold M (1999) Late Quarternary organic carbon and biomarker records from the Laptev Sea continental margin (Arctic Ocean): implications for organic carbon flux and composition. In: Kassens H, Bauch HA, Dmitrenko I, Eicken H, Hubberten HW, Melles M, Thiede J, Tomokhov L (eds) Land-ocean systems in the Siberian Arctic: dynamics and history. Springer-Verlag, Heidelberg, pp 635–655
Strub PT, Mesias JM, Montecino V, Rutllant J (1998) Coastal ocean circulation off western South America. In: Brink K, Robinson A (eds) The sea, vol. 11. John Wiley & Sons, New York, pp 273–313
Takahashi K (1998) The Okhotsk and Bering Seas: critical marginal seas for the land-ocean linkage. In: Saito Y, Ikehara K, Katayama H (eds) Land-sea link in Asia. STA (JISTEC) and Geological Survey of Japan, pp 341–353
Takizawa J (1982) Characteristics of the Soya Warm Current in the Okhotsk Sea. Journal of Oceanographical Society of Japan 38:281–292
Talley LD (1991) A Okhotsk sea water anomaly: implications for ventilation in the North Pacific. Deep-Sea Res 38:171–190
Talley LD, Nagata Y (eds) (1995) The Okhotsk Sea and Oyashio region. PICES Science Report 2, 227 pp
Tarran GA, Burkill PH, Edwards ES, Woodward EMS (1999) Phytoplankton community structure in the Arabian Sea during and after SW monsoon, 1994. Deep-Sea Res Pt II 46:655–676
Thierry MF, Wambeke V, Thingstad FT, Sempere R, Garcia N, Raimbault P, Marie D, Queguiner B, Dolan J, Claustre H (2000) Phosphate as a key factor controlling production and carbon export in the Mediterranean Sea. JGOFS Open Science Meeting, Japan Marine Science Foundation, Tokyo, 13–18 April, 2000
Thomas AC, Strub PT, Huang F, James C (1994) A comparison of the seasonal and interannual variability of phytoplankton pigment concentrations in the Peru and California current system. J Geophys Res 99:7355–7370
Thomas H, Schneider B (1999) The seasonal cycle of carbon dioxide in Baltic Sea surface waters. J Marine Syst 22:53–67
Thompson DWJ, Wallace JM (1998) The Arctic oscillation signature in the wintertime geopotential height and temperature fields. Geophys Res Lett 25:1297–1300
Torres T, Turner DR, Silva N, Rutllant J (1999) High short-term variability of CO_2 fluxes during an upwelling event off the Chilean coast at 30°S. Deep-Sea Res Pt I 46:1161–1179
Tsunogai S, Watanabe S, Nakamura J, Ono T, Sata T (1997) A preliminary study of carbon system in the East China Sea. J Oceanogr 53:9–17
Tyrrell T, Holligan PM, Mobley CD (1999) Optical impacts of oceanic coccolithophore blooms. J Geophys Res 104:3223–3241
Uzuka N, Watanabe S, Tsunogai S (1997) DMS in the North Pacific and its adjacent seas. In: Tsunogai S (ed) Biogeochemical processes in the North Pacific. Japan Marine Science Foundation, Tokyo, pp 127–135
van Geen A, Takesue RK, Goddard J, Takahashi T, Barth JA, Smith RL (2000) Carbon and nutrient dynamics during coastal upwelling off Cape Blanco, Oregon. Deep-Sea Res Pt II 47:975–1002
Ver LMB, Mackenzie FT, Lerman A (1999) Biogeochemical responses of the carbon cycle to natural and human perturbations: past, present and future. Am J Sci 299:762–801
Walsh JE (1991a) The Arctic as a bellwether. Nature 352:19–20
Walsh JE, Zhou X, Portis D, Serreze MC (1994) Atmospheric contribution to hydrologic variations in the Arctic. Atmos Ocean 32:733–755
Walsh JJ (1977) A biological sketchbook for an eastern boundary current. In: Goldberg ED, McCave IN, O'Brien JJ, Steele JH (eds) The sea, vol. 6. John Wiley & Sons, London, pp 923–968
Walsh JJ (1981) A carbon budget for overfishing off Peru. Nature 290:300–304
Walsh JJ (1988) On the nature of continental shelves. San Diego: Academic Press, 520 pp
Walsh JJ (1989) Arctic carbon sinks: present and future. Global Biogeochem Cy 3:393–411
Walsh JJ (1991b) Importance of continental margins in the marine biogeochemical cycling of carbon and nitrogen. Nature 350:53–55
Walsh JJ (1994) Particle export at Cape-Hatteras. Deep-Sea Res Pt II 41:603–628
Walsh JJ (1995) DOC storage in Arctic Seas: the role of continental shelves. Coastal and Estuarine Studies 49:203–230
Walsh JJ, Dieterle DA (1994) CO_2 cycling in the coastal ocean. I – a numerical analysis of the southeastern Bering Sea with applications to the Chukchi Sea and the north Gulf of Mexico. Prog Oceanogr 34:335–392
Walsh JJ, Rowe GT, Iverson RC, McRoy CPM (1981) Biological export of shelf carbon is a sink of the global CO_2 cycle. Nature 291:196–201
Walsh JJ, Premuzic ET, Gaffney JS, Rowe GT, Harbottle G, Stoenner RW, Balsam WL, Betzer PR, Macko SA (1985) Organic storage of CO_2 on the continental slope off the mid-Atlantic bight, the southeastern Bering Sea and the Peru coast. Deep-Sea Res 32:853–883
Walsh JJ, McRoy CP, Coachman LK, Goering JJ, Nihoul JJ, Whitledge TE, Blackburn TH, Parker PL, Wirick CD, Shuert PG, Grebmeier JM, Springer AM, Tripp RD, Hansell DA, Djenidi S, Deleersnijder E, Henriksen K, Lund BA, Andersen P, Muller-Karger FE, Dean K (1989) Carbon and nitrogen cycling within the Bering/Chukchi Seas: source regions for organic matter effecting AOU demands of the Arctic Ocean. Prog Oceanogr 22:277–359
Walsh JJ, Carder KL, Müller-Karger FE (1992) Meridional fluxes of dissolved organic matter in the North Atlantic Ocean. J Geophys Res 97:15625–15637
Watson AJ (1995) Are upwelling zones sources or sinks of CO_2? In: Summerhayes CP, Emeis KC, Angel MV, Smith RL, Zeitzschel B (eds) Upwelling in the oceans: modern processes and ancient records. Dahlem Workshop Reports. Envorinment Science Research Report 18. John Wiley & Sons, New York, pp 321–336
Watts LJ, Owens NJP (1999) Nitrogen assimilation and the *f*-ratio in the northwestern Indian Ocean during an intermonsoon period. Deep-Sea Res Pt II 46:725–743
Weatherhead EC, Morseth CM (1998) Climate change, ozone, and ultraviolet radiation. In: AMAP Assessment report: Arctic pollution issues. Arctic Monitoring and Assessment Programme (AMAP), Oslo, Norway, Chap. 11, pp 717–774
Weller G, Lange M (1999) Impacts of global climate change in the Arctic regions. International Arctic Science Committee, University of Alaska, Fairbanks
Weiss RF, Van Woy FA, Salameh PK (1992) Surface water and atmospheric carbon dioxide and nitrous oxide observations by shipboard automated gas chromatography: results from expeditions between 1977 and 1990. Oak Ridge National Laboratory, NDP–044, 123 pp
Wijffels SE, Schmitt RW, Bryden HL, Stigebrandt A (1992) Transport of freshwater by the oceans. J Phys Oceanogr 22:155–162
Wollast R (1998) Evaluation and comparison of the global carbon cycle in the coastal zone and in the open ocean. In: Brink KH, Robinson AR (eds) The sea, vol. 10. John Wiley & Sons, New York, pp 213–252
Wollast R, Mackenzie FT, Chou L (1993) Interactions of C, N, P and S biogeochemical cycles and global change. Springer-Verlag, Berlin, 507 pp
Woodward EMS, Rees AP, Stephens JA (1999) The influence of the south-west monsoon upon the nutrient biogeochemistry of the Arabian Sea. Deep-Sea Res Pt II 46:571–591
Wu CR, Shaw PT, Chao SY (1999) Assimilating altimetric data into a South China Sea model. J Geophys Res 104:29987–30005
Wyrtki K (1971) Oceanographic atlas of the International Indian Ocean Expedition. National Science Foundation, Washington D.C., 531 pp
Yeats PA, Westerlund S (1991) Trace metal distributions at an Arctic Ocean ice island. Mar Chem 33:261–277

Apendix 3.1 Continental Margins: Site Descriptions

Agulhas Bank
Medium-width shelf influenced by the strong Agulhas Current; modest winds and surface heating but weak riverine outflow; 6×10^4 km^2

Amazon Shelf
Medium-to-wide shelves strongly influenced by large rivers, the Brazil Current and tides, but moderate winds; 8.3×10^4 km^2

Andaman Sea
Semi-enclosed narrow-to-medium width shelves with weak currents, moderate winds but strong tides and freshwater inputs; 2.4×10^5 km^2

Arabian Peninsular Shelf
Narrow shelf with weak currents, tides and freshwater but strong winds; 1.2×10^5 km^2

Baltic Sea
Semi-enclosed, shallow sea with strong tides but weak oceanic and moderate freshwater influences; 0.42×10^6 km^2

Banda Sea
Semi-enclosed deep basin with narrow shelves, shallow sills, strong tides and freshwater; 0.70×10^6 km^2

Barents Sea
Semi-enclosed with wide shelves; large freshwater inputs and winds but exports ice; 6.0×10^5 km^2

Bay of Bengal Shelf
Narrow-to-medium width shelves influenced by the moderate E Indian Coastal Current; strong freshwater and winds, but weak tides; 7.2×10^4 km^2

Beaufort Sea
Narrow-to-medium shelves with large freshwater inflow; 1.8×10^5 km^2

Benguela Current Shelf
Classic wind-forced upwelling system with deep shelf break; influenced by the Agulhas Rings and the Angolan Current; strong winds, but little freshwater or tides; 1.44×10^5 km^2

Bering Sea Basin
Deep basin with a maximum depth of 5 121 m; deep connections with the North Pacific; deep winter convection; 1.1×10^6 km^2

Bering Sea Shelf
Large, wide, shallow shelf area influenced from shore by large rivers and cyclonic eddies of the Bering Sea; exchange time <6 months; 1.1×10^6 km^2

Biscay-French Shelves
Narrow in the south, widening northwards; influenced by moderate winds and tides but weak upwelling; 7.5×10^4 km^2

Black Sea
Semi-enclosed sea with narrow-to-wide shelves; strong freshwater but weak ocean and tidal influences; 0.46×10^6 km^2

Brazil Shelf
Narrow shelves in the NE and E; strongly influenced by the Brazil and the N Brazil Currents; moderate-to-strong winds but weak tides and freshwater; narrow-to-medium shelves in the south; influenced strongly by the Brazil and Malvinas Currents; moderate-to-strong winds, but weak-to-moderate tides and freshwater; 5×10^5 km^2

Buenos Aires Shelves
Medium-width shelves influenced by the strong Malvinas and Brazil Currents but weak-to-moderate tides and freshwater; 1.6×10^5 km^2

Canadian Arctic Archipelago Shelves
Semi-enclosed; narrow shelves with moderate freshwater inflow; 3.0×10^5 km^2

Caribbean Sea
Semi-enclosed sea with deep basin and wide shelves; strong currents; 1.94×10^6 km^2

Central Chilean Shelf
Narrow shelf influenced by the strong Peru-Chile Coastal Current; strong winds but weak freshwater and upwelling; 0.5×10^5 km^2

Chukchi Shelf
Medium-to-wide shelves influenced by the Siberian Coastal Current and large freshwater inflow; 5.2×10^5 km^2

East China Sea Shelf
Large, wide, shallow shelf strongly influenced from the shore by large river and from the ocean by the Kuroshio; clear seasonal monsoon winds, but moderate tides and surface heating; 0.9×10^6 km^2

East Japan Shelf
Narrow shelf strongly influenced by the Oyashio and Kuroshio Currents and other deep-ocean interactions; moderate surface heating and weak tides; freshwater outflow and moderate winds; 1.0×10^5 km^2

East African Shelf
Narrow shelf influenced by the strong E African Coastal Current; moderate winds but weak tides and little freshwater; 1.3×10^5 km^2

East Madagascar Is. Shelf
Narrow shelf influenced by the strong E Madagascar Current; moderate freshwater and winds but weak tides; 1.0×10^5 km^2

East Siberian Sea
Semi-enclosed with wide shelves and large freshwater inflow; 8.9×10^5 km^2

Equador-Peru Shelves
Narrow shelf influenced by strong upwelling, winds and the Peru-Chile Count Current, but weak tides and no freshwater; 0.1×10^5 km^2

Equatorial W African Shelf
Narrow shelf influenced by the Equatorial Counter Current and upwelling; weak winds, moderate tides, but abundant freshwater; 1.0×10^5 km^2

Flores Sea
Semi-enclosed deep basin with narrow shelves, shallow sills, strong tides and freshwater; 1.6×10^5 km^2

Great Barrier Reef
Medium-width shelf influenced by the strong Hiro Current, winds and seasonal upwelling, but moderate tides and freshwater; 1.5×10^5 km^2

Gulf of California Shelves
Narrow shelves except in the north; strong tides; little freshwater inflow; 0.16×10^6 km^2

Gulf of Carpentaria
Shallow shelf with strong tides, currents and freshwater; 4×10^5 km^2

Gulf of Maine
Semi-enclosed, with wide shelves weakly influenced by the Labrador Current and the Gulf Stream, but strong tides, modest freshwater and winds; 1.0×10^5 km^2

Gulf of Mexico
Semi-enclosed sea with narrow-to-medium shelves slightly influenced by the Loop Current and tides, but moderate winds; strong freshwater outflow in the north, moderate in the west; 2.3×10^5 km^2

Gulf of St. Lawrence
Nearly closed bay with medium-wide shelf and a weak influence from the Labrador Current; modest winds and tides but strong freshwater outflow; 1.6×10^5 km^2

Gulf of Thailand
Narrow-to-medium width shelf trending N to S hundreds of km with large riverine, tidal and monsoon influences; driven by seasonal upwelling and possibly coastal trapped waves; water exchange time of about 1 year; flushing time with respect to freshwater input ~25 years; 4×10^5 km^2

Halmahera Sea
Semi-enclosed deep basin with narrow shelves, shallow sills, strong tides and freshwater; 1.0×10^5 km^2

Iberian Shelf
Narrow shelf influenced by upwelling and the Portugal Current; moderate winds; small freshwater input; 1.0×10^5 km^2

Indonesian Seas
Open and semi-enclosed seas with narrow-to-wide shelves; strongly influenced by ocean, tides and freshwater.

Irish Sea
Semi-enclosed shelf with through flow, strong tides and winds; 0.18×10^6 km^2

Java Sea
Semi-enclosed shelf with strong tides and freshwater; 0.48×10^6 km^2

Kamchatka Shelf
Narrow shelf influenced by the strong East Kamchatka Current and surface heating; moderate winds and weak deep-ocean influences; tides, freshwater inflow and ice; very high surface nutrient concentration in winter (NO_3 about 20 μM l^{-1}; PO_4 about 2.25 μM l^{-1}; and SiO_2 about 60 μM l^{-1}), but oxygen is 5% below saturation at $T < -1$ °C; 1.8×10^5 km^2

Kara Sea
Semi-enclosed with wide shelves; very large freshwater input but exports ice; 8.8×10^5 km^2

Labrador Shelf
Subpolar shelves of medium width; strongly influenced by the Labrador Current with modest amounts of freshwater; winds and tidal influences; 0.9×10^5 km^2

Laptev Sea
Semi-enclosed; wide shelves with large freshwater inflow but exports ice; 6.6×10^5 km^2

Luzon-Taiwan Mindanao Shelves
Narrow shelves with strong influences from the Kuroshio and other deep-ocean interactions, but weak tides; freshwater inflow, winds and surface heating; 7.3×10^4 km^2

Mackenzie Shelf
Wide shelf dominated by the Mackenzie River that freezes annually; coastal current; exchange time <1 year; 0.06×10^6 km^2

Malacca Straits
Semi-enclosed shallow shelf with weak currents, moderate winds but strong tides and freshwater; 2.4×10^5 km^2

Maluku Sea
Semi-enclosed deep basin with narrow shelves, shallow sills, strong tides and freshwater; 1.6×10^5 km^2

Mediterranean Sea
Semi-enclosed sea with narrow-to-wide shelves; moderate ocean influence but weak tides; 2.51×10^6 km^2

Mid-Atlantic Bight
Narrow-to-medium width shelves moderately influenced by the Gulf Stream and Labrador Current; weak tides, modest freshwater and winds; 1.5×10^5 km^2

Mindanao Shelves
Narrow shelves with strong influences from the Kuroshio and other deep-ocean interactions, but weak tides, freshwater inflow, winds and surface heating; 6.1×10^5 km^2

Mozambique Channel
Semi-enclosed, narrow shelf influenced by the strong Mozambique Current and freshwater, but moderate tides and winds; 9×10^4 km^2

Natal/E. Cape Shelf
Narrow shelf influenced by the strong Agulhas Current; moderate freshwater but weak tides and winds; 4×10^4 km^2

New Zealand Shelves
Open, narrow shelves with a strong ocean influence; moderate tides and freshwater; 2.8×10^5 km^2

Newfoundland Shelf
Medium-width shelf with strong influences from the Labrador Current; weak tides and modest freshwater and winds; 4.5×10^5 km^2

North Sea
Semi-enclosed shallow shelf with strong tides and freshwater; 0.58×10^6 km^2

N Chilean Shelf
Narrow-to-medium width with seasonal wind-forced upwelling; Peru-Chile Counter Current; weak tides but no freshwater; 0.4×10^5 km^2

N Equador-Panama Shelf
Narrow shelf with influences from the Columbia Current, winds and strong precipitation; generally downwelling, but with upwelling north of 4° N in winter; weak tides; 1.0×10^5 km^2

North Sea
Shallow shelf sea with water depth ranging from 40 m in the south to 200 m at the shelf edge in the north; strong tides, freshwater inflow and winds; 0.58×10^6 km^2

NW African Shelves
Generally narrow shelves influenced by upwelling, the Canary Current and the North and South Atlantic Counter Current; strong winds but weak tides or freshwater inflow; 2×10^5 km^2

NW American Shelf
Narrow shelf with strong influences from the California and Davidson Currents, upwelling, seasonal storms, and river water (730 km^3 yr^{-1}); buoyancy forced coastal current; little freshwater inflow and weak tides in the south, strong in the north; 0.5×10^5 km^2

NW European Shelf
Wide shelf influenced by the North Atlantic Current; strong winds but moderate freshwater and upwelling; 0.9×10^6 km^2

Norwegian Shelf
Narrow shelf influenced by the Norwegian Current, strong winds and freshwater, but little upwelling except in fjords; 1.0×10^5 km^2

Panama-Mexican Shelf
Narrow shelf with influences from the Costa Rican Coastal Current and offshore winds; little precipitation or freshwater inflow; 1×10^6 km^2

Patagonia Shelf
Wide shelf influenced by the strong Malvinas Current, tides and winds, but weak freshwater; 0.8×10^6 km^2

Persian Gulf
Shallow semi-enclosed sea with strong tides; evaporation higher than precipitation plus runoff; 0.24×10^6 km^2

Red Sea
Deep semi-enclosed sea with narrow shelves; strong evaporation, little precipitation or runoff; incoming surface flow and outgoing subsurface flow; 0.44×10^6 km^2

Scotian Shelf
Medium-width shelf with weak influence from the Labrador Current and the Gulf Stream; modest tides, freshwater and winds; 1.5×10^5 km^2

Sea of Japan Basin
Deep basin with deep winter convection; straits connecting to the open ocean: all <130 m deep; 7.4×10^5 km^2

Sea of Japan Shelves
Narrow shelves; strong surface heating; moderate influences from the Kuroshio and winds; weak tides, freshwater inflow and ice; 2.6×10^5 km^2

Sea of Okhotsk Basin
Deep basin with deep winter convection and deep straits connecting the basin to the North Pacific; strong influence from the strong East Kamchatka Current and the Oyashio; 1.01×10^6 km^2

Sea of Okhotsk Shelf
Medium-width shelf with strong ice and surface heating influences; moderate tides, freshwater inflow and winds; weak deep-ocean influences; 0.51×10^6 km^2

Somalia Shelf
Narrow shelf influenced by strong winds, upwelling and the moderate Somali Current, but little river outflow or tides; 4.6×10^4 km^2

S Atlantic Bight
Narrow shelf strongly influenced by the Gulf Stream; weak tides, modest freshwater and winds; 0.3×10^5 km^2

S Chilean Shelf
Medium-width shelf influenced by the West Wind Drift and Cape Horn Current; strong winds, tides and freshwater (2.5 m yr^{-1}); downwelling; 1.2×10^5 km^2

South China Sea Basin
Deep basin with moderate monsoon winds, upwelling, river water buoyancy-forced coastal current, and deep connections to the Philippine Sea; weak tides; 1.1×10^6 km^2

South China Sea Shelf
Large, wide, shallow shelf moderately influenced from shore by large rivers from the South China Sea Basin by eddies and by surface heating and seasonal monsoon winds; weak tides; exchange time <6 months; 1.1×10^6 km^2

SE Australian Shelf
Narrow shelf influenced by the strong E Australia Current and winds, but weak tides and freshwater; 0.4×10^5 km^2

S Indonesian Shelf
Narrow shelves with weak currents, weak tides; moderate freshwater but strong winds; 0.67×10^6 km^2

Sulawesi (Celebes) Sea
Semi-enclosed deep basin with narrow shelves, shallow sills, strong tides and freshwater; 2.6×10^5 km^2

Sulu Sea
Semi-enclosed deep basin with narrow shelves, shallow sills, strong tides and freshwater; 0.35×10^6 km^2

W Canadian Shelf
Medium-to-wide shelves with strong influences from winds and the North Pacific and Alaskan Currents; intermittent upwelling in the southern shelf; downwelling in the north; moderate tides and freshwater inflow; 0.1×10^6 km^2

W Florida Shelf
Narrow-to-medium width shelves with a moderate influence from the Loop Current; weak tides and freshwater but strong winds; 0.4×10^5 km^2

W Indian Shelf
Narrow-to-medium width shelves with weak currents or fresh-water; moderate tides but strong winds; 0.3×10^6 km^2